Analysis of Precipitable Water Vapour in Angola Using GNSS Observations

Versão Final Após Defesa

Isíldo Ntemo Gomes

Dissertação para obtenção do Grau de Mestre em
Sistemas de Informação Geográfica
(2^{o} ciclo de estudos)

Orientador: Prof. Doutor Rui Manuel da Silva Fernandes
Co-orientadores: Prof. Doutor Pedro Almeida e Doutor Machiel Bos

Abril de 2022

Dedicatória

Dedico este trabalho em primeira instância ao Isildo Ntemo Gomes (Eu);

Aos meus pais: Pedro Gomes e Nsanga Jaqueline;

A minha mulher, Lando Adolfina Kiala Gomes;

Ao INAMET e a SUGGEST-AFRICA;

E por fim a todos quanto foram fundamentais na conclusão de mais uma fase deste projecto nomeadamente: SEGAL e aos meus professores.

Agradecimentos

Aos meus pais e irmãos, que me apoiaram, incentivaram nos momentos mais difíceis e comemoraram os momentos mais felizes.

A minha mulher, pelo incentivo e força que vinhas me dado durante este 2 ano, e agradece-lho pela paciência, meu muito obrigado Lando Adolfina Kiala Gomes (Mãe Grande Dorkiz Única Mamã Béton).

Ao meu orientador Professor Dr. Rui da Silva Manuel Fernandes, na verdade não tenho palavras para expressar por que tudo fizeste para chegarmos até aqui acreditaste em mim e partilhaste todo seu conhecimento, e que fez de tudo para que projecto continuasse ao longo da dissertação. Obrigado pelos puxões de orelha, tenho a plena certeza que vai ajudar-me a crescer muito! Muito obrigado, Professor.

Aos meus Co-orientadores Pedro de Almeida e o ao Doutor Machiel Bos, meu muito obrigado pela vossa disponibilidade prestada em mim não sei como vos agradecer, mais uma vez meu muito obrigado.

A minha instituição INAMET (Instituto Nacional de Meteorologia e Geofísica), pela oportunidade concedida de eu ser o focal point para este projecto. A SUGGEST-AFRICA pela oportunidade concedida será sempre uma honra poder voltar a trabalhar pelo projecto, e a toda staff da SEGAL. Meu muito obrigado vai também na pessoa que preferiu escolher-me para eu fazer parte deste projecto Domingos Nascimento.

Aos meus colegas da instituição que sempre estiveram comigo nomeadamente: António Gaspar (Lameira), Amílcar José, Rita Capitã e o Chefe Eurico da Rocha. Aos meus professores e colegas do curso de SIG especialmente ao Armando Vicente e ao Ipalibo Bala meus mais velhos foi muito bom conhecê-los levar-vos-ei para vida. Aos meus amigos da UBI (Moisés Nsabi, Evanilson Miza e o Bartolomeu Kapalandanda), que me apoiaram e acolheram-me com tanto carinho, e que me ajudaram nos momentos de dificuldade ao longo da pesquisa. E sem esquecer o meu amigo e o Doutor Arlindo Meque. Enfim a todos que me ajudaram direita e indiretamente meu muito obrigado.

A maior ventura da minha vida foi aceitar o desafio do projecto de fazer o trabalho inteiramente em inglês com tantas dificuldades, mas, fi-lo como eu sempre digo:

Ninguém se perde no caminho certo!

Resumo Alargado

Para precisão da previsão do tempo e análise de eventos extremos é fundamental uma boa estimativa do vapor da água na atmosfera. O vapor da água na atmosfera é fornecido por várias técnicas como radio sondagem que mede este parâmetro em várias alturas. No entanto, muito dessas técnicas são limitadas devido a resolução espacial e temporal ou sofrem restrições específicas de medição. Para completar estas limitações encontrado nas demais técnicas, o vapor da água precipitável (PWV) pode ser medido pelo GNSS (Sistemas de navegação global por satélite) CORS (Rede nacional de estações de referência de operação continua). PWV pode ser obtido a partir do atraso do sinal de GNSS através da troposfera, quando a temperatura e a pressão também são conhecidas derivado da localização duma estação meteorológica.

No âmbito da SUGGEST-ÁFRICA, esta ser implementado um sistema de modo a calcular o PWV de uma maneira automática em Angola. Assim, nesta dissertação pretende descrever os passos necessários para desenvolver tal sistema a ser utilizado para apoiar aplicações meteorológicas e climáticas em Angola. SUGGEST-ÁFRICA também financiou a instalação de 5 estações meteorológicas, colocada com estações GNSS em Angola, nomeadamente: Benguela, Cabinda, Cuito, Luanda e Namibe, a fim de obter a pressão e a temperatura necessárias para obter as estimativas PWV. Aconselha-se o uso dos modelos globais/regionais para aquisição de valores de pressão e temperatura quando não existe dados nas estações meteorológicas adjacentes.

As metodologias foram otimizadas para o acesso passivo e ativo dos dados GNSS; a estimação do vapor de água precipitável é calculada usando a técnica PPP (Posicionamento do ponto preciso), que permite a determinação de cada estação individualmente e separadamente; as soluções foram validadas usando valor interno. Além disso, são apresentadas análises para avaliar a fiabilidade da rede.

Este trabalho, também apresenta resultados preliminares para a variação de todo dados do ZTD disponível em Angola e a forma como se relacionam com as variações sazonais do vapor de água. Também, apresenta variação da série temporal do PWV na estação meteorológica de Luanda (instalado pela SEGAL).

Este estudo é suportado pela SUGGEST-ÁFRICA, financiado pela fundação Aga Khan e FCT. Utiliza recurso computacional fornecido pela C4G – Colaboração de Geociências

(PINFRA/ 22151/2016). Também é apoiado pelo projecto FCT/UIDB/50019/2020 – IDL financiado pela FCT.

.

Palavras-chave

GNSS;Atraso Total de Zenith;Vapor de Água Precipitável;SIG

Abstract

For accurate weather predictions and analysis of extreme events, a good estimate of the amount of water content in the atmosphere is essential. This information is provided by several techniques like radiosondes that measure this parameter at various heights. However, most of them are very limited spatially and temporarily or suffer from measurement specific constraints. To complement these techniques, Precipitable Water Vapor (PWV) can be measured with GNSS (Global Navigation Satellite System) at CORS (Continuously Operating Reference Stations) networks. when the temperature and pressure are also known at the station location. PWV can be derived from the delay in the GNSS signal when it passes through the troposphere.

In the framework of SUGGEST-AFRICA, it is being implemented a system to use the national GNSS stations for the automatic computation of PWV in Angola. Thus, this dissertation intends to describe the necessary steps to develop a system to be used for supporting meteorological and climate applications in Angola. SUGGEST-AFRICA also funded the installation of 5 weather stations, collocated with GNSS stations in Angola namely: Benguela, Cabinda, Cuito, Luanda and Namibe, in order to obtain pressure and temperature which is necessary to obtain the PWV estimates. When there are no nearby meteorological stations, the potential alternative is to use values from global/regional models.

Methodologies have been optimized to passive and actively access the GNSS data; the PWV estimations are computed using PPP (Precise Point Positioning), which permits the estimation of each station separately; solutions have been validated using internal values. In addition, analyses are presented to evaluate the reliability of the network.

This work presents preliminary results for the variation of the ZTD data available all around the territory in Angola and how they relate to the seasonal variations in water vapour. Also, presents preliminary results for the time-series variation of PWV in the Luanda station (collocated by the SEGAL group).

This study is supported by SUGGEST-AFRICA, funded by Fundação Aga Khan and FCT. It uses computational resources provided by C4G – Collaboratory for Geosciences (PINFRA/22151/2016). It is also supported by project FCT/UIDB/50019/2020 – IDL funded by FCT.

Keywords

GNSS, Zenith Total Delays, Precipitable Water Vapour, GIS.

Contents

1Introduction 1
1.1 Scientific Research Design 2
1.1.1 Motivation and Justification 2
1.1.2 Problem Statement 3
1.1.3 Study Subject 3
1.1.4 Main Objective 3
1.1.5 Specific Objectives 3
1.1.6 Hypotheses 3
1.1.7 Methodology 3
1.1.8 Expected Result 4
1.1.9 Tasks 4
1.2 Main Contributions 4
1.3 Dissertation Structure 4
2State of the Art 7
2.1 Atmosphere Water Vapour 7
2.1.1 Water Vapour Overview 7
2.2 GNSS Overview 7
2.2.1 GNSS Network in Angola 9
2.2.2 GNSS Data Collection Methods 11
2.2.3 GNSS Meteorology 12
2.3 GNSS Processing 15
2.3.1 Processing Methods 15
2.3.1.1 Double Difference 15
2.3.1.2 Precise Point Positioning 16
2.3.2 Offline Processing Software 17
2.3.3 Online Processing Software 17
2.3.3.1 Jet Propulsion Laboratory – Global Differential GPS 18
2.4 Satellite Orbits 18
2.5 Meteorological Parameter Pressure and Temperature 19
2.6 Water Vapour by Other Techniques 20
2.6.1 Radiosondes 20
2.6.2 Microwave Radiometer 21
2.7 GNSS, PWV in Geographical Information Systems 22
2.7.1 GIS 22
2.7.2 GIS Data Capture Considerations 22
2.7.3 World Geodetic and Local Coordinates System 23
2.7.4 Using GNSS and PWV with GIS 23
2.7.5 Input GNSS, Pressure and Temperature Data to GIS 24
2.7.6 Applications and case studies 24
3Study Area Characterization 27
3.1 Geographic Location and Extension 27
3.1.1 Delimitation of the Study Area and Population 27
3.2 Climatological Characterization of the Study Area 28
3.2.1 Precipitation 29
3.2.2 Temperature 32
3.2.3 Topography 35
3.2.4 Drivers Over Study Area Climate 36
4Material and Methods 37
4.1 Data Acquisition 37
4.1.1 GPS Network Management System Software (The TeroNet) 37
4.1.2 GPS Data Flow 39

4.2 Network 39
4.2.1 RINEX Files Acquisition 41
4.3 Technologies, Technique and Software Used in the Dissertation 41
4.3.1 Programming Language 41
4.3.2 Linux Tools 42
4.3.3 GDGPS – APPS 42
4.3.4 ZTD2PWV 42
4.3.5 ArcGIS Desktop 10.7.1 (ArcMap, ArcToolbox and ArcCatalog) 42
4.3.6 Technique for Spatial interpolation 43
4.4 Processing of GNSS Observations Data 43
4.5 Estimating Process of the PWV 44
4.5.1 Pressure and Temperature Parameter 44
4.5.2 PWV Obtained from GPS and Meteorological Observations Dataset 45
5Results and Discussion 47
5.1 Network Reliability 47
5.1.1 GNSS Data Availability 48
5.2 Meteorological Stations Reliability 49
5.3 PPP ZTD Values 50
5.3.1 Climatological Characterization of the ZTD of Study Area 50
5.4 Validation of Estimated PWV 54
6Conclusion and future work 57
6.1 Final Notes 58
6.2 Future Work 58
Bibliography 59
A Data availability per year per station 67
B The maximum, minimum and average values of ZTD per station 75
C Equipment status at the station including the status after intervention 77

List of Figures

Figure 2.1 - Representation of a GPS constellation with six orbital planes (Cai, 2020). 8
Figure 2.2 - The equipment's and the systems installed in the REPANGOL network (Adapted from Fernandes et al., 2011). 9
Figure 2.3 - Permanent GNSS network in Angola (Fernandes et al., 2011). 10
Figure 2.4 - GNSS Stations of a) Cuito and b) Namibe with Meteorological Stations. 10
Figure 2.5 - Representation Layers of the Earth's atmosphere (Layers, 2021). 13
Figure 2.6 - Schematic of the satellite signal path through atmosphere Earth's atmosphere (adapted from Jones et al., 2020). 13
Figure 2.7 - Schematic representation of the Double Difference (Sickle & Dutton, 2021). 16

Figure 2.8 - Weather balloon carrying a RS (ALSA, 2021). 20
Figure 2.9 - MWR profiles (MWRc, 2021). 21
Figure 2.10 - Procedure for obtaining GNSS-derived PWV (Liu et al., 2019). 24
Figure 2.11 - Scheme for the comparison of the interpolation performances of the new method (based on extended virtual PWV sample points) and conventional one (based on original PWV sample points)(Liu et al., 2019). 25
Figure 2.12 - Co-Kriging interpolation results for PWV provided by Schemes I and II. Graphs (a, c), and (e) is generated by Scheme I, while graphs (b, d), and (f) are generated by Scheme II (Liu et al., 2019). 25
Figure 2.13 - Flow chart of the G4M procedure (Ferrando et al., 2018). 26
Figure 2.14 - 30-minute extraction from the 6-min HI maps for the severe event on November 4, 2011 (Ferrando et al., 2018). 26
Figure 3.1 - The map of the location of the study area. 27
Figure 3.2 - The map of the provinces of the study area. 28
Figure 3.3 - Map showing the climatological charecterization of the over Angola (Adapted from Climat, 2021). 29
Figure 3.4 - The monthly average rainfall in Dundo, Saurimo, Uige and Malanje (National Institute of Meteorology and Geophysics (1981-2010) (INAMET)[1]). 29
Figure 3.5 - Map of the mean annual rainfall in Angola (Dw, 2014). 30
Figure 3.6 - The monthly average rainfall in Luanda, Cabinda, Benguela and Namibe (1981-2010) (INAMET). 31
Figure 3.7 - The monthly average rainfall in Luena, Huambo and Lubango (1981-2010) (INAMET). **Error! Bookmark not defined.**
Figure 3.8 - Map of the Average annual temperature in Angola. 32
Figure 3.9 - The monthly average temperature in Mbanza Congo (Climat, 2021). 33
Figure 3.10 - The monthly average temperature in Luanda (Climat, 2021). 33
Figure 3.11 - The monthly average temperature in Namibe (Climat, 2021). 34
Figure 3.12 - The monthly average temperature in Huambo (Climat, 2021). 34
Figure 3.13 - The monthly average temperature in Ondjiva (Climat, 2021). **Error! Bookmark not defined.**
Figure 3.14 - Map of topography in Angola (Huntley et al., 2019). 35
Figure 3.15 - Impact of southward and northward displacement of the ITCZ on rainfall seasonality in the study area during 2009/2010 Mendelsohn et al. (2013 in Huntley et al., 2019). 36
Figure 4.1 - The TeroNet user interface with the GNSS network of Angola (Repangol, 2021). 37
Figure 4.2 - The TeroNet user interfaces with detail of each station as the actions that can be performed on each station inserted in the web platform (Repangol, 2021). 38

Figure 4.3 - Example of data that may download from the TeroNet web platform (Repangol, 2021). 38
Figure 4.4 - The web platform TeroNet software (Adapted from TeroMovigo, 2019). 39
Figure 4.5 - Distribution Map of GNSS stations with five Meteo stations in Angola. 40
Figure 4.6 - Flowchart GNSS annual data download. 41
Figure 4.7 - The GNSS observations data processing from software Jet Propulsion Laboratory - Global Differential GPS. 44
Figure 4.8 - Processing summary file. 44
Figure 4.9 - Flowchart to obtain ZTD and Conversion to PWV (Adapted from Liu et al., 2019). 46
Figure 5.1 - The average percentage of data values per station. 48
Figure 5.2 - The Total and average percentage value of the Luanda and Cuito station per year. 49
Figure 5.3 - ZTD time-series variation for the GNSS Station of Cuito. 50
Figure 5.4 - ZTD time-series variation for the GNSS Station of Luena. 51
Figure 5.5 - The monthly average of the ZTD obtained from three stations. 51
Figure 5.6 - Daily average of ZTD among sixteen stations in the different zone. 52
Figure 5.7 - The maximum, minimum and average values of the ZTD. 53
Figure 5.8 - Summary of the climatological characterization of the ZTD in the study area (Adapted from ZTD values available 11/5/2010 to 27/11/2021). 54
Figure 5.9 - Time-series variations average daily of the PWV at the LDIG station. 55
Figure 5.10 - The monthly Average of the PWV obtained from the LDIG station. 56
Figure A.1 - The Total possible percentage value of the Benguela station per year. 67
Figure A.2 - The Total possible percentage value of the Caxito station per year. 67
Figure A.3 - The Total possible percentage value of the Cabinda station per year. 68
Figure A.4 - The Total possible percentage value of the Cuito station per year. 68
Figure A.5 - The Total possible percentage value of the Huambo station per year. 69
Figure A.6 - The Total possible percentage value of the Lubango station per year. 69
Figure A.7 - The Total possible percentage value of the Luanda station per year. 70
Figure A.8 - The Total possible percentage value of the Luena station per year. 70
Figure A.9 - The Total possible percentage value of the Mbanza Congo station per year. 71
Figure A.10 - The Total possible percentage value of the Malanje station per year. 71
Figure A.11 - The Total possible percentage value of the Ndalatando station per year. 72
Figure A.12 - The Total possible percentage value of the Namibe station per year. 72
Figure A.13 - The Total possible percentage value of the Ondjiva station per year. 73
Figure A.14 - The Total possible percentage value of the Saurimo station per year. 73
Figure A.15 - The Total possible percentage value of the Sumbe station per year. 74
Figure A.16 - The Total possible percentage value of the Uíge station per year. 74
Figure B.1 - The maximum, minimum and average values of ZTD per station. 75

List of Tables

Table 2.1 - Different Methods for GNSS Data Collection 11
Table 2.2 - Different types of offline software for processing GNSS data (Adapted from Couto, 2016)..17
Table 2.3 - Different types of software online for processing GNSS data (Adapted from Ulukavak, 2019). 18
Table 2.4 - Different types of global models for acquiring meteorological parameters..19
Table 4.1 - REPANGOL network with Location Information, including the longitude, latitude, and heights. 40
Table 4.2 - Solution strategy for acquiring ZTD (Adapted from Liu et al., 2019). 43
Table 5.1 - Summary Information of GNSS Stations. 47

List of Acronyms

PWV	Precipitable Water Vapour
ZTD	Zenith Total Delays
GIS	Geographic information systems
SEGAL	Space and Earth Geodetic Analysis Laboratory
FCT	Fundação Ciência e Tecnologia
IWV	Integrated Water Vapour
RS	Radiosondes
MWR	Microwave Radiometers
GNSS	Global Navigation Satellite System
GPS	Global Positioning System
GLONASS	Russia Global Navigation Satellite System
Galileo	Europe global navigation satellite system
BDS	China BeiDou Navigation Satellite System
TOA	Time Of Arrival
IGCA	Geographic and Cadastral Institute of Angola
GPRS	General Packet Radio Service
VPNs	Virtual Private Network
RTK	Real-Time Kinematic
AFREF	African Geodetic Reference Frame
IGS	International GNSS Service
DTM	Digital Terrain Model
COST	Cooperation in the field of Scientific Technical Research
TOUGH	Targeting Optimal Use of GPS Humidity
ZWD	Zenith Wet Delay
ZHD	Zenith Hydrostatic Delay
GMF	Global Mapping Function
VMF 1	Vienna Mapping Function 1
NMF	Neill Mapping Function
NWM	Numerical Weather Models
DD	Double Difference
PPP	Precise Point Positioning
JPL	Jet Propulsion Laboratory
G4M	GNSS for meteorology
HI	Heterogeneity Index
DRC	Democratic Republic of the Congo
INAMET	National Institute of Meteorology and Geophysics
ITCZ	Intertropical Convergence Zones
CORS	Continuously Operating Reference Station
UBI	University of Beira Interior
PWV	Precipitable Water Vapour
ZTD	Zenith Total Delays
GIS	Geographic information systems

Chapter 1

Introduction

According to Isioye et al. (2017), Earth's atmosphere plays a fundamental role in several areas of knowledge, in particular meteorology. Due to its dynamism and the complexity of its processes, observing the atmosphere is a challenging task.

Water vapour in the Earth's atmosphere is often being studied by meteorologists and climatologists, because it plays an important role in atmospheric processes, including energy transport, condensation, cloud formation and precipitation (Nykiel et al., 2019).

Given the seasonal variability of water vapour, there is a need for more comprehensive data collection of atmospheric water vapour in space and time to fully understand the weather and climate patterns (Isioye et al., 2017). Thus, having a precise measure of precipitable water vapour (PWV) can improve the monitoring/evaluation of weather and climate (Revuelta et al., 1985).

According to Abbasy et al., (2017); Alshawaf et al., (2015); Zhang et al., (2018), there are different methods to compute PWV. In general, it can be divided into two categories: Satellite-based (space to Earth) and ground-based (Earth to space). These methods will be discussed in the second chapter.

The PWV obtained from GNSS can reflect the inflow and outflow of water vapour in a vertical air column above a determined site, which is important in studying severe water vapour variations. PWV obtained from GNSS have also been widely used in meteorology applications such as climate studies, precipitation forecasts and analysis (Yao et al., 2017).

As a result, this study aims to Compute PWV from Zenith Total Delays (ZTD) + meteorological (Pressure and Temperature) parameters, and analysis of the time-series to investigate the PWV variation in Angola.

Although the study aims to compute the PWV in the absence of meteorological parameters, this study will aim at only analyzing the ZTD. According to some studies, the ZTD value also is useful for meteorology applications such as climate studies, numerical weather prediction and analysis of the relationship between intense precipitation (see, Benevides et al., 2013; Dousa, 2004; Van der Marel, 2004; Vedel & Huang, 2004).

1.1 Scientific Research Design

1.1.1 Motivation and Justification

In Angola, the weather forecast is used as strategic planning information for several areas of economic and social activity & security. This information can present a large margin of error since atmospheric conditions can change in a matter of minutes and there are not enough instruments available to monitor water vapour. Therefore, weather phenomena can occur without a warning of the responsible service which can cause extreme losses in economic and social activity.
Given this limitation, some countries such as Europe, North America and Japan use a new method based on GNSS observation. This method helps in forecasting these weather phenomena because, from GNSS observations data, it is possible to compute the PWV, which plays a fundamental role in atmospheric processes.

In Angola, GNSS stations have already been installed by IGCA, with the support of the Space & Earth Geodetic Analysis Laboratory (SEGAL). GNSS observation stations have been mounted in each capital of Angola's 18 provinces. One of the biggest challenges is to transmit the know-how to national technicians on how to process data from GNSS networks. For this reason, the stations only serve for data download but are not analyzed and applied for weather forecasting (Kitoko, 2014).

The motivation for this dissertation is to demonstrate the procedures of data processing of GNSS networks. This work will serve to transfer of know-how to Angolan national technicians so that the stations do not work only to download data but provide information that will improve weather forecasting. This dissertation is supported by SUGGEST-AFRICA, funded by Fundação Aga Khan and FCT. It uses computational resources provided by C4G — Collaboratory for Geosciences (PINFRA/22151/2016). It is also supported by project FCT/UIDB/50019/2020 – IDL funded by FCT.

SUGGEST-AFRICA was the one responsible for assigning the dissertation topic.

On the personal side, what motivated me to embrace the assigned topic, was knowing that it is common to see water vapour in the atmosphere is studied by meteorologists and climatologists. Being a meteorologist, I would be the first in Angola to compute the PWV using a new method based on GNSS observation.

The analysis of the PWV will provides knowledge on its influence on rainfall distribution, climate and the prediction of extreme events.

1.1.2 Problem Statement

This dissertation addresses the processing of GNSS observations and computing precipitable water vapour (PWV) to research the variation of the ZTD and PWV in Angola using GNSS techniques.

1.1.3 Study Subject

Zenith Total Delays (ZTD) and Precipitable Water Vapour (PWV) in Angola using GNSS techniques.

1.1.4 Main Objective

Investigate long-term variations of Zenith Total Delays (ZTD) and Precipitable Water Vapour (PWV) using GNSS data available all around the territory in Angola.

1.1.5 Specific Objectives

- ✓ Analyse the network reliability according to the observations data recorded on the servers;
- ✓ Processing of GNSS observations to obtain Zenith Tropospheric Delays (ZTD);
- ✓ Compute PWV from ZTD + meteorological (Pressure and Temperature) parameters;
- ✓ Validate GNSS-derived PWV with meteorological (Pressure and Temperature) parameters;
- ✓ Create analyze daily time-series.

1.1.6 Hypotheses

- ✓ If the using GNSS data available all around the territory is processed one can determine the ZTD;
- ✓ If the precipitable water vapour (PWV) is determined from the ZTD + meteorological (Pressure and Temperature), one can investigate the variation using GNSS data available all around the territory.

1.1.7 Methodology

To comply with the proposed objectives, the deductive and dialectical method of analogy will be used developed in 2 steps:

- ✓ Bibliographic research;
- ✓ Survey research.

1.1.8 Expected Result

- ✓ Determine ZTD and validate PWV values atmosphere derived GNSS data available all around the territory and meteorological (Pressure and Temperature) parameters to investigate the variation of the ZTD and PWV.

1.1.9 Tasks

In the framework of the research and development work to be carried out in preparing the master's thesis, the following tasks are proposed: Study and familiarization with the main concept underlying the estimation of PWV using GNSS data.

1. Study and familiarization with the main concepts underlying the estimation of PWV using GNSS data.
2. Study and familiarization with the acquisition of meteorological values (Pressure and Temperature) directly observed or from models.
3. Integration of the conversion from ZTD to PWV in the entire system to produce daily and sub-daily time-series of PWV estimates.
4. Execution of tests and validation of results.
5. Analysis of the time-series to investigate the ZTD and PWV variation in Angola.
6. Writing of a scientific article.
7. Writing of the M.Sc. thesis.

1.2 Main Contributions

The main contributions of this dissertation are here presented.

The first contribution consists of the development of several computer applications which, based on the existing software packages, have implemented an integrated system to:

- ✓ Download GNSS data;
- ✓ Generation of RINEX files;
- ✓ Process the acquisition data using (APPS-GDGPS) software;
- ✓ Extract ZTD values;
- ✓ Conversion from ZTD to PWV.

During this dissertation the following posters and conference papers were presented:

- A poster with the title "Precipitable Water Vapor Derived from GNSS data in Angola" was submitted and accepted for 2º edition of the workshop "Numerical weather forecast in Portugal: modelling the surface-atmosphere interaction". University of Évora, Évora, 11-12 November 2021 (IPMA, 2021).
- Abstract with the title "Evaluating the estimation of GNSS-based PWV in Angola, Mozambique, and Nigeria" was submitted and accepted for the AGU Fall Meeting 2021. New Orleans, LA & Online Everywhere 13-17 December 2021 (Fernandes et al., 2021).

1.3 Dissertation Structure

This dissertation is organized into six chapters, where:

Chapter 1 – Introduction The scientific research design is presented, with the motivation and justification, statement of the problem, object of study, objectives, hypotheses, methodology, expected result, tasks and chronograms. It also contains the main contribution of this dissertation.

Chapter 2 - State of the Art In this chapter, the relation between the water vapour and the GNSS is described in more detail, namely the definitions, an explication regarding GNSS meteorology, GNSS data collection methods and different methods for processing GNSS raw data. Analyses the different GNSS orbit types, the different techniques to compute GNSS data, and some software available to processing for it. It also analyses some pressure and temperature models, a small comparison between GNSS-PWV and other methods to obtain PWV. The relation between GNSS, PWV and GIS finally addresses applications and case studies.

Chapter 3 – Study area characterization the area of study is identified and characterized concerning demographic and climatological aspects.

Chapter 4 – Material and Methods In generally, this chapter discusses all materials and methods used for the elaboration of this dissertation.

Chapter 5 – Results and Discussion This chapter shows the network reliability of observations data recorded on the servers. And finally, the analysis of the time series to investigate the variation of the ZTD and PWV in Angola.

Chapter 6 – Conclusion and future work Present the main conclusions of this dissertation and future work is described.

Chapter 2

State of the Art

2.1 Atmosphere Water Vapour

2.1.1 Water Vapour Overview

Water vapour is defined as the amount of water in the gas phase (in grams per cubic meter) of air. The water vapour content of an air parcel can also be expressed as the thickness of a layer liquid water that is equal to the amount of, combined all the water vapour in the vertically integrated total in any one column of air above it. There are two the most commonly used terms which are Integrated Water Vapour (IWV) or PWV (Jones et al., 2020). According to Abbasy et al. (2017), PWV is an indicator of the water vapour quantity in the atmosphere.

The highest water vapour values are located mainly in the warmer zones. However, the vast predominance of all atmospheric water vapour is limited in the lower part of the troposphere, with a certain degree of variability depending on the season, latitude and atmospheric conditions (Jones et al., 2020).

Water vapour is one of the most fundamental factors controlling the average atmospheric temperature by absorbing radiation. Life on Earth depends on the greenhouse effect. As a result, this effect plays a vital role in absorbing solar radiation into the atmosphere, which keeps the Earth's atmosphere at a habitable temperature. The Earth has an average temperature of approximately 14°C, where this temperature would be around -18°C if it were not for the existence of gases such as water vapour and carbon dioxide in the atmosphere. These gases are responsible for making life on Earth possible (Jones et al., 2020).

Water vapour has a crucial role in the transfer of energy in the atmosphere (Rocken et al., 1997). It is also is a fundamental natural greenhouse gas (Bevis et al., 1992; Bleisch et al., 2011). Water vapour is one of the most variable constituents of the atmosphere, which plays a fundamental role in the global hydrological cycle and the climate system (Isioye et al., 2015).

With such a crucial role in the earth's atmosphere, meteorologists have created several methods to measure the distribution of water vapour in the atmosphere. The methods are, among others, radiosondes (RS), microwave radiometers (MWR), spectrometers, lidars and GNSS which is the method described in this dissertation.

2.2 GNSS Overview

The technology that includes all space-based navigation systems refers to GNSS, a name given to all satellite space positioning techniques with global coverage. Currently, there are several systems, namely, the Global Positioning System (GPS) from the United States, Russia Global Navigation Satellite System (GLONASS), Europe's Global Navigation Satellite System (Galileo) and China's BeiDou Navigation Satellite System (BDS) (Okey, 2015). Therefore, the combination of these systems involves satellites, ground reference stations and user equipment (Rizos et al., 2005). These systems provide accurate information in almost every part of the globe at any hour, minute and second of an individual or object, thus discarding traditional paper maps into digital solutions with greater accuracy than before (Couto, 2016).

According to Jones et al., (2020); Kaplan & Hegarty (2006); Rizos et al., (2005), they defined the three segments involving all GNSS: Satellites (space), ground and user. The space segment consists of satellites orbiting at an altitude of (in the case of GPS) is approximately 26,600 km in orbital planes of 55° to the equator. Considering the previously exposed, GPS will be the primary focus of this dissertation.

According to Cai (2009); Kaplan & Hegarty (2006), the GPS satellite navigation system consists of 24 satellites distributed in six orbital planes where one plane contains four satellites. GPS also provides a form of Coordinated Universal Time (UTC). GPS services can support multiple users because GPS receivers only receive data. GPS satellites provide separate services to civilian and military users (Kaplan & Hegarty, 2006). Figure 2.1 will show a representation of a GNSS with orbital planes.

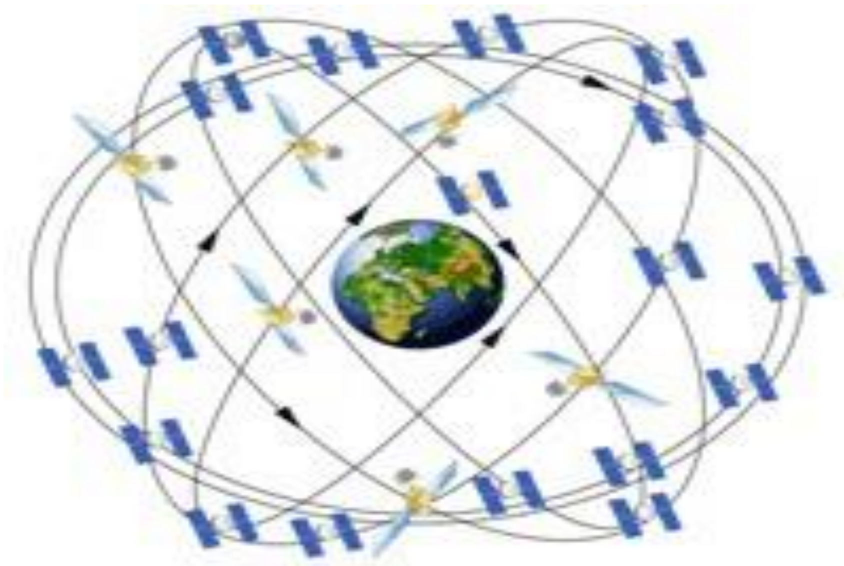

Figure 2.1 - Representation of a GPS constellation with six orbital planes (Cai, 2020).

GPS satellites broadcast ranging codes and navigation data on four L-band frequencies: L1 - 1575.42 MHz, L2/LC - 1227.60, L5 - 1176 MHz an L1C – 1575 MHz (GPS, 2020). Each satellite transmits a different carrier signal. The different carrier signal allows the use of a technique is known as a one-way Time of Arrival (TOA). TOA consists of determining the propagation time of the signal and consequently calculating the satellite-to-user distance while the navigation data allow each receiver to know the position of each satellite in the transmission signal (Kaplan & Hegarty, 2006).

It is possible to measure the three-dimensional position of the receivers. For this measurement to be possible, at least four satellites are required to measure the position (Jones et al., 2020; Kaplan & Hegarty, 2006). Three satellites would be enough if the clock in the GNSS receiver would be very accurate. Since this is normally not the case, data from a fourth GNSS satellite is needed to correct for this clock error.

2.2.1 GNSS Network in Angola

The permanent GNSS network in Angola was intended and established by the Geographic and Cadastral Institute of Angola (IGCA) in the REPANGOL project. This project was developed with the support of the Space and Earth Geodetic Analysis Laboratory (SEGAL) (Kitoko, 2014).

According to Fernandes et al. (2011), The project included the following installed systems:

- **GNSS System** - Topcon NetG3A;
- **Router** - Transmission based on mobile networks (GPRS and 3G). Software developed by SEGAL using VPNs (Virtual Private Network);
- **Power Management** - Solar panels are used to give all the necessary power. In Angola, the streaming of Real-Time Kinematic (RTK) corrections is possible when there is power from the electrical grid (or using an additional battery).

Figure 2.2 illustrates the equipment's and the systems installed.

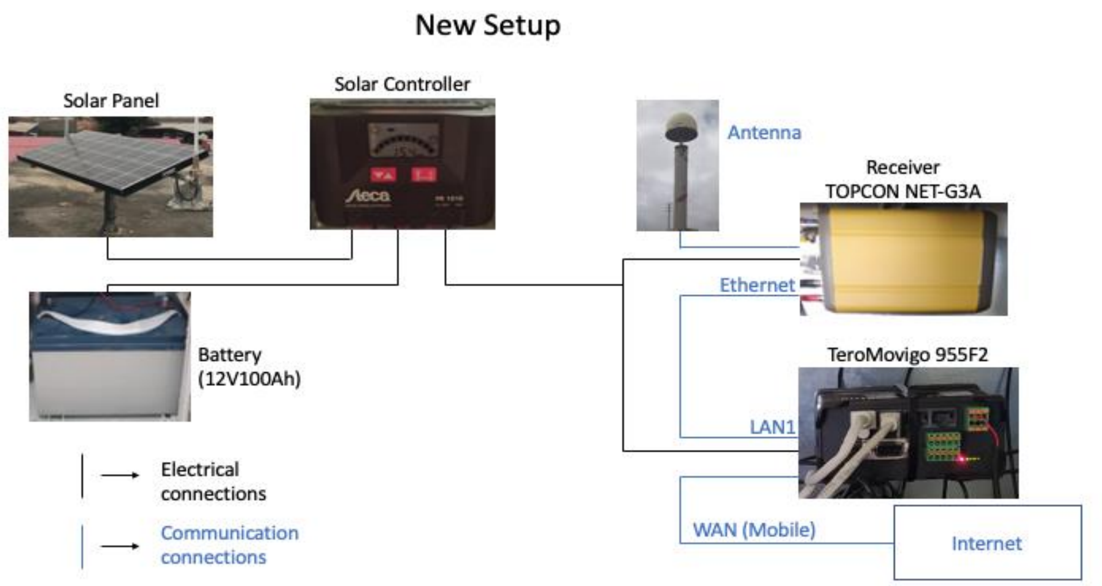

Figure 2.2 - The equipment's and the systems installed in the REPANGOL network (Adapted from Fernandes et al., 2011).

However, SEGAL has installed Topcon GNSS stations in all 18 provinces, one per capital of provincial (see, Figure 2.3) (Fernandes et al., 2011; Kitoko, 2014).

Figure 2.3 - Permanent GNSS network in Angola (Fernandes et al., 2011).

The REPANGOL network before 2010 has not been collocated with meteorological sensors. However, in 2020, in the framework of SUGGEST-AFRICA, SEGAL placed five meteorological stations nearby REPANGOL: Luanda, Benguela, Cuito, Cabinda and Namibe (see Figure 2.4).

Figure 2.4 - GNSS Stations of a) Cuito and b) Namibe with Meteorological Stations.

This project is part of the African Geodetic Reference Frame (AFREF) project, which advocates the establishment of the same geodetic reference frame for the African continent

(Kitoko, 2014). According to Fernandes et al. (2011), There reasons for promoting the project are:

- Adoption of modern geodesic infrastructures fully compatible with the actual geo-referencing techniques;
- Poor quality of the existing network based on observations made with old techniques;
- Conformity with the reference frameworks of neighboring countries through a collaboration with international projects, namely AFREF and IGS.

2.2.2 GNSS Data Collection Methods

Many methods are employed to collect high precision differential GNSS data. The technique used depends on many factors, including desired precision, survey objective, available equipment, and field logistics. There are several methods to collect GNSS data following table shows four some of the most common GPS survey methods (Blume, 2010):

Table 2.1 - Different Methods for GNSS Data Collection

Survey Methods	Accuracy	Occupation Period	Applications
Continuous	< 0.5 cm	Months or more	Geophysics, Crustal deformation, reference stations
Static	0.5 cm – 2.5 cm	Hours to days	Crustal deformation, geodetic control, geophysics, very long baseline surveys
Kinematic (post-processing and real-time	1 cm – 5 cm	Seconds	Short baselines, vehicle positioning, feature surveys, closely spaced points, GIS and mapping
Point positioning	100 cm – 500 cm	Minutes to hours	Rough positioning

- ✓ **Continuous** stations are continuously operating long-term or permanent GPS station installations and often involve data telemetry. It can be used as pre-existing base stations in campaign surveys (rapid static, static, and kinematic).
- ✓ A **static** method is regional, sub-cm precision GPS surveys with portable equipment and is the standard campaign data collection method for crustal deformation surveys. The static survey collects at least 6 hours of non-stop data every day for processing and repeats benchmark occupations if possible.
- ✓ The **kinematic** method is local surveys (<10 km). Kinematic uses mobile GPS equipment for mapping features or measuring point locations where many cm precisions are sufficient. Kinematic surveys depend on continuous tracking to resolve the integer ambiguity. Since the data processing software can simultaneously delete the ambiguity and track the antenna motion, fixed-integer solutions are acquired nearly instantaneously.

- ✓ **Point positioning** uses only data from a single receiver to compute its coordinates. This technique is very coarse, but sometimes it is the only way to determine base station coordinates while in the field.

2.2.3 GNSS Meteorology

The use of GNSS for meteorological purposes has become quite popular nowadays (the last few decades) because of its advantages (Ferrando et al., 2018). According to Li et al. (2014), GNSS has many significant advantages compared to other existing methods. Although GNSS they do not provide humidity profiles in their measurements. The most fundamental one is the good temporal resolution (less than one hour, down to 5 min). And the fact can be run unattended and operated in all weather conditions (Baelen et al., 2005).

GNSS meteorology is the remote sensing of the atmosphere (particularly troposphere) using GNSS to obtain information about its state (Bosy et al., 2012; Bosy et al., 2010). Continuous observations from GNSS receivers provide an excellent tool for monitoring PWV in the Earth's atmosphere, with particular reference to its lower layer (Troposphere) (Bosy et al., 2012; Boutiouta & Lahcene, 2013; Ferrando et al., 2018).

Sguerso et al. (2013) implemented a new element in this field. Proposed to use several existing regional, national and international permanent GPS stations to estimate the ZTD for climatological applications and to monitor the PWV of a wide area with the Digital Terrain Model (DTM) Sguerso et al. (2013 in Ferrando et al., 2018).

According to Bosy et al. (2012), many research projects were initiated in Europe and overseas to derive the water vapour in the atmosphere from GPS observation data. For example, COST Action 716 (European Cooperation in the field of Scientific Technical Research-exploitation of ground-based GPS for climate and numerical weather prediction applications, 1998–2004) (Dousa, 2004; Van der Marel, 2004), TOUGH (Targeting Optimal Use of GPS Humidity Data in Meteorology, 2003–2006) (Vedel & Huang, 2004). The main input of these projects was to connect the fields of meteorology and geodesy, in a way to operationalize and test the use of ground-based GNSS for meteorological applications. The idea was that the GNSS stations would provide near real-time observations to be assimilated into the numerical weather prediction. The result was positive since the test indicated that ZTD based on ground-based GNSS had good accuracy (Dousa, 2004; Gonçalves, 2016; Huang & García-Moya, 2003).

GNSS propagation signals arrive in the atmospheric environment from different directions. The magnitude of these differences depends on the elevation angle as azimuths. The GNSS signal is delayed in the atmosphere (Rohm et al., 2014).

The GNSS meteorology is based on the tropospheric delay, one of the results of GNSS data processing. The tropospheric delay received from GNSS data processing is represented by the ZTD (Bosy et al., 2012; Bosy et al., 2010).

Figure 2.5 shows the vertical profile of the atmosphere with different layers. The signal delay is mainly due to the two primary sources Ionosphere and the troposphere. However, the delay caused by the ionosphere can be eliminated by the linear combination of two frequencies, in case of delay caused by troposphere, has to be modelled (Szafranek et al., 2014).

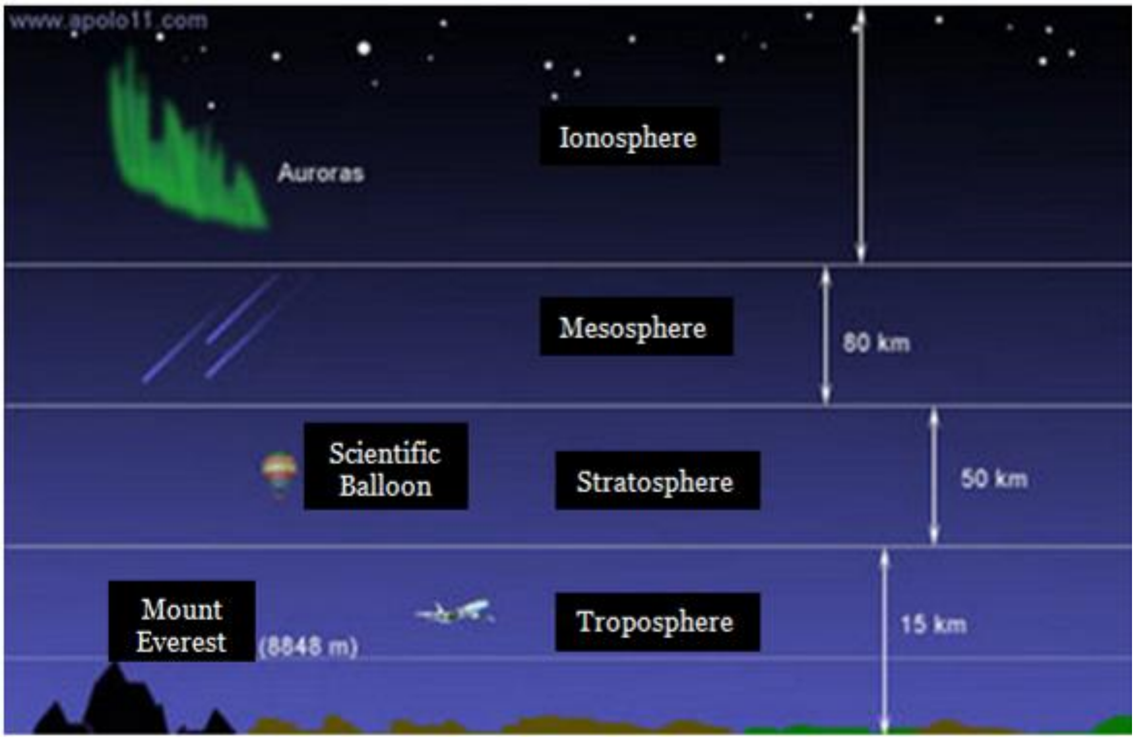

Figure 2.5 - Representation Layers of the Earth's atmosphere (Layers, 2021).

Figure 2.6 shows a Schematic of the satellite signal path through the atmosphere, zenith direction and elevation angle (a).

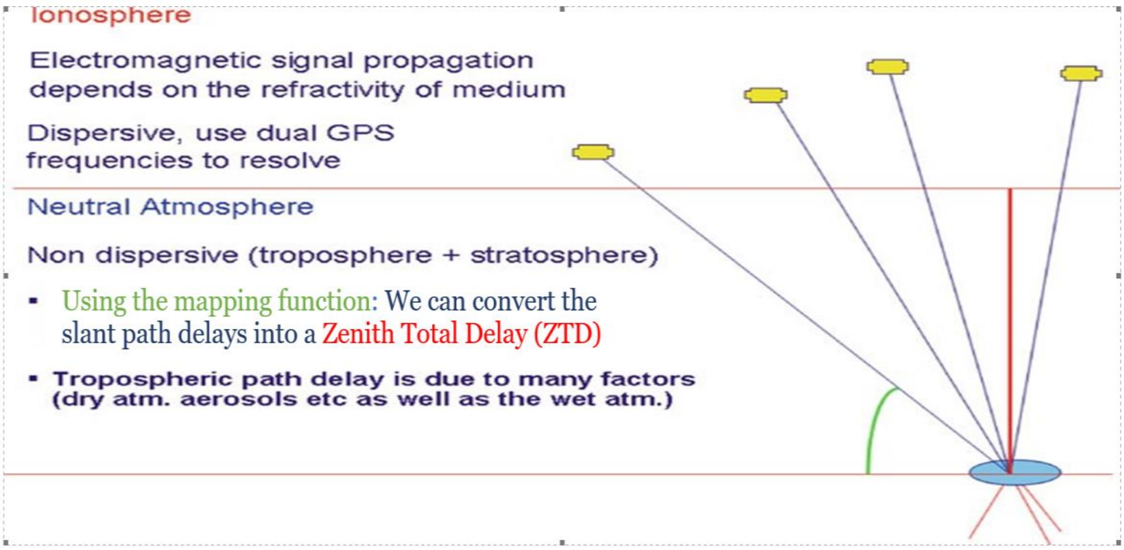

Figure 2.6 - Schematic of the satellite signal path through atmosphere Earth's atmosphere (adapted from Jones et al., 2020).

ZTD consists of delays caused by the passing of the signal through the wet part (known as Zenith Wet Delay, ZWD) and the dry part of the troposphere (known as Zenith Hydrostatic Delay, ZHD), in other words, can say it is the sum of the ZWD and ZHD. ZHD can be determined using surface meteorological data, and ZWD is not easy to calculate in the atmosphere due to time-varying water vapour content (Szafranek et al., 2014).

According to Bosy et al. (2012), The ZHD is determined based on the pressure and temperature. This parameter can be derived from deterministic atmosphere models or with station observed meteorological. ZWD is the foundation for the computing of PWV in the atmosphere, is computing by applying empirical equations (Bevis et al., 1992, 1994).

The GNSS meteorology has reached a point where there is a need to develop methods not only to compute PWV over the GPS receiver. But also, to investigate the PWV distribution in space and time (4DWVD) (Bosy et al., 2012; Vedel & Huang, 2004). GNSS tomography is one of the methods to resolve the spatial structure and temporal behaviour of the tropospheric water vapour. Tomography, in general, is a technique by which many line-of-sight integral observations in different directions and different locations are employed to derive 3D images of a PWV distribution.

Also, other techniques can be used to model the propagation of GNSS signals, such as ray-tracing (Petovello, 2016) and neural networks (Kanhere et al., 2022). According to Petovello (2016), ray-tracing methods are often employed to model the propagation of GPS signals in constrained environments. The neural network is the technique that is useful in improving GNSS Positioning (Kanhere et al., 2022; Munin et al., 2019). The main input of these techniques is the synthetic environment, virtual modelling of a realistic environment in terms of both geometry and physics, and the correction of errors generated by multipath signals reflected by the terrain that distort the direct signal transmitted by the satellite.

For Ha et al. (2005 in Won et al., 2010), GNSS uses empirical models in its processing to obtain more accurate data. Therefore, it is essential to use the most accurate models for the delay of the atmosphere to reduce errors (Boehm et al., 2006).

GNSS employs mapping functions to convert the tropospheric signal delay from the zenith direction to the line-of-sight direction (Won et al., 2010). There are different mapping functions in GNSS processing data such as Global Mapping Function (GMF), Vienna Mapping Function 1 (VMF 1) and Neill Mapping Function (NMF).

Neill (1996 in Won et al., 2010), NMF was the most widely used for years. The construction of the NWM was based only on radiosondes profiles from the Northern Hemisphere (Boehm et al., 2006). However, recently developed mapping functions were based on Numerical Weather Models (NWM) provided by the European Centre for Medium-range Weather Forecasts (ECMWF) to bridge the observed NMF difficulty (Boehm et al., 2006). Thus, the representative mapping functions based on NWM are the Vienna Mapping Function 1 (VMF1) and the Global Mapping Function (GMF).

According to Won et al. (2010), Some previously researched showed that Mapping functions VMF 1 and GMF also influence vertical position tropospheric estimates. Boehm et al. (2006), observed the height changes by testing NMF, GMF, and VMF1 in GNSS analysis and found that VMF1 and GMF are very good, but VMF1 is currently the mapping function the most accurate available. But recently, a refined version of VMF1, VMF3, was released. The results from VMF3 agree very well with the results from GMF and VMF1, although small biases can be found, especially for the height component (Putri et al., 2020).

2.3 GNSS Processing

2.3.1 Processing Methods

Two methods mainly used for processing GNSS data will be discussed in the subsection below: Double Difference (DD) (Hernández-Pajares et al., 2001), and Precise Point Positioning (PPP) (Gao, 2006; Zumberge et al., 1997).

2.3.1.1 Double Difference

The Double Difference technique processes GNSS data in a set of stations simultaneous. The idea is to form baselines between GNSS stations and thus eliminate clock errors (Couto, 2016). This technique results in a combination of two other methods:

✓ **Between-Receivers Single Difference:** For Sickle & Dutton (2014 in Couto, 2016) is a method where two GNSS receivers are synced to the same satellite. This technique can provide better positioning by subtracting each receiver observations equation since common error sources are cancelled when the difference is eliminated.

✓ **Between-Satellites Single Difference:** A method that consists of one receiver observing two satellites. However, here the code and/or phase from the satellite are subtracted to the other satellite. This technique eliminates the receiver clock error but does not provide a better position estimate Sickle & Dutton (2014 in Couto, 2016).

According to Couto (2016), when the two types of single differences are combined, it is possible to highlight the best of both. In this case, Between-Receivers single difference, it is possible to have improved position estimates while Between-satellites single Difference, it is possible to eliminate the clock error (see Figure 2.7).

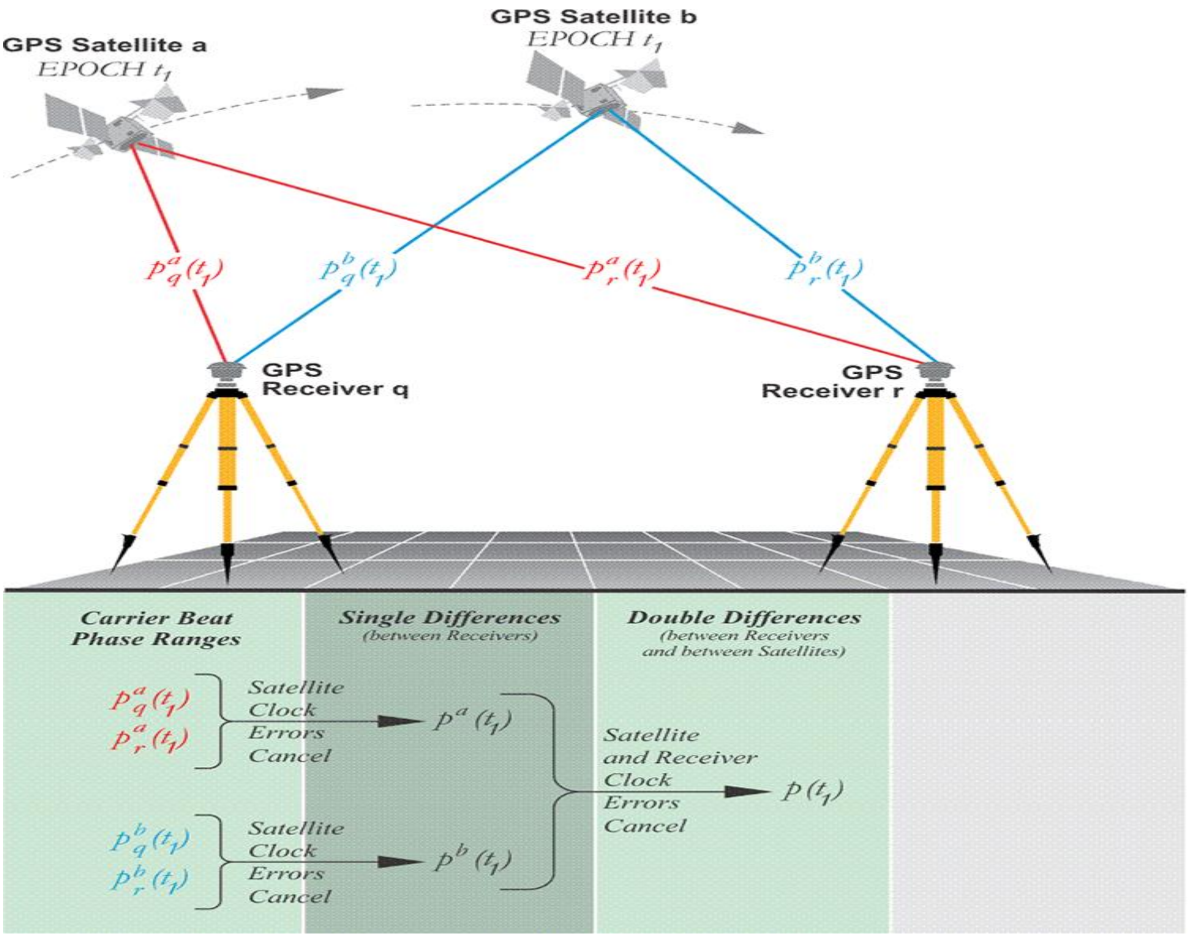

Figure 2.7 - Schematic representation of the Double Difference (Sickle & Dutton, 2021).

2.3.1.2 Precise Point Positioning

According to Gao (2006), the technique for performing precise position determination using a single GNSS receiver is known as Precise Point Positioning (PPP). This technique is dependent on accurate products of GNSS orbit and clock data, with an accuracy of a centimetre. This data can be applied to dramatically reduce errors in the orbits and clocks of GNSS satellites. Those are two of the most frequent sources of error in GNSS positioning.

For dual-frequency GNSS receiver is combined, with satellite clocks and precise positions, PPP can provide highly accurate solutions with centimetre accuracy. That fact might be enticing to many applications. While double-difference positioning requires observations from at least one base station, PPP does not require such observations. PPP differs from the conventional point positioning method due to the precise part. The other ones only use code or phase-smoothed code as the principal observable to estimate the position (Gao, 2006).

According to Gao (2006), There are several significant advantages the PPP technique can provide compared to differential precise positioning method:

1. PPP involves only one GNSS receiver mean that is not necessarily establishing a base station for GNSS users. As a result, it removes the constraint of simultaneous observations as well on both rover and base receivers imposed by the differential RTK technique;

2. PPP technique in its positioning approach can be considered global because, its positioning solutions are referred, to as a global reference frame. As a result, it provides better positioning consistency than the differential approach. This fact is because the positioning solutions the differential approach are relative to the local base station or stations;
3. Equipment cost and Labor are reduced with PPP than differential approach since it removes the dependency on the base station(s);
4. Beyond its global position, PPP can also be applied to support other applications. Since PPP needs to estimate receiver clock and tropospheric effect parameters, this fact, provides a new way for precise time transfer and water vapour estimation using a single GNSS receiver.

Despite its vast advantage, the PPP method may also have some limitations. One of its limitations is based on the accurate estimation of the transmitter's clock because if a clock error is observed, it will influence the solutions with centimetre accuracy (Zumberge et al., 1997).

2.3.2 Offline Processing Software

There are different offline GNSS data processing programs, some are free, and others are commercial (Couto, 2016). In this dissertation, five offline services were listed (see Table 2.2), although this work will not use offline processing software.

Table 2.2 - Different types of offline software for processing GNSS data (Adapted from Couto, 2016).

Software	Distribution	License Details
RTKLib	Open-Source	BSD 2-clause license
GPSTK	Open-Source	GNU LGPL
BERNESE	Commercial	-
GAMIT/GLOBK	Commercial with Free License for Universities or personal uses	-
GIPSY-OASIS	Commercial with Free License for Universities or personal uses	-

2.3.3 Online Processing Software

Online GPS data processing services have been gaining more users. This fact is due to its simplicity of use and because it is a more accessible processing technique for people with low financial resources or specific knowledge. What characterizes this type of service is its precise calculation (Centimeter level) in a global reference frame, without requiring specifying a set of reference stations. Currently, there are free online services and commercial (Couto, 2016).

In this work, four online services were chosen (see Table 2.3), but only one will be discussed (NASA/JPL - USA).

Table 2.3 - Different types of software online for processing GNSS data (Adapted from Ulukavak, 2019).

Software	Organization
magicGNSS	GMV Aerospace and Defense S.A.U.
GAPS	University of New Brunswick (UNB)
CSRS-PPP	Natural Resource Canada (NRC)
GDGPS-APPS	NASA/JPL - USA

2.3.3.1 Jet Propulsion Laboratory – Global Differential GPS

The Jet Propulsion Laboratory (JPL) was established in the United States of America to research orbit, space and Earth sciences is a federally funded research and development center managed for NASA by Caltech (Nas, 2021). One of the largest terrestrial networks of real-time reference receivers is employed by JPL, with innovative network architecture and real-time data processing software (JPL, 2021).

The GDGPS – APPS (Global Differential GPS - Automatic Precise Positioning Service) is a system that also users real-time, daily and weekly GNSS orbit and clock products produced by JPL (Ulukavak, 2019). The GDGPS service provided by JPL utilizes the GIPSY–OASIS software. Thus, It can also determine for static and kinematic (including high-speed) observation (Couto, 2016). For its use, a web platform is available at https://pppx.gdgps.net/submitx, and currently, the GDGPS-APPS system supports such RINEX 2, RINEX 2.11 and RINEX 3 and GIPSY TDP files (NASa, 2021).

2.4 Satellite Orbits

Section 2.2 discusses the GPS, which consists of satellites distributed in orbits. With this, one can conclude that satellite orbits are one of the most fundamental components for each GNSS based processing. NASA's Jet Propulsion Lab (JPL) and International GNSS Services (IGS) are the two orbital observation providers mainly used. Usually, there are three types of products: Final, Rapid and Ultra-Rapid (NASb, 2021).

- ✓ **Final -** They have an accuracy of 2,5cm and are available after 14 days.
- ✓ **Rapid -** They have an accuracy of 3,5cm and are available after 1 day.
- ✓ **Ultra-Rapid -** IGS also provides the Ultra-Rapid orbit (IGS, 2021). But in this section, only the JPL Ultra-Rapid orbit will be discussed. The JPL Ultra-Rapid products have as based on observations. They contain a 30-hour window with an accuracy of 5cm. Since these are observations, they present a delay in this case of 2 hours and are updated every hour (NASb, 2021).

There are other types of orbits for which GPS data collection is possible, for example, NRC (see Cai, 2009). This dissertation is limited in discussing the most used orbits.

2.5 Meteorological Parameter Pressure and Temperature

The meteorological data (mostly temperature and pressure) is necessary for the PWV compute, and the accuracy of this data is of high fundamental. Thus, the meteorological data used for the computing must be corresponding to the location of GNSS stations to eliminate the uncertainties related to the spatial distance between meteorological stations and GNSS stations (Szafranek et al., 2014).

The ideal would be the GPS stations fitted with high precision Temperature and Pressure sensors. As our GNSS data providers did not have their stations fitted with these kinds of sensors, SUGGEST-AFRICA collocated five of the stations of weather stations to obtain the pressure and temperature. When there are no meteorological stations nearby, it is advised to use the values from global/regional models.

There are different models to acquire these meteorological parameters. Although, it was not chosen a standard model to download these meteorological data. The ideal is to research a model with good temporal resolution since the GNSS has a temporal resolution (less than an hour, down to 5 min). Table 2.4 illustrates five different global models with their respective resolutions and temporal availability.

Table 2.4 - Different types of global models for acquiring meteorological parameters.

Dataset	Spatial Resolution	Temporal Resolution	Temporal Availability	Web Pages (March 2021)
NCEP/NCAR Reanalysis	209 km	6-hourly	1948-01-01 to current	https://rda.ucar.edu/datasets/ds090.0/ (NOAA, 2021)
ECMWF Operational Model Reanalysis	0.08 degrees	6-hourly	2016-01-01 to current	https://rda.ucar.edu/datasets/ds113.1/ (ECMWF, 2021)
ERA-Interim	1.125 to 0.703 degrees	6-hr (analysis) 1-hr (forecast)	1979-01-01 to current	https://rda.ucar.edu/datasets/ds627.0/ (ERA-Interimim, 2021)
ERA5 Reanalysis	31 km	1-hourly	1979-01-01 to current	https://cds.climate.copernicus.eu/cdsapp#!/dataset/reanalysis-era5-single-levels?tab=overview (Hersbach et al., 2021)
MERRA-2	0.5 degrees	1-hourly 3-hourly 6-hourly	1981-01-01 to current	https://gmao.gsfc.nasa.gov/pubs/docs/Bosilovich785.pdf (Bosilovich et al., 2016)

2.6 Water Vapour by Other Techniques

There are several techniques. But only traditional methods have been chosen for discussions, such as radiosondes (RS) and microwave radiometer (MWR) (He et al., 2020; Yao et al., 2017; Zhao et al., 2018). Water vapour information has mainly been obtained by using these techniques for many years (Zhao et al., 2019).

2.6.1 Radiosondes

This observation is usually performed with the release of a helium gas balloon in the high atmosphere, allowing the measurement of meteorological parameters (Elhaty et al., 2019). These observations can obtain high accuracy and high vertical resolution, and their observation covers the range from the earth's surface to an altitude of 30 km. RS stations provide two to four times observations per day (Zhang et al., 2018). According to Abbasy et al., (2017); Elhaty et al., (2019); Zhang et al., (2018), RS observations can provide pressure, relative humidity, temperature, dew point, geo-potential height, wind direction, and wind speed.

The information obtained can be seen in real-time or on a computer. The data obtained is used to (IPM, 2021):

- ✓ Initialization of the numerical weather prediction models;
- ✓ Local/regional prediction of the stability of the atmosphere and the distribution of water vapour;
- ✓ Studies about atmospheric pollution;
- ✓ Ballistic Precision and reach, by calculating the density of the air for a given pressure;
- ✓ Prediction of the effects of atmospheric refraction on the propagation of electromagnetic radiation or sound waves;
- ✓ Climate studies.

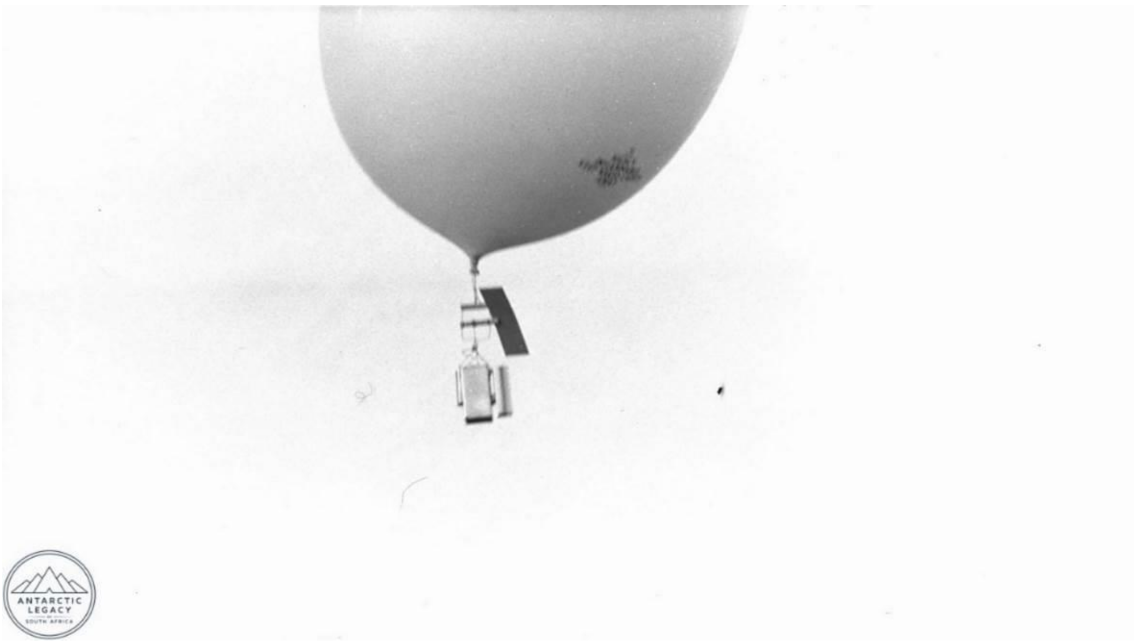

Figure 2.8 - Weather balloon carrying a RS (ALSA, 2021).

2.6.2 Microwave Radiometer

MWR provides time-series measurements of water vapour and liquid water (MWRa, 2021). The instrument itself detects emission from water vapour (five frequencies in the 22–30-GHz domain) and molecular oxygen (seven frequencies in the 51–59-GHz). It is a commercially available 12-channel (20 to 60 GHz) WP3000 system from Radiometric. The 22–30-GHz channels are regulated by automated tipping and are specified at 0.5 K. The 51–59-GHz channels are calibrated using a liquid nitrogen target with a specified accuracy of 0.5 K. The MWR provides profiles of temperature and humidity up to 10 km, PWV and liquid water (Baelen et al., 2005). The instrument provides invaluable real-time upper air information. The data obtained is used to (MWRb, 2021):

- ✓ Studies regarding air quality;
- ✓ Predicting Lightning;
- ✓ High-Impact local weather alerts
- ✓ Studies regarding improving local nowcasting;
- ✓ Fog prediction;
- ✓ Characteristics of snowpack;
- ✓ Study of the vegetation and soil moisture.

Figure 2.9 - MWR profiles (MWRc, 2021).

RS provide accurate measurement of the water vapour, but its temporal and spatial resolution is low. MWR provide a high temporal resolution of water vapour but low spatial resolution. Besides these limitations, these techniques involve high costs (Joshi et al., 2013). However, Comparing the traditional techniques with the GNSS solutions, GNSS solutions can provide information in all-weather conditions, is do not expensive and have High Spatial-temporal resolution (Abbasy et al., 2017; He et al., 2020; Jin & Luo, 2009; Joshi et al., 2013; Zhao et al., 2019).

2.7 GNSS, PWV in Geographical Information Systems

2.7.1 GIS

Geographic information systems (GIS) is employed in many subject areas (Pinto, 2009; Taha, 2008). According to Sadoun & Al-Bayari (2006), the GIS tool allows the processing of spatial data into information. According to Lange & Gilbert (2005), The interest in the GIS tool has been used by the development of several enabling technologies, one of the more important of which is the GNSS. GPS has contributed effectively to the growth of GIS worldwide due to its capability and efficiency in collecting, organizing, managing, updating, operating and presenting spatial data cost-effectively and in a speedy manner. The combination between GPS receivers and GIS tools gives more facilities for data collection and instantaneous map updating (Sadoun & Al-Bayari, 2006). One fundamental factor in the combination of GIS and GPS application is working in the same coordinate system or datum. Working in different coordinate systems creates data mismatching in GIS/GPS applications (Sadoun & Al-Bayari, 2006, 2007).

While GIS offers tremendous capabilities for decision making, rendering competent decisions still depends on having reliable data. To realize the benefits of GNSS and not misapply the technology, it is fundamental to understand its limitations (Lange & Gilbert, 2005).

The applications of GPS/GIS are evolving rapidly but, present some limitations such as (Sadoun & Al-Bayari, 2007):

- ✓ GIS data and maps should be periodically updated;
- ✓ There should be Standards to control the quality of the GIS data;
- ✓ The transformation between GNSS reference systems such as World Geodetic System, 1984 (WGS-84) and the local coordinate systems should be well known for those working in GIS data collection;
- ✓ Standards for developing GPS/GIS solutions are do not been discussed yet.

2.7.2 GIS Data Capture Considerations

According to Kaplan & Hegarty (2006), with GNSS, it is possible to capture position-referenced data in the field with a simple handheld computer. Every GIS database must be referenced to a base map very accurately, and the reference datum of the various data layers must be the same (Lange & Gilbert, 2005). According to Weibel & Dutton (1999), They considered as an example a set of four maps of the same locality, drawn at the scale 1:1000, 1:25 000, 1:100 000, and 1:250 000. They presented the analysis of the different scales using as a study area the dwellings of a determinate settlement. They concluded that the 1:250 000 scale map showed only block aggregations, tinting entire cities as one polygonal feature and transforming smaller towns into point symbols. They also concluded that at a smaller scale (i.e., 1:550 000), all settlements might be viewed as point symbols.

2.7.3 World Geodetic and Local Coordinates System

The Coordinate System is a method that has a base set of points marked on the Earth's surface, which allows to geographically locate any point on Earth. The geometric location of any point in the world can be defined by a triplet of coordinates, where your representation uses different conventions: Cartesian (X, Y, Z); Planimetric (East, North); Geodetic (Latitude, Longitude, Ellipsoidal Height) +Vertical (Couto, 2016).

Understanding the concept of a map datum is fundamental if useful results are to be acquired from any GNSS mapping exercise. Since GNSS is a worldwide system, so has a datum applicable over the whole earth. However, GNSS uses WGS-84 for GIS data capture. There are several local datums like European Datum 1950 (ED-50), North America Datum 1927 (NAD-27), and North America Datum 1983 (NAD-83) (Lange & Gilbert, 2005). In the Angola case, use Camacupa / UTM zone 33S (IOGP, 2021; Kitoko & Painho, 2015), which have been used to make local maps. Two elements make up the surface component: latitude (Varying between -90º and +90º, where your measurements are positive in the northern hemisphere and negative in the southern hemisphere) and longitude (Varying between -180º and +180º, where your measurements are positive to East of the prime meridian and negative to West of the prime meridian) (Couto, 2016).

All data should be collected and displayed in the most up-to-date datum available for the GIS tool. It is fundamental to use the same datum for all data layers if the data are will to be overlaying in a GIS (Lange & Gilbert, 2005).

2.7.4 Using GNSS and PWV with GIS

There are several ways in which GNSS to use alongside GIS (Ferrando et al., 2018; Lange & Gilbert, 2005). This dissertation will be choosing some of those ways for the uses alongside GIS:

- ✓ The use of GNSS may be to identify or refine the geographical coordinates associated with satellite imagery;
- ✓ The use of GNSS can be in the ground-truthing of satellite images;
- ✓ GNSS has developed into a cost-effective tool for updating GIS (Lange & Gilbert, 2005).
- ✓ Comparison between different methods for Spatial Interpolation of the GNSS ZWD, ZTD and ZHD (Benvenuto et al., 2018; Ferrando et al., 2018; Lo & El-mowafy, 2011).
- ✓ The introduction of a simplified mathematical model including different methods for Spatial Interpolation data, to describe the atmospheric Pressure and Temperature behaviour and improve the interpolation of Pressure and Temperature data;
- ✓ The ability to produce high-resolution 2D PWV maps, even from few input data;
- ✓ localize severe meteorological and climatologist events in time and space (Benvenuto et al., 2018; Ferrando et al., 2018).
- ✓ Time-series maps to investigate the PWV variation and its implication for the climate (Benvenuto et al., 2018; Ferrando et al., 2018; Liu et al., 2019).

2.7.5 Input GNSS, Pressure and Temperature Data to GIS

The final step of this process of GNSS-based data collection for GIS is to export the data from the field device to the target database (Lange & Gilbert, 2005). The Export (e.g., ZTD, ZWD, ZHD, Pressure and Temperature) data in a GIS environment is the most often carried out by running a translation program (Lange & Gilbert, 2005) see in Benvenuto et al. (2018). But this task can be accomplished more easily by putting the coordinates and attributes in a comma-delimited file (e.g., Excel) (Lange & Gilbert, 2005), joining related tabulated information to the shapefiles.

However, with these data loaded into the GIS environment applying the equations proposed by Bevis et al. (1992), it is possible to produce PWV maps (Ferrando et al., 2018).

2.7.6 Applications and case studies

There are several applications and case studies that use GNSS-PWV with GIS. This work will be to choose some of those applications and case studies using the GIS tool.

Liu et al. (2019) adapted the GIS tool to present A New Method for Refining the GNSS-Derived PWV Map new interpolation in Hong Kong (China). This method is called the LZ method (the LZ method consists of densifying the sample points by providing virtual sample points). The algorithm developed to produce the refined PWV maps derived from GNSS was implemented the DTM for the studies of the influence of height on the amount of PWV. However, Figures 2.10 and 2.11 illustrate the Algorithm developed to produce the refined PWV maps derived from GNSS.

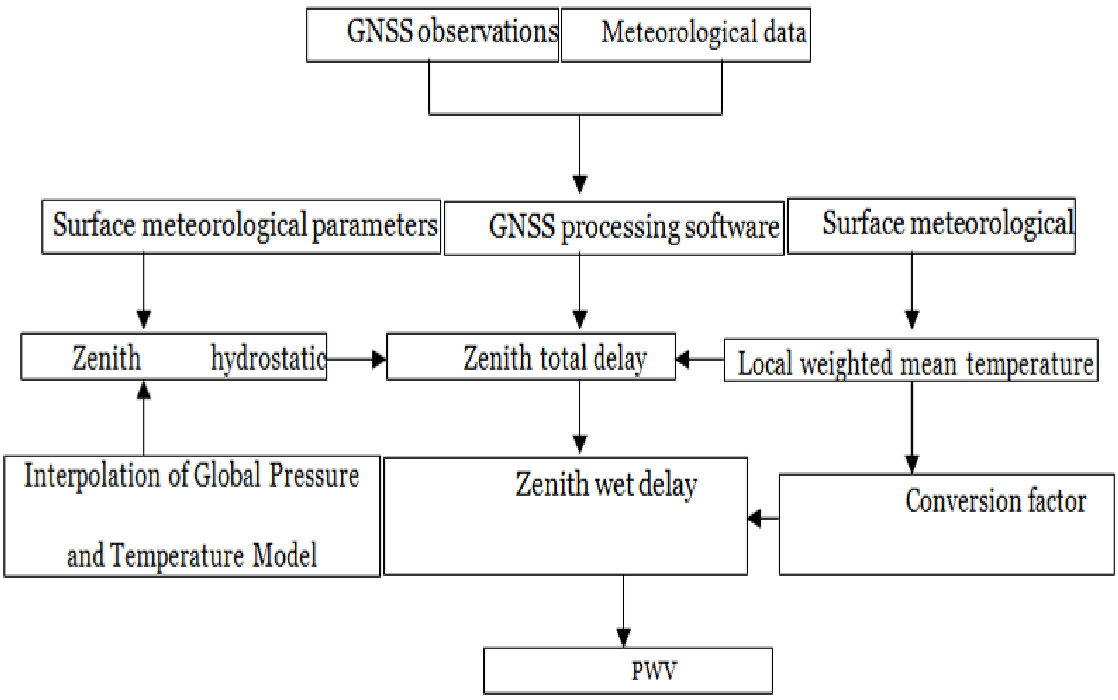

Figure 2.10 - Procedure for obtaining GNSS-derived PWV (Liu et al., 2019).

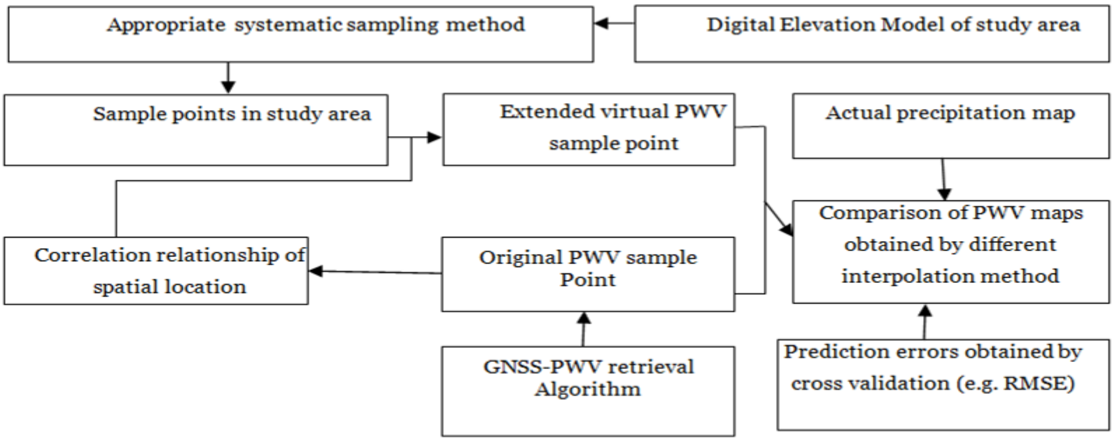

Figure 2.11 - Scheme for the comparison of the interpolation performances of the new method (based on extended virtual PWV sample points) and conventional one (based on original PWV sample points) (Liu et al., 2019).

However, for the result (see Figure 2.12). Liu et al. (2019) used a geostatistical approach.

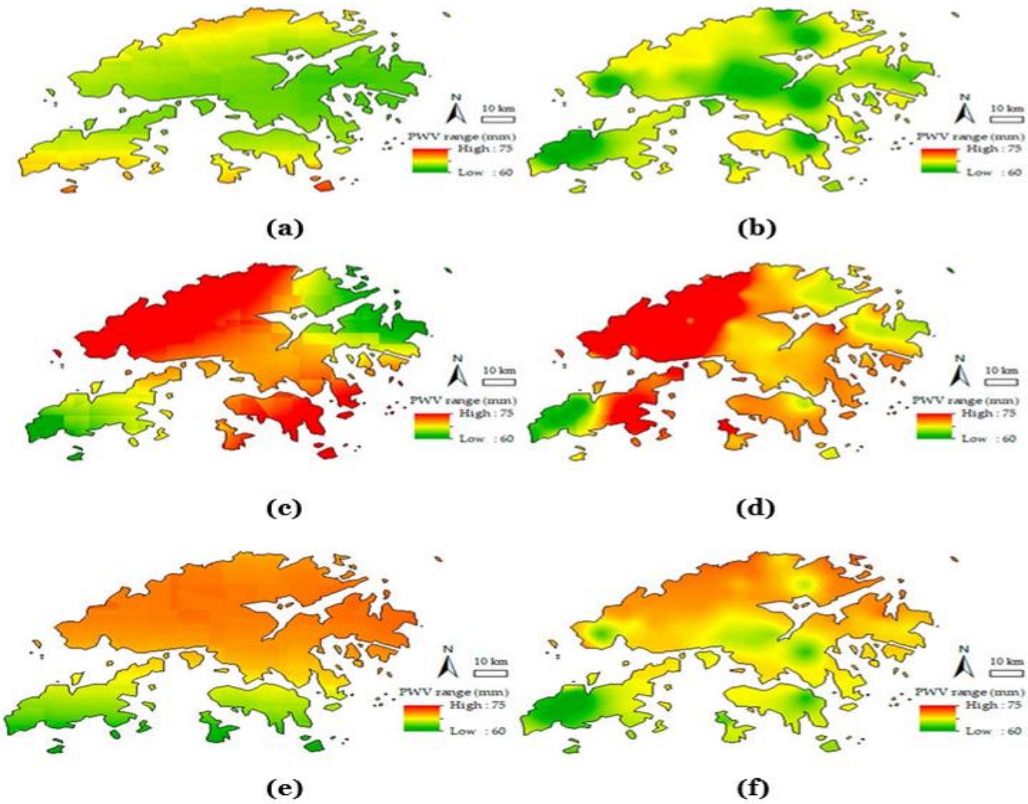

Figure 2.12 - Co-Kriging interpolation results for PWV provided by Schemes I and II. Graphs (a, c), and (e) is generated by Scheme I, while graphs (b, d), and (f) are generated by Scheme II (Liu et al., 2019).

That, among the techniques of the geostatistical, they used the kriging technique. According to (Liu et al., 2019), the Kriging technique is a geostatistical approach that generates a continuous surface that does not pass through all sample points.

Ferrando et al. (2018) developed studies to localize severe weather events in Genoa (Italy). Thanks to GIS, an intense rainfall indicator called the heterogeneity index (HI) was calculated. This index is responsible for determining where the severe weather event will occur. Therefore, this technique has been called an innovative G4M (GNSS for meteorology) procedure. The innovative G4M procedure can monitor the PWV content of a large and orographically complex area by analysing not necessarily located GNSS and meteorological parameter (Pressure and Temperature) observations. However, Figure 2.13 illustrate the Algorithm developed to produce G4M.

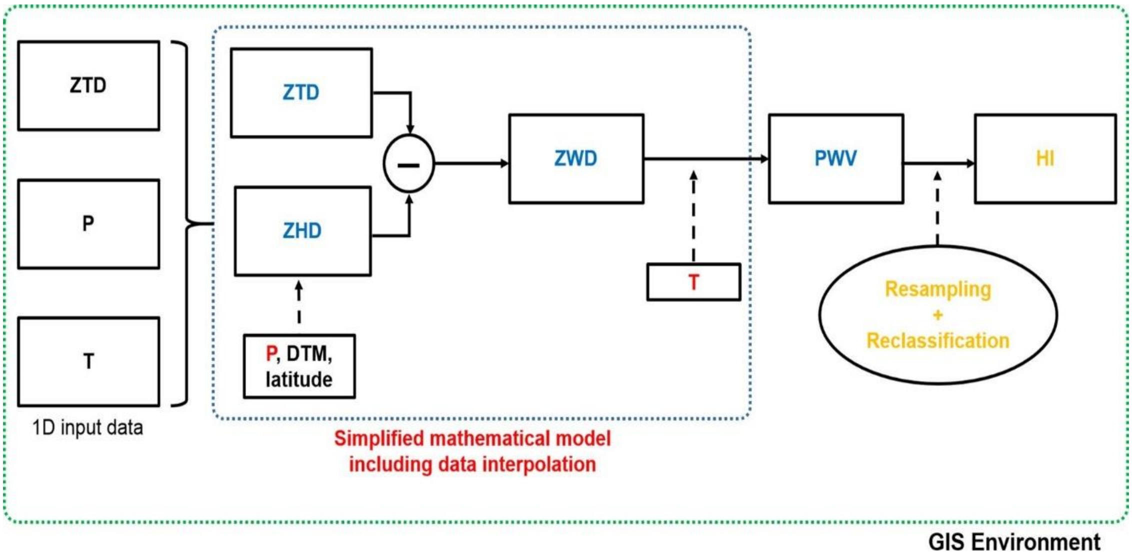

Figure 2.13 - Flow chart of the G4M procedure (Ferrando et al., 2018).

Figure 2.14 shows the result of the case study in Genoa, where the red circle reports the time of the most elevated HI values (Ferrando et al., 2018).

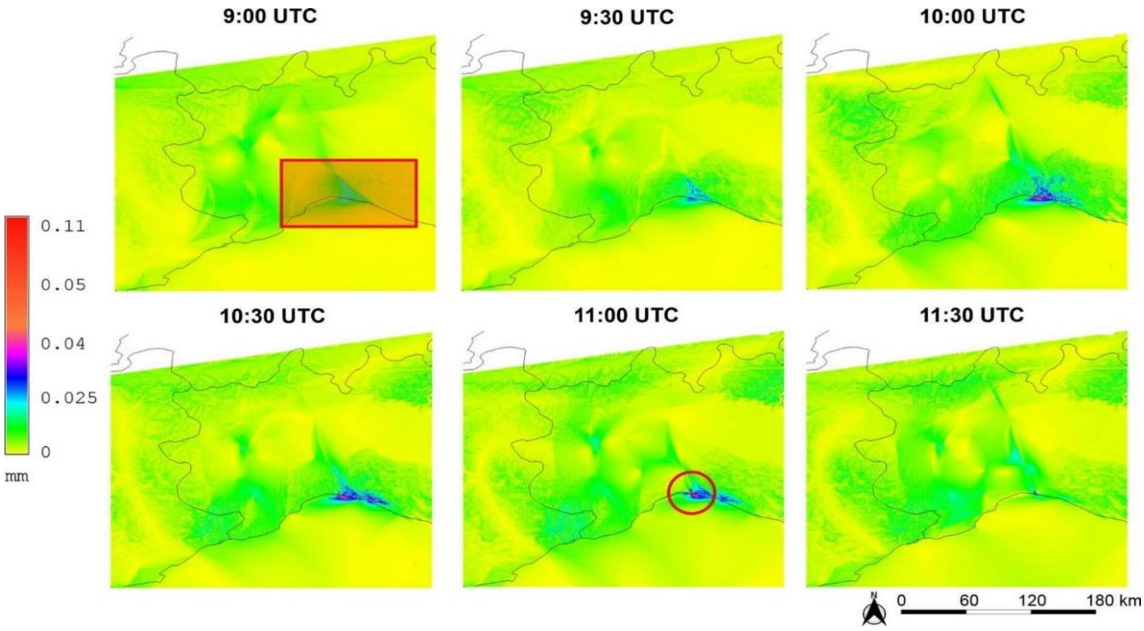

Figure 2.14 - 30-minute extraction from the 6-min HI maps for the severe event on November 4, 2011 (Ferrando et al., 2018).

Chapter 3

Study Area Characterization

3.1 Geographic Location and Extension

The geographical area selected for carrying out the analyses is Angolan territory. Angola is the country located on the Southwest coast of Africa, between latitude 4° 22' and 18° 02' South and longitude 11° 41' and 24° 05' East (Azevedo, 2005; Huntley et al., 2019). The map of the study area location will be seen in Figure 3.1.

Boundaries (Azevedo, 2005; CLOG6, 2021; Huntley et al., 2019): North: Republic of the Congo and the Democratic Republic of the Congo (DRC); South: Namibia; East: Zambia; West: Atlantic Ocean.

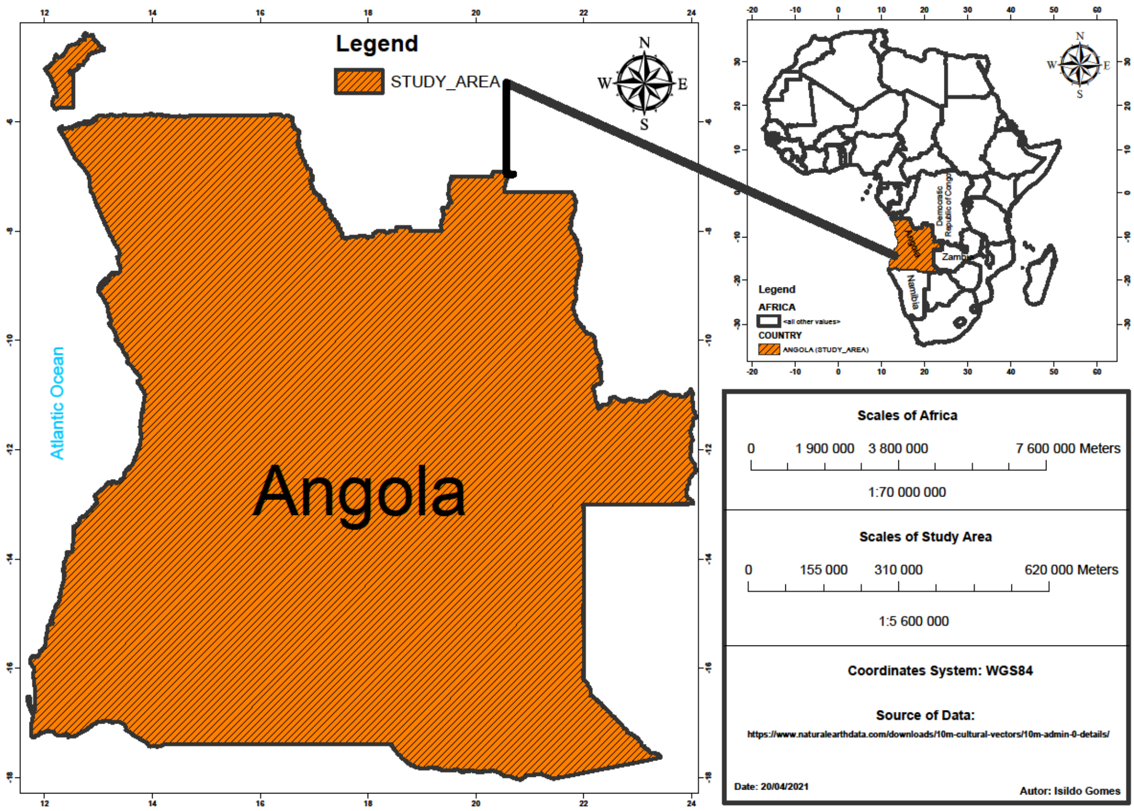

Figure 3.1 - The map of the location of the study area.

3.1.1 Delimitation of the Study Area and Population

The study area selected to carry out the analyses is composed of 18 provinces which are: Cabinda, Zaire, Uige, Malanje, Lunda Norte, Lunda Sul, Cuanza Norte, Bengo, Luanda (Capital), Cuanza Sul, Benguela, Huambo, Bie, Moxico, Namibe, Huila, Cunene, Cuando Cubango see, Figure 3.2.

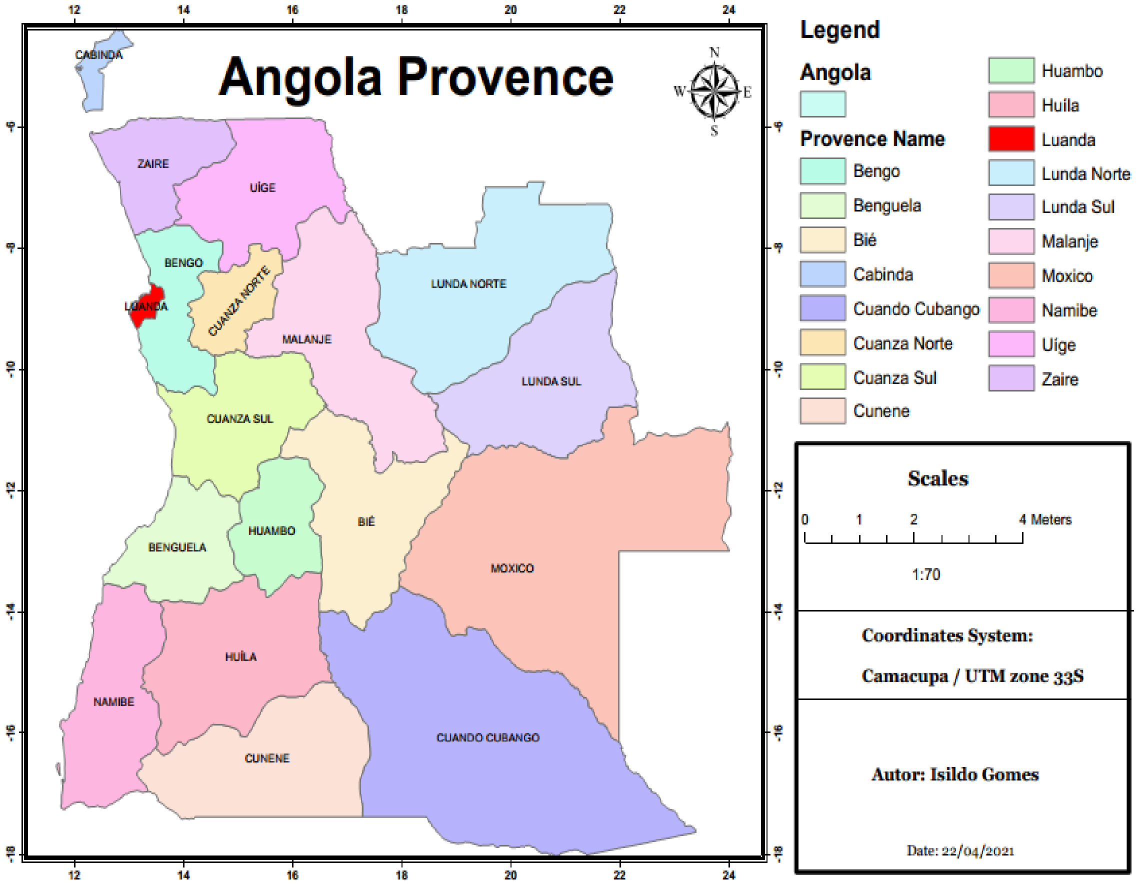

Figure 3.2 - The map of the provinces of the study area.

The selected study area has approximately 25,789,024 inhabitants. According to (INE, 2014), the geographical distribution of the population, seven provinces are the most populous, and six provinces are the least.

With these results comes the importance of water vapour analysis using GNSS observations. Since analysis based on this type of technique will help to predict, identify and monitor extreme events. Since the GNSS observations method provides good temporal resolution (less than one hour, down to 5 minutes). In this way, we can avoid the loss of life, especially of young people who are the driving force of a country.

3.2 Climatological Characterization of the Study Area

The climate of Angola presents variability in the north-south direction and with the proximity to the coast (Azevedo, 2005; Jesus, 2018; Xavier, 2013). Climate is tempered by altitude on the plateau in the interior regions and by a cold current along the coast (Azevedo, 2005; Climat, 2021). Angola has two seasons: a dry (cold) season (called Cacimbo) and a hot (rainy) season (Climat, 2021; Xavier, 2013). Generally speaking, the dry season starts in May and lasts until mid-September, while the rainy season begins in mid-September and lasts until April or May (Azevedo, 2005; Climat, 2021; Xavier, 2013).

3.2.1 Precipitation

In the northernmost part of the study area and the northern exclave of Cabinda (see Figure 3.3), the climate is tropical (Climat, 2021).

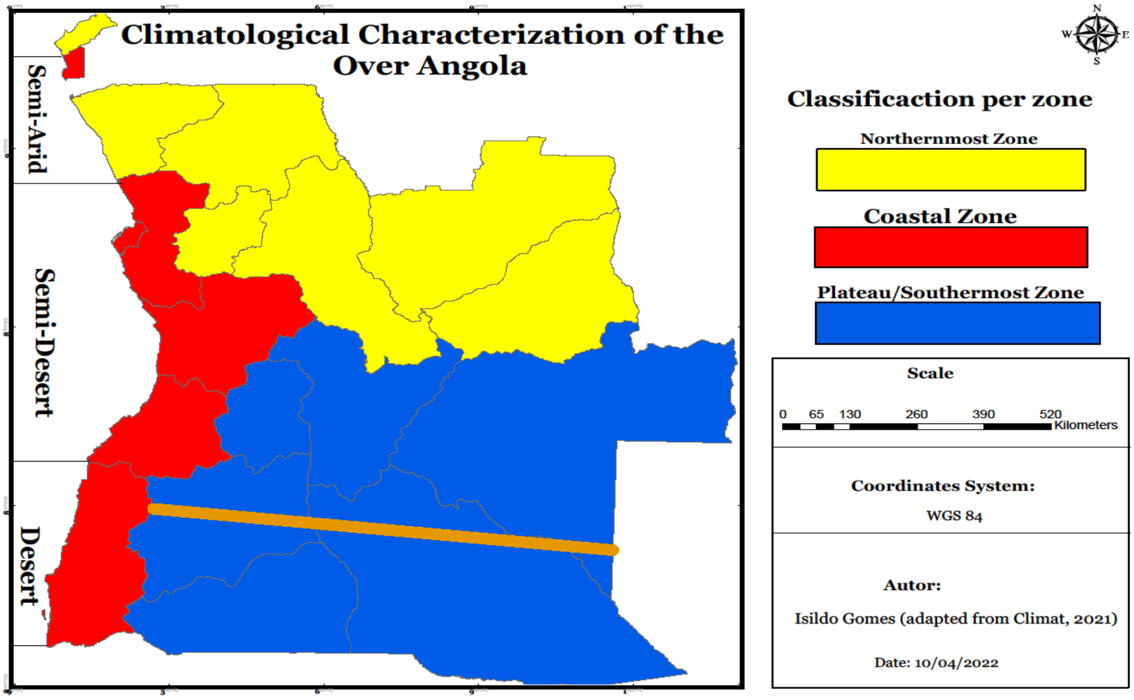

Figure 3.3 - Map showing the climatological characterization of the over Angola (Adapted from Climat, 2021).

With a rainy season from mid-September to mid-May (see Uige, Malanje, Dundo and Saurimo Figure 3.4) (Climat, 2021). Rainfall exceeds 1,200 mm per year in most parts of the area (see Fig. 3.5) (Azevedo, 2005; Climat, 2021).

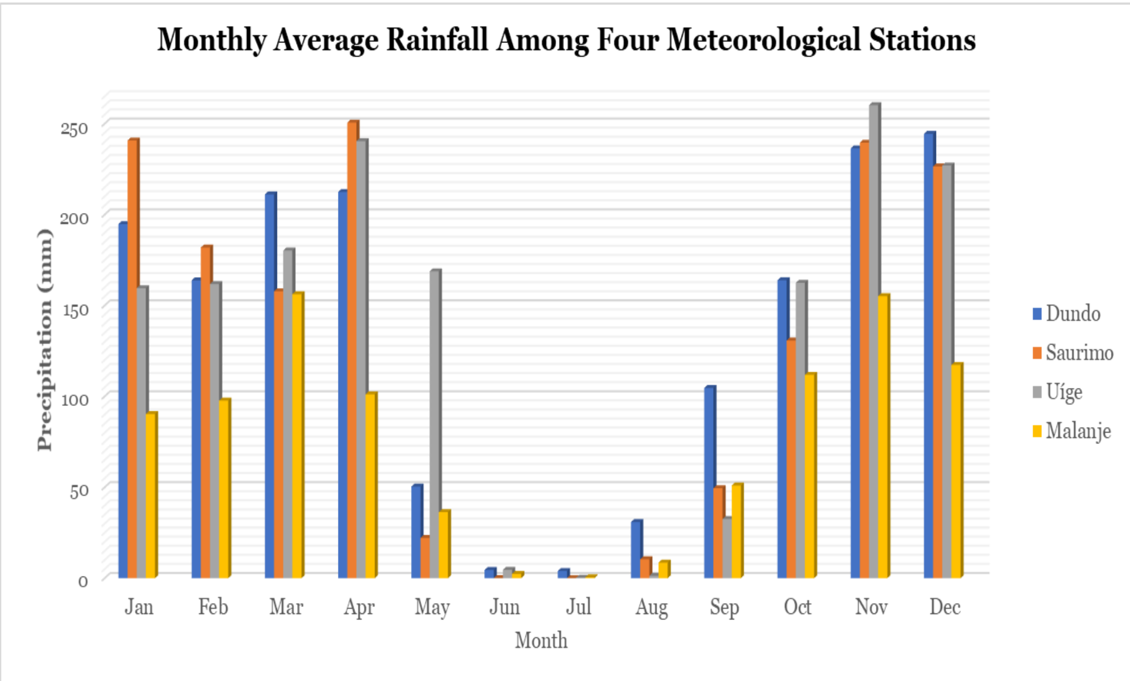

Figure 3.4 - The monthly average rainfall in Dundo, Saurimo, Uige and Malanje (1981-2010) (National Institute of Meteorology and Geophysics (INAMET)[1]).

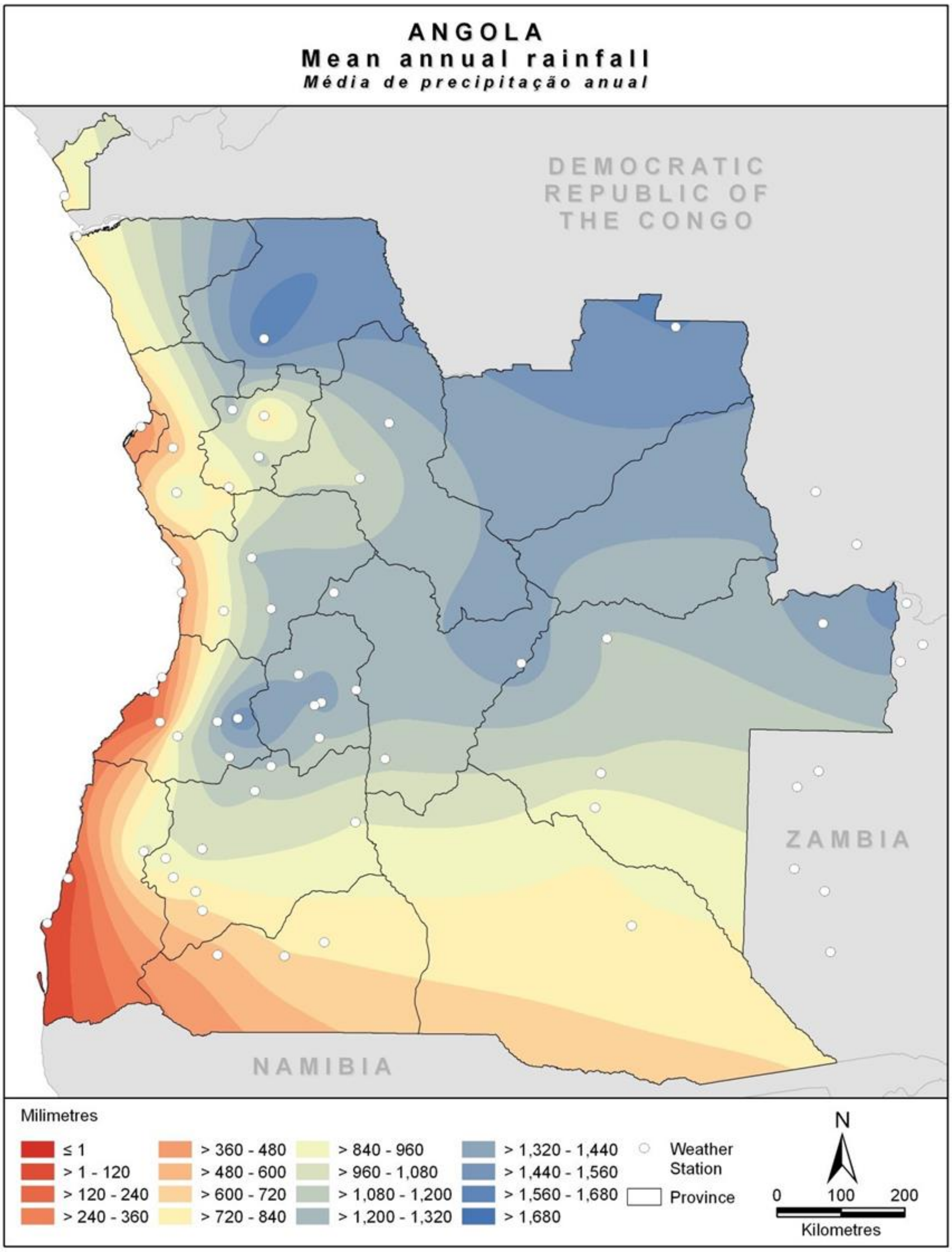

Figure 3.5 - Map of the mean annual rainfall in Angola (Dw, 2014).

In the coastal zone, including the southern part of Cabinda province, the climate is semi-arid in the north, semi-desert in the central area and desert in the southern part (though mild) (see Figure 3.3 or Climat, 2021). In the northern part rainfall, is more than 500 mm per year. In the southern part of the coast, the rains are rare, as they fall below or equal to 50 mm per year (See Figure 3.5 or Azevedo, 2005; Climat, 2021; Xavier, 2013).

With a rainy season from October to April/mid-May (see Luanda, Cabinda, Benguela and Namibe Figure 3.6 or Climat, 2021).

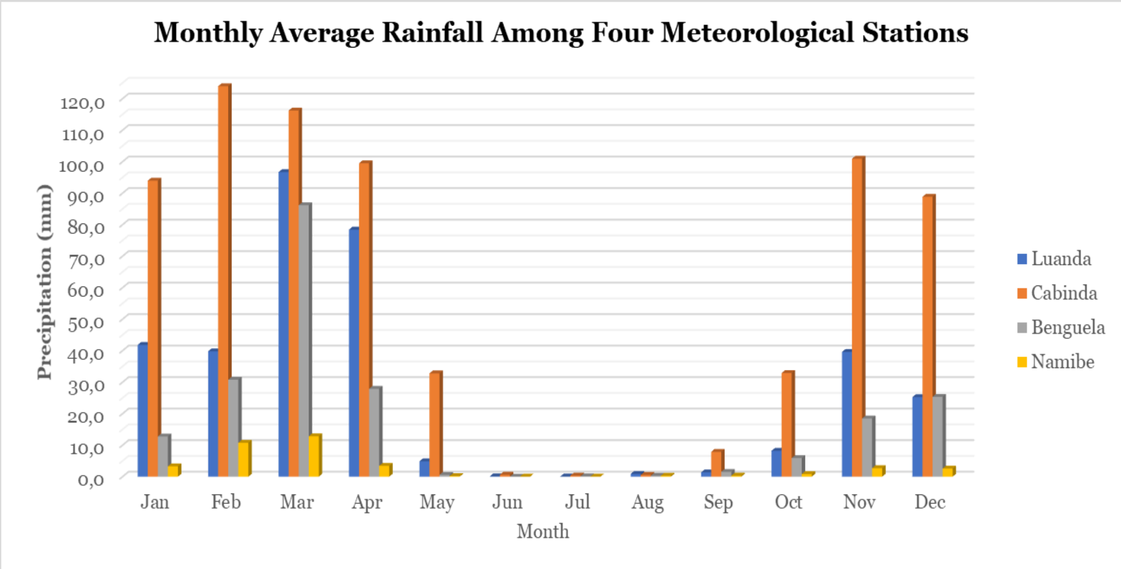

Figure 3.6 - The monthly average rainfall in Luanda, Cabinda, Benguela and Namibe (1981-2010) (INAMET).

In the interior plateau, in the Bie Plateau zone, climate is close to tropical. While in the lower plateau regions in the east of the country, a subtropical climate with hot summers predominates (Jesus, 2018). Rainfall generally varies between 1,200 and 1,600 mm per year in the north-central region (above the orange line on the map, see Figs. 3.5 and 3.3) (Climat, 2021), while it falls below 1,000 mm in the south (Climat, 2021; Xavier, 2013).

The rainy season is from October to April in the north-central (see Huambo and Luena Fig. 3.7), and December to March in the south (see Lubango Figure 3.7) (Azevedo, 2005; Climat, 2021; Xavier, 2013).

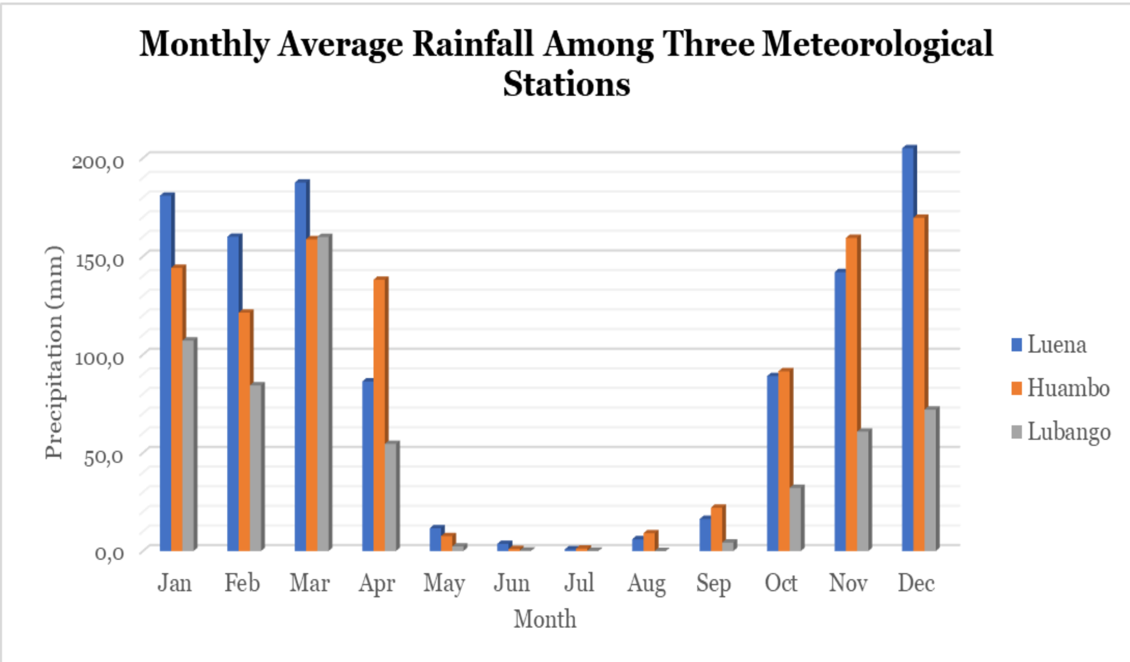

Figure 3.7 - The monthly average rainfall in Luena, Huambo and Lubango (1981-2010) (INAMET).

However, what was discussed above regarding precipitation can also be concluded that the different zones discussed present different months rainier. Thus, in a general way, the months are:

November, December, March and April for the northernmost zone (see Figure 3.4);

February, March and April for the coastal area (see Figure 3.6);

For part of the plateau. November, December, and March (see Figure 3.7).

---

[1]INAMET is a Public Institute of Angola, responsible for the research and provision of scientific services in meteorology and geophysics. Its purpose is to coordinate operational and applied research activities in the respective fields (INAMET).

3.2.2 Temperature

Using temperature, it's also possible to identify the previously referenced zones (northernmost, coast and plateau). Thus, in the northernmost zone, the average temperature registers 21/22 degrees in the dry season, from June to August. While in the hot season, it registers around 25/26 degrees, from October to May (Climat, 2021). The average temperature generally varies between 23/25 degrees per year (see Figure 3.10).

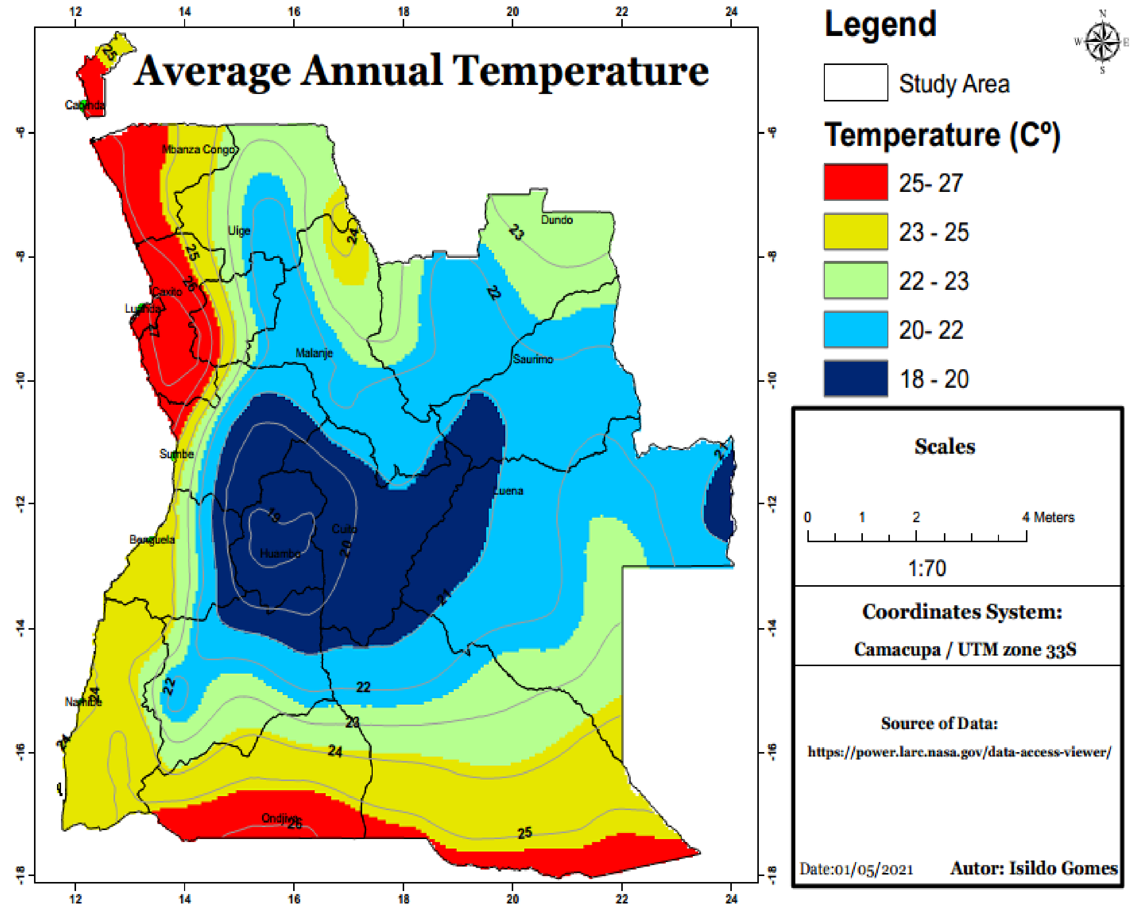

Figure 3.8 - Map of the Average annual temperature in Angola.

In this case, the Mbanza Congo weather station shows records of average monthly temperatures (see Figure 3.9).

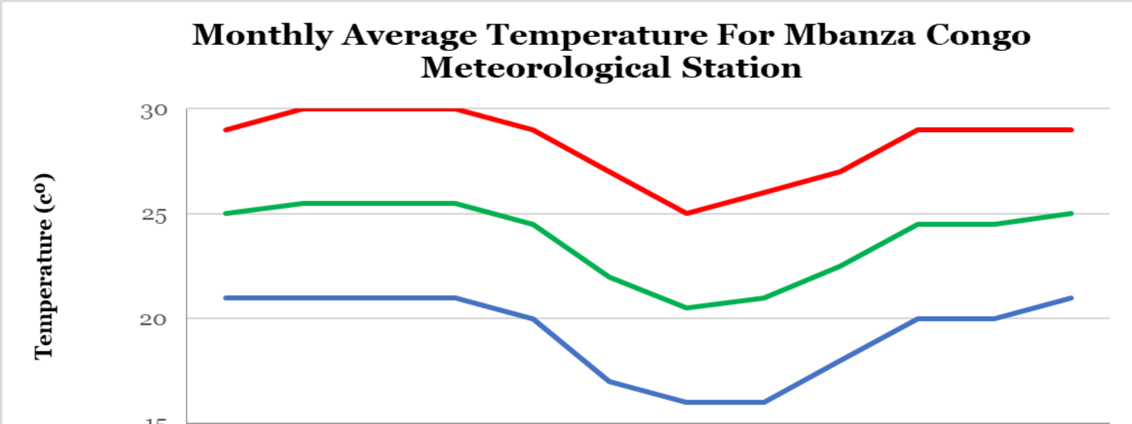

	Jan	Feb	Mar	Apr	May	Jun	Jul	Aug	Sep	Oct	Nov	Dec
Min	21	21	21	21	20	17	16	16	18	20	20	21
Average	25	25,5	25,5	25,5	24,5	22	20,5	21	22,5	24,5	24,5	25
Max	29	30	30	30	29	27	25	26	27	29	29	29

Figure 3.9 - The monthly average temperature in Mbanza Congo (Climat, 2021).

In the coastal zone, the average temperature is higher in the central and northern parts of the coast: Cabinda and Luanda (Azevedo, 2005; Climat, 2021). The average temperature generally oscillates around 25/26 in the central and northern parts, and the southern part 24 degrees per year (see Figure 3.8) (Climat, 2021). In Cabinda, the average temperature around from 26 degrees in February to April to 21 °C in July. While in Luanda, it varies from 26 degrees in February to April to 20 °C in July and August (see Figure 3.10) (Climat, 2021).

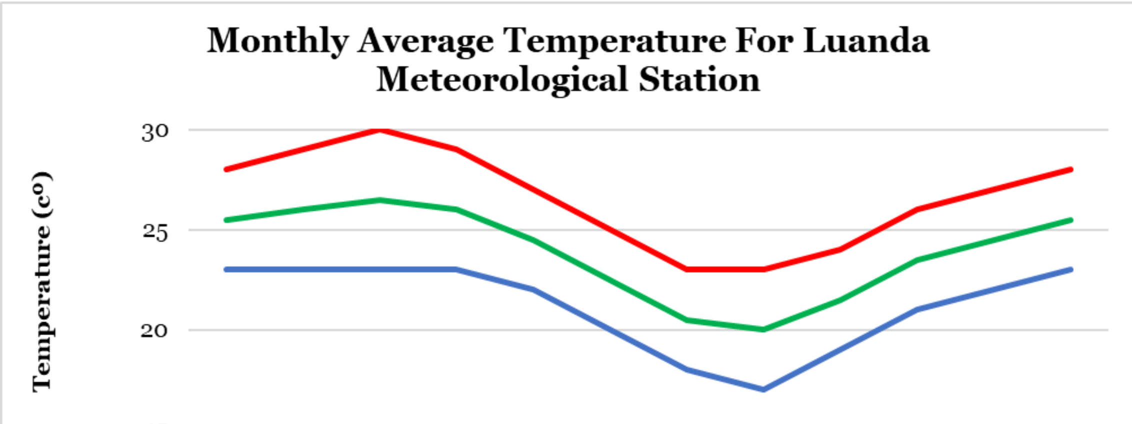

	Jan	Feb	Mar	Apr	May	Jun	Jul	Aug	Sep	Oct	Nov	Dec
Min	23	23	23	23	22	20	18	17	19	21	22	23
Average	25,5	26	26,5	26	24,5	22,5	20,5	20	21,5	23,5	24,5	25,5
Max	28	29	30	29	27	25	23	23	24	26	27	28

Figure 3.10 - The monthly average temperature in Luanda (Climat, 2021).

The southern part of the coast is colder. Thus, the average temperature in Namibe is around 24 degrees in February and March to 16.5 °C in July (see Figure 3.11) (Climat, 2021).

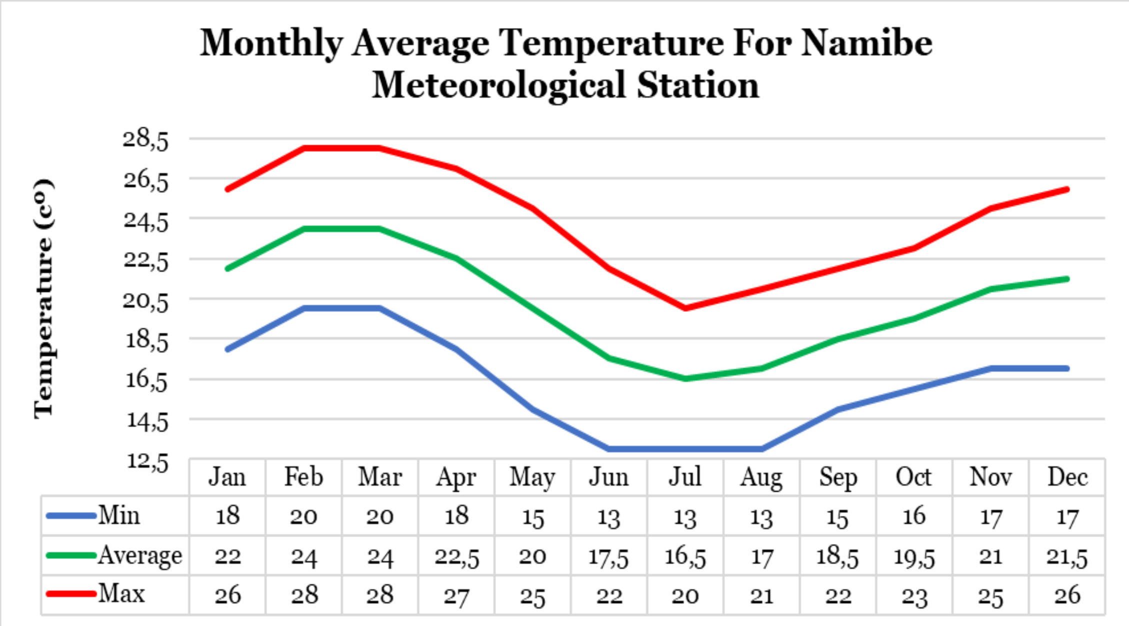

	Jan	Feb	Mar	Apr	May	Jun	Jul	Aug	Sep	Oct	Nov	Dec
Min	18	20	20	18	15	13	13	13	15	16	17	17
Average	22	24	24	22,5	20	17,5	16,5	17	18,5	19,5	21	21,5
Max	26	28	28	27	25	22	20	21	22	23	25	26

Figure 3.11 - The monthly average temperature in Namibe (Climat, 2021).

In the plateau areas, the coldest period is from May to August (see Figures 3.12 and 3.13), there are measurable temperature variations between night and day. Therefore, nights are cold, with possible frost. While during the day it can even be warm. The southernmost part of the plateau, between September and November, is very hot, to the point where maximum temperatures oscillate around 33/35 degrees. But it can sometimes reach 40°C, as it can be seen in the temperatures in Ondjiva (Climat, 2021). The average temperature generally varies around 18/19 in the central, northern part 20/22, and the southern part 23/26 degrees per year (see Figure 3.8) (Climat, 2021).

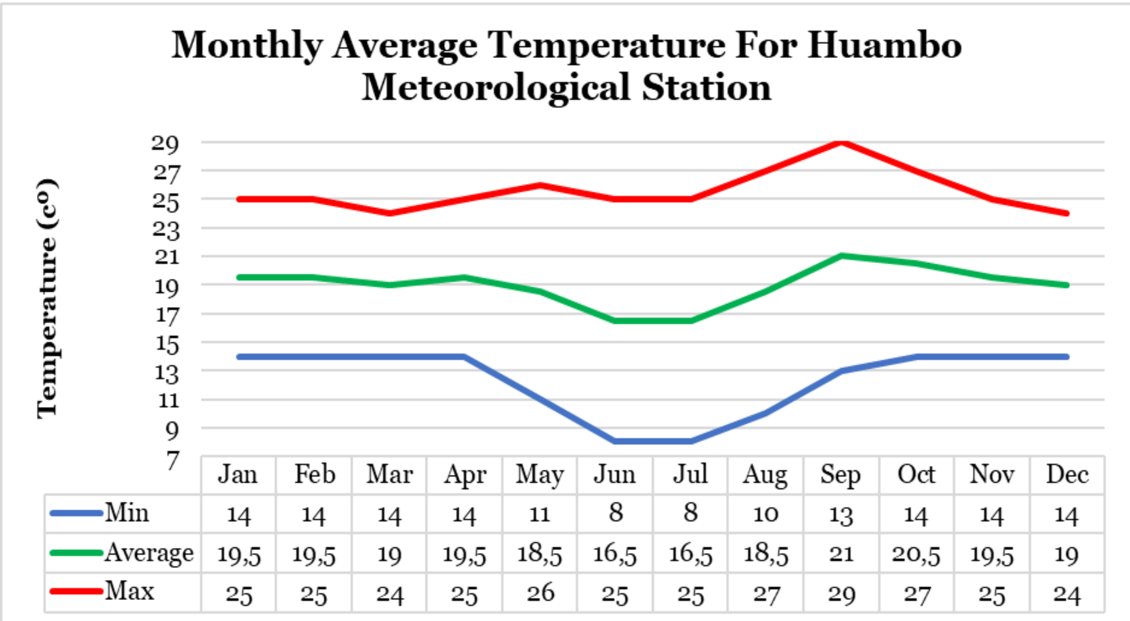

	Jan	Feb	Mar	Apr	May	Jun	Jul	Aug	Sep	Oct	Nov	Dec
Min	14	14	14	14	11	8	8	10	13	14	14	14
Average	19,5	19,5	19	19,5	18,5	16,5	16,5	18,5	21	20,5	19,5	19
Max	25	25	24	25	26	25	25	27	29	27	25	24

Figure 3.12 - The monthly average temperature in Huambo (Climat, 2021).

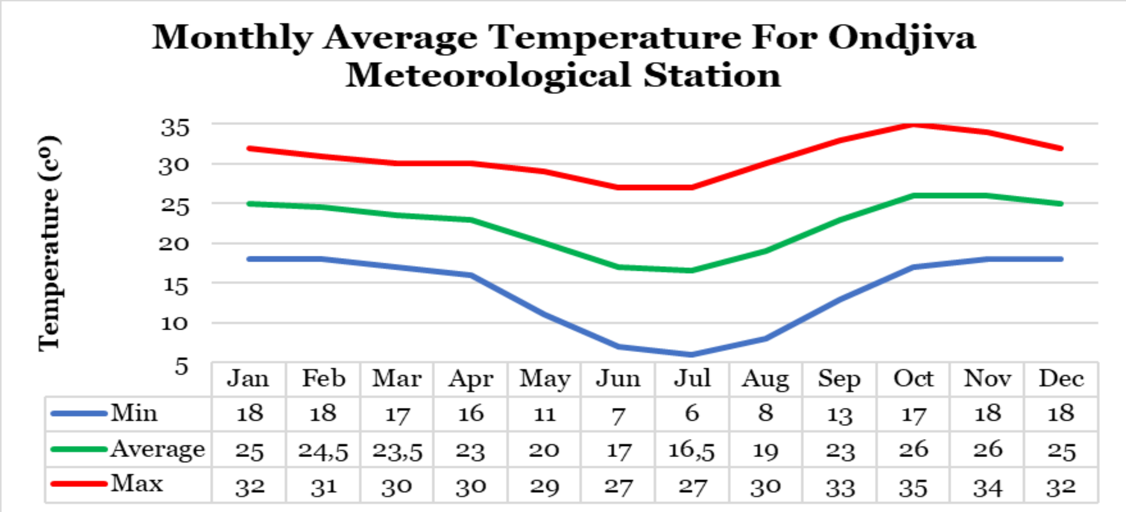

Figure 3.13 - The monthly average temperature in Ondjiva (Climat, 2021).

3.2.3 Topography

According to (Huntley et al., 2019; Jesus, 2018), they divided the Angolan terrain into three main parts: the coastal plain, escarpment and plateau (see Figure 3.14).

- ✓ **The coastal plains**: located below 200 m altitude and vary in width between 10 and 150 km, they occupy 5% of the study area (Huntley et al., 2019).
- ✓ **Escarpment**: situated at an altitude of 1000 m, occupy 23% of the study area (Huntley et al., 2019).
- ✓ **The plateau**: situated at an altitude of 1000-1500 m, occupies 65% of the study area (Azevedo, 2005; Huntley et al., 2019). Since 7% of the study area is above 1500 m, its highest point (Moco) ranges between 2600 and 2620 m. Moco is the highest point in the study area (Azevedo, 2005; Climat, 2021; Huntley et al., 2019; Jesus, 2018).

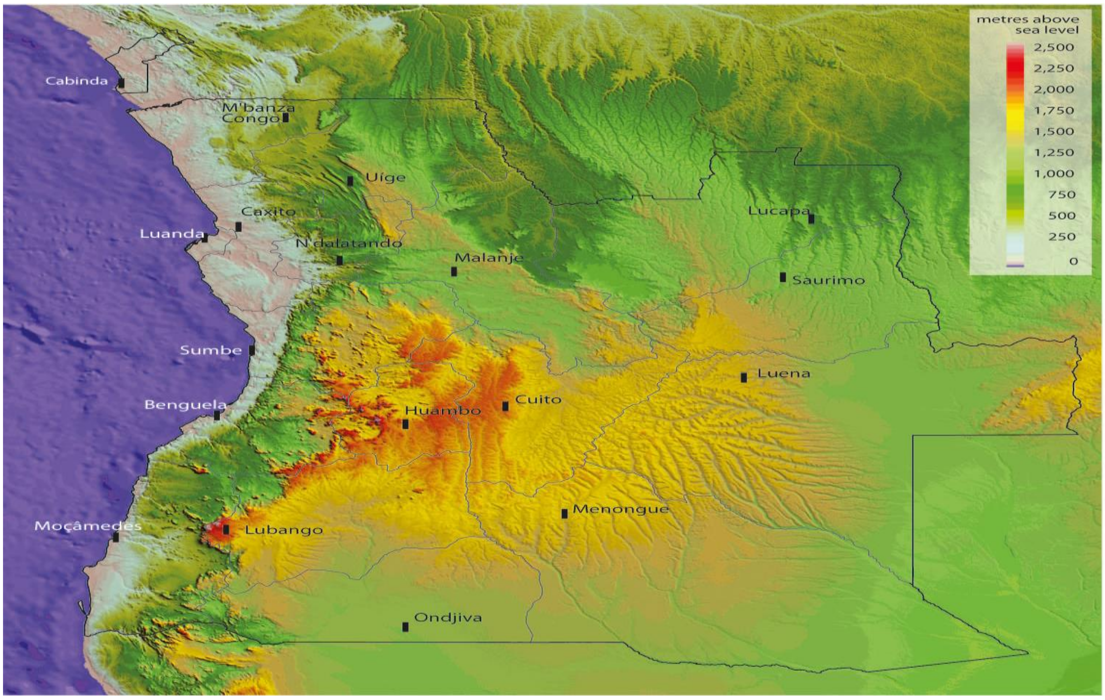

Figure 3.14 - Map of topography in Angola (Huntley et al., 2019).

3.2.4 Drivers Over Study Area Climate

Several drivers are acting on the selected study area. But in this section, some systems that influence the climate of the study area will be discussed.

Firstly, the geographical location of the study area is from near the equator to near the Tropic of Capricorn, along 14 degrees latitude. This fact explains the general reduction in solar radiation received and, as also the average annual temperatures recorded from north to south. Secondly, both temperature and precipitation are driven by altitude and seasonality (Huntley et al., 2019). Thirdly, the cold Benguela current results in a precipitation gradient increasing from south to north and west to east. Rainfall is also locally accentuated by the orographic influence (Azevedo, 2005; Huntley et al., 2019; Xavier, 2013). Areas of 1000 m altitude can register rainfall locally influenced by orographic (Huntley et al., 2019). And finally, Intertropical Convergence Zones (ITCZ) Azevedo (2005); Huntley et al., (2019); Xavier (2013), an atmospheric system that dominates Central Africa and is the most fundamental to the rainfall patterns of the study area. ITCZ is a cloud band accompanied by low pressure and precipitation that moves south over the study area during summer and then returns north towards the equator as winter approaches. The rainy season driven by ITCZ travels north over the study area from early summer, reaching the south at the end of this season (Huntley et al., 2019). Figure 3.15 shows the impact of southward and northward displacement of the ITCZ on rainfall seasonality in the study area.

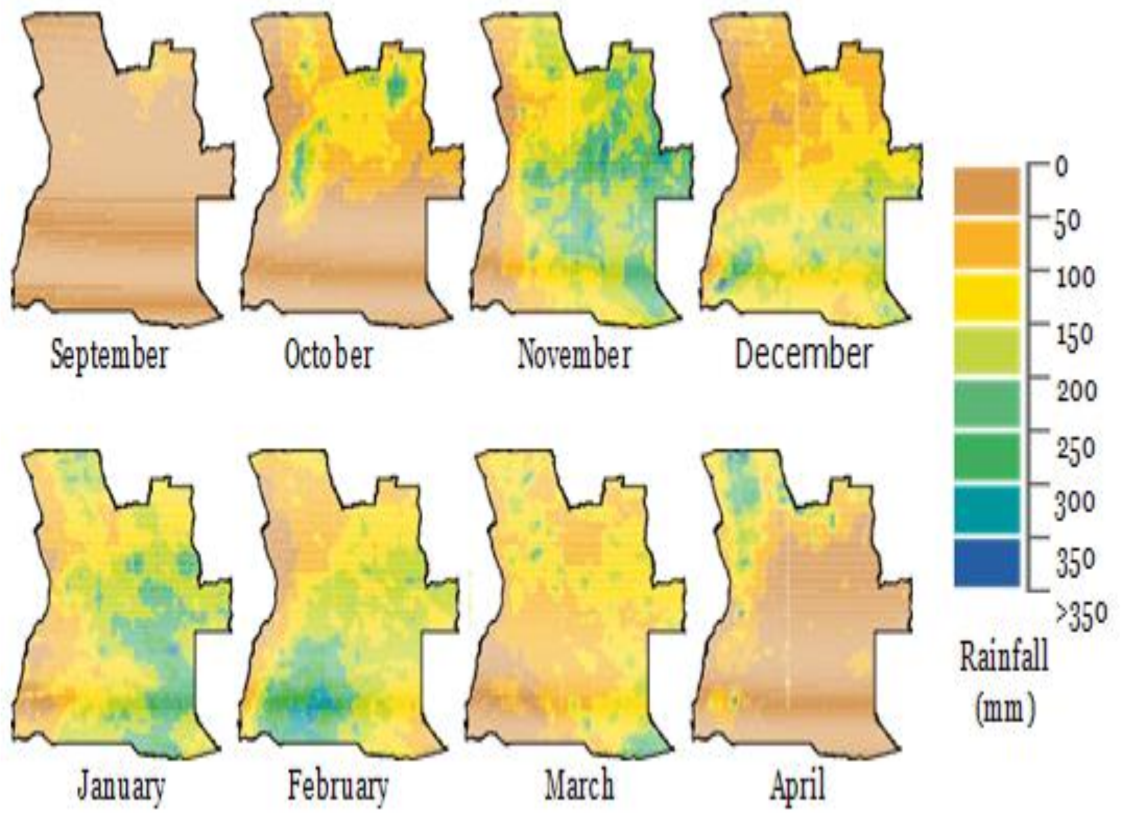

Figure 3.15 - Impact of southward and northward displacement of the ITCZ on rainfall seasonality in the study area during 2009/2010 Mendelsohn et al. (2013 in Huntley et al., 2019).

Chapter 4

Material and Methods

4.1 Data Acquisition

For the present work, two types of data were used:

- ✓ GNSS observations (RINEX files, ZTD);
- ✓ Surface meteorological parameters (Temperature and pressure).

In the sections below in more details will be presented on how these data were acquired.

4.1.1 GPS Network Management System Software (The TeroNet)

GPS network management system such as TeroNet is a web platform consisting of a complex set of tools for CORS (Continuously Operating Reference Station) network management. TeroNet software is advantageous to help with the following scenarios (Teromovigo, 2019):

- ➢ Storage and pre-processing of GPS data;
- ➢ Making pre-processed data available to TeroNet registered users;
- ➢ Monitoring of the CORS connection status;
- ➢ Quality assurance of the received GPS data.

The platform web TeroNet was developed by TeroMovigo with the partnership of SEGAL in Portugal. Since the installer of the permanent GNSS network in Angola is the SEGAL (Fernandes et al., 2011; Kitoko & Painho, 2015). Figure 4.1 shows the TeroNet user interface with the GNSS network of Angola. The web platform is currently also managed by the IGCA in Angola (see, Figure 4.2).

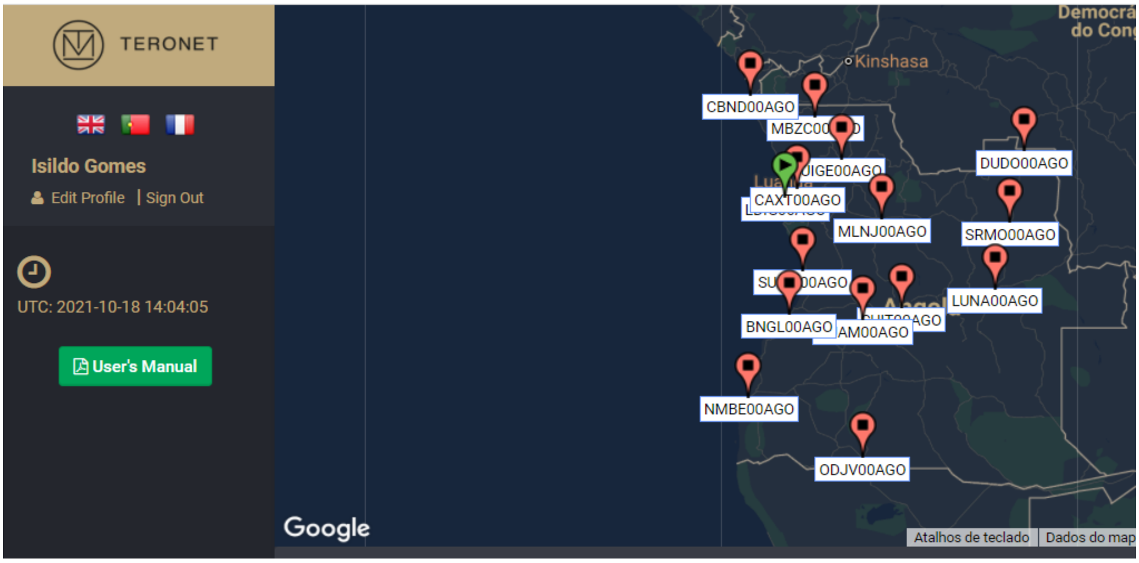

Figure 4.1 - The TeroNet user interface with the GNSS network of Angola (Repangol, 2021).

The web platform is not limited to illustrating the installed GNSS networks, as seen in Figure 4.1. The TeroNet software also includes details of each station as the actions that can be performed on each station inserted in the web platform (see Figure 4.2).

Site name	Location	Agency	Action
BNGL00AGO	Benguela - Angola	IGCA	Details Daily Hourly Ephemeris
CAXT00AGO	Caxito - Angola	IGCA	Details Daily Hourly Ephemeris
CBND00AGO	Cabinda - Angola	IGCA	Details Daily Hourly Ephemeris
CUIT00AGO	Kuito - Angola	IGCA	Details Daily Hourly Ephemeris
DUDO00AGO	Dundo - Angola	IGCA	Details Daily Hourly Ephemeris
HUAM00AGO	Huambo - Angola	IGCA	Details Daily Hourly Ephemeris
LDIG00AGO	Luanda - Angola	IGCA	Details Daily Hourly Ephemeris
LUNA00AGO	Luena - Angola	IGCA	Details Daily Hourly Ephemeris

Figure 4.2 - The TeroNet user interfaces with detail of each station as the actions that can be performed on each station inserted in the web platform (Repangol, 2021).

With the actions illustrated in Fig. 4.2, the platform also may download the RINEX files same (daily or hourly).

Download CAXT00AGO - 2020-03-16

Daily file with 100% of data:

RINEX v2.11 RINEX v3.00

Download CAXT00AGO - 2016-03-15

Hour of day	Completeness	%	Download
00:00:00 - 00:59:59		0%	N/A
01:00:00 - 01:59:59		0%	N/A
02:00:00 - 02:59:59		0%	N/A
03:00:00 - 03:59:59		0%	N/A
04:00:00 - 04:59:59		0%	N/A
05:00:00 - 05:59:59		0%	N/A
06:00:00 - 06:59:59		100%	RINEX v2.11 RINEX v3.00

Figure 4.3 - Example of data that may download from the TeroNet web platform (Repangol, 2021).

4.1.2 GPS Data Flow

Upon the arrival of RAW GPS data at the TeroNet server, they are stored and automatically converted into RINEX and ephemeris files. After this processing, the quality of the processed files is determined for later download to the registered users on the TeroNet web platform (Teromovigo, 2019). Figure 4.4 illustrates GNSS data flow.

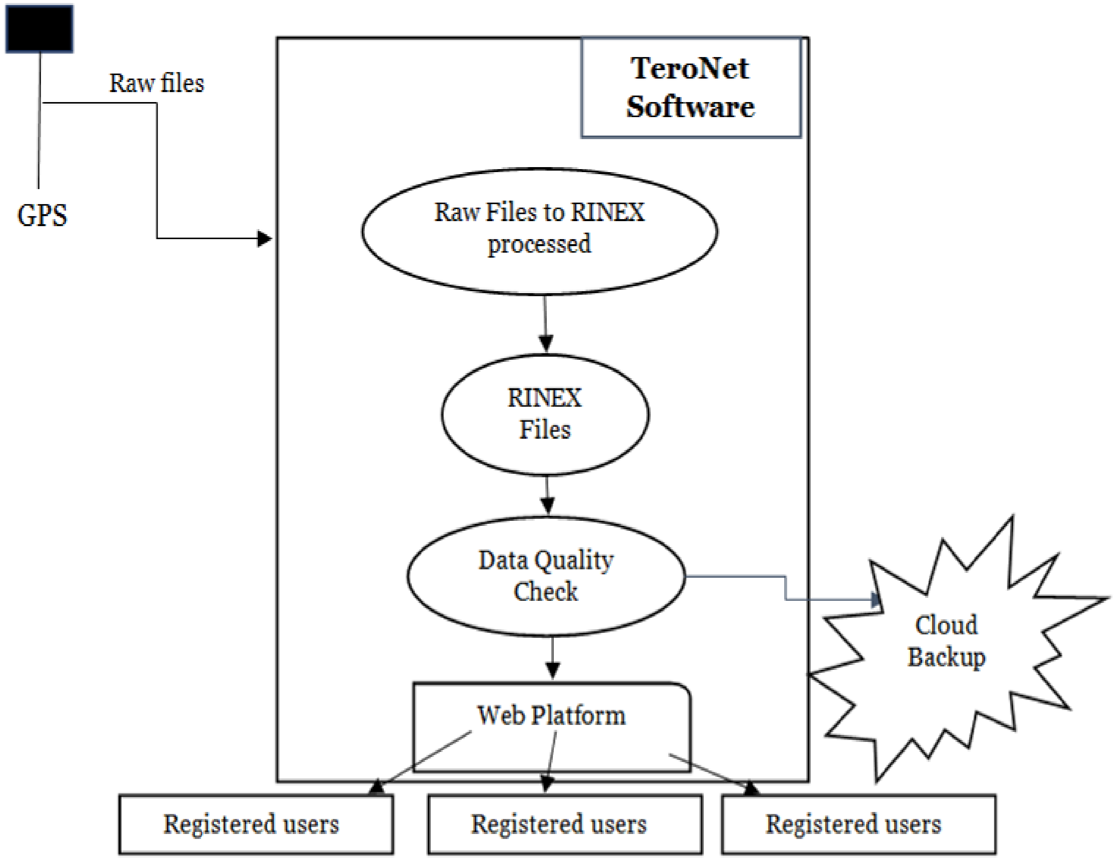

Figure 4.4 - The web platform TeroNet software (Adapted from TeroMovigo, 2019).

4.2 Network

As was already discussed in **section 2.2.1** on GNSS networks in Angola, in this work, we will use the data from the existing GNSS network in Angola. This data will be obtained from the only existing GNSS network in Angola, called REPANGOL.

REPANGOL is a network containing 18 GNSS stations. Currently, only 12 stations are operational according to the REPANGOL network survey report prepared with the supervision of SEGAL (see Appendix C). GNSS data can be collected in the server of the University of Beira Interior (UBI). The acquisition of the data depends on the timely payment of the internet subscription at each site for sending data to the servers.

Unfortunately, the lack of internet connection prevented the collection of data for most stations. Because the choice of the GNSS stations studied or analysed in this dissertation depends on the consistency of the available data, two stations with large data gaps were discarded (i.e., Dundo and Menongue). Figure 4.5 illustrate the REPANGOL network with five Meteo stations in Angola. Table 4.1 show the GNSS stations with location information.

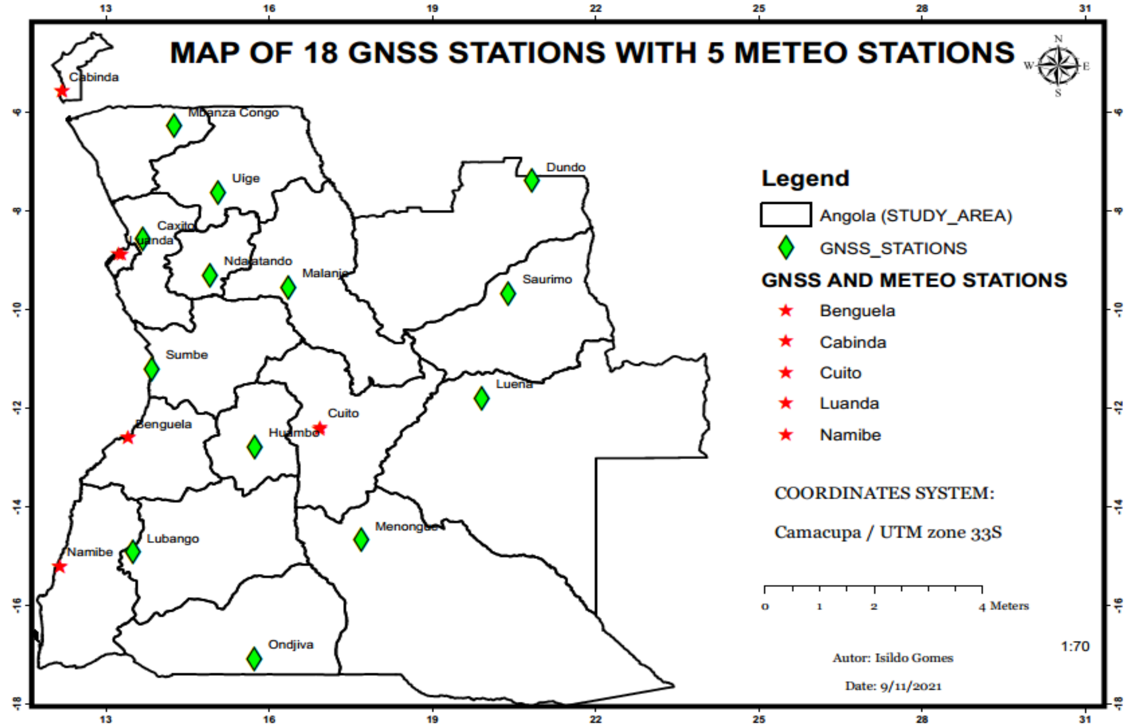

Figure 4.5 - Distribution Map of GNSS stations with five Meteo stations in Angola.

Table 4.1 - REPANGOL network with Location Information, including the longitude, latitude, and heights.

Station ID	Latitude S (°)	Longitude E (°)	Height (m)	City
BNGL	-12,58402851	13,40823961	47.159	Benguela
CBND	-5,55802347	12,19103808	35.627	Cabinda
CUIT	-12,38219111	16,94176731	1717.785	Cuito
DUDO	-7,38358304	20,83021287	743.217	Dundo
HUAM	-12,77395835	15,73266293	1738.627	Huambo
LBNG	-14,9157803	13,49754338	1783.088	Lubango
LUNA	-11,78837011	19,90819367	1351.051	Luena
MBZC	-6,26698628	14,24931505	572.951	MBanza Kongo
MLNJ	-9,54619427	16,34592391	1178.112	Malanje
NDLT	-9,3013202	14,9112362	815.659	Ndalatando
NMBE	-15,19728969	12,14444302	40.454	Namibe
ODJV	-17,06771889	15,72507817	1139.187	Ondjiva
SRMO	-9,65505174	20,39346134	1086.109	Saurimo
SUMB	-11,20219076	13,83744859	45.7	Sumbe
UIGE	-7,6123205	15,05339908	873.413	Uíge
LDIG	-8,85568186	13,28848349	109.94	Luanda
CAXT	-8,56645021	13,67648365	38.685	Caxito
MNNG	-9,3013202	14,9112362	1383.263	Menongue

4.2.1 RINEX Files Acquisition

After identifying the GNSS stations that will be used for this dissertation, The next step is to obtain the data from these stations. The data acquired from these GNSS stations supports a RINEX format. For this work, the UBI server was used to obtain annual data for its processing. Another server that can be used is the TeroNet. The TeroNet is a versatile web platform for downloading GNSS data from the REPANGOL network. At the same time, on the UBI server scripts are running that continuously download data from the REPANGOL network for scientific research. Figures 4.6 illustrate the flowchart of how the data was obtained from the UBI server.

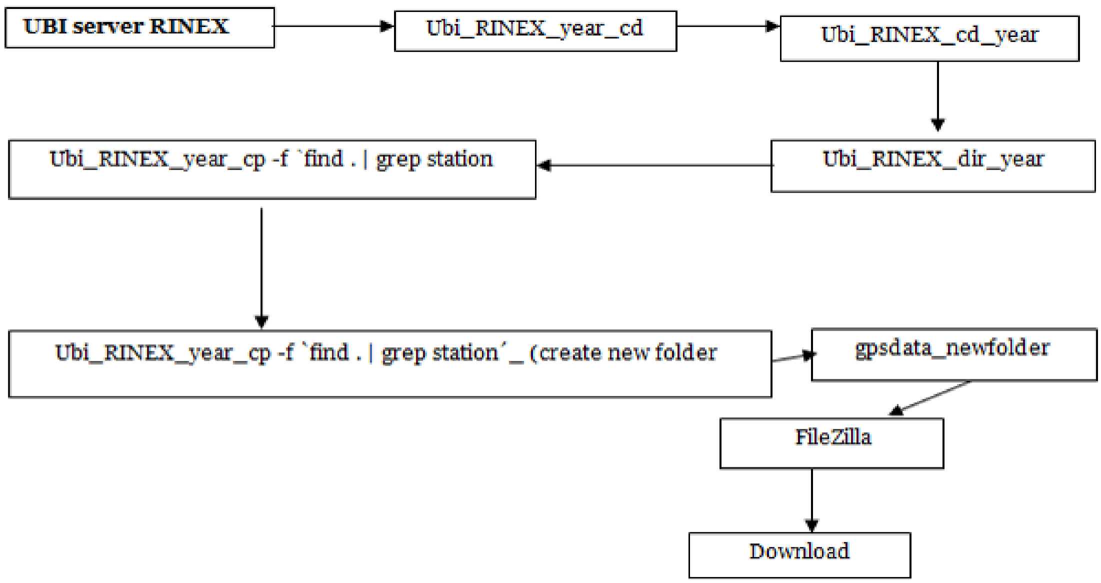

Figure 4.6 - Flowchart GNSS annual data download.

4.3 Technologies, Technique and Software Used in the Dissertation

This section will present the technologies, techniques and software used during the implementation of the system to determine ZTD and compute the PWV.

4.3.1 Programming Language

In this work, scripts to automate repetitive command line operations were created for which the TCSH language was used. This choice is justified by the fact that there is vast experience using Linux shell scripting language by the SEGAL group.

TCSH is a Unix-like operating system based on the C shell (csh). Its main features are programmable command completion and command-line editing (TCSH, 2021).

4.3.2 Linux Tools

As a Linux shell scripting language was implemented this led to the use of a set of Linux tools. it was used some simple and common commands like: "cat, grep, cut, find" but also was used other more complex and more relevant to work as:

awk: is a scripting language, but it offers many useful features because it is easy to analyse files process and manipulate text, do calculations with it and strings (Awk, 2021).

crontab: This is the Linux task scheduler running at regular time intervals on the system (Crontab, 2021).

rsync: is a scripting language that allows a complete synchronisation between files from a source to a destination. This synchronisation can also be done on a local machine or between different machines (Rsync, 2021).

4.3.3 GDGPS – APPS

Since the services provided by the software established by the project are based on the GIPSY-X software. Thus, the processing technique established was PPP since it is the method used by GIPSY-X (see Fernandes et al., 2006).

4.3.4 ZTD2PWV

In this work, the PWV was calculated automatically for which we used ZTD2PWV which incorporates the equations discussed in section 4.5.

The ZTD2PWV is an application developed by SEGAL to convert the ZTD into PWV for the day in question with a set second period (SEGAL, 2017).

According to (SEGAL, 2017) ZTD2PWV uses on the command line the following arguments:
ztd2pwv -m file -z file -l latitude -H value -o value -p file
-m Input meteo rinex file (required)
-z Input ztd sinex file (required)
-l latitude station (decimal deg) (required)
-H Orthometric Height station (required)
-o offset between antenna and sensor. Positive if antenna higher (required)
-p Output pwv sinex file (required)

4.3.5 ArcGIS Desktop 10.7.1 (ArcMap, ArcToolbox and ArcCatalog components)

In this way, based on the information that will be collected the following tasks will be developed:

- ✓ Delimitation of the study area;
- ✓ Spatial interpolation;

- ✓ Extraction;
- ✓ Elaboration of maps.

4.3.6 Technique for Spatial interpolation

Spatial interpolation is a technique used to obtain information within an unmeasured area. Spatial interpolation is based on applying the known result to surrounding stations which are known as sampling points. An interpolated value is also known as a predicted value (Liu et al., 2019).

Lo & El-mowafy (2011), describe, there several spatial interpolation techniques. According to Liu et al. (2019), interpolation Kriging, inverse distance weighted, natural neighbour, and two-dimensional minimum curvature spline are often used.

Therefore, for this dissertation, the kriging technique has been used, specifically the ordinary kriging interpolation. This choice was motivated by the study elaborated by Lo & El-mowafy, (2011).

4.4 Processing of GNSS Observations Data

The first step to compute the PWV is to obtain the ZTD parameter. This parameter is acquired by processing the GNSS data. With the software Jet Propulsion Laboratory - Global Differential GPS was processed available data used in this dissertation for analysis of the PWV. To respond to the main objective of the work, daily data were processed.

The daily ZTD data were used to investigate the long-term variations over Angola. Table 4.2 illustrates the solution strategy in processing the data to obtain the ZTD.

Table 4.2 - Solution strategy for acquiring ZTD (Adapted from Liu et al., 2019).

Parameter	Strategy
Troposphere Model – Mapping Function	GMF
GNSS Orbit & Clock State – Satellite Orbit	JPL Precise
Elevation Angle Cutoff	7.5
Solution Period	300

The choice of the GMF as the Troposphere Model was based on the study done by Boehm et al., (2006). Section 2.3 was discussed the different satellite orbits. The software chosen in the dissertation can use the Rapid and Final products except for the Ultra-Rapid of IGS. GIPSY - X needs an orbit with accurate satellite clocks. Here is the reason for the choice of the JPL Ultra-Rapid satellite orbit (JPL Precise), although its possible solutions have a delay of 2 hours when generated. Solution Period = 300 shows that ZTD values are estimated every 5 min. Thus, figure 4.7 shows the GNSS observations data processing in software Jet Propulsion Laboratory - Global Differential GPS.

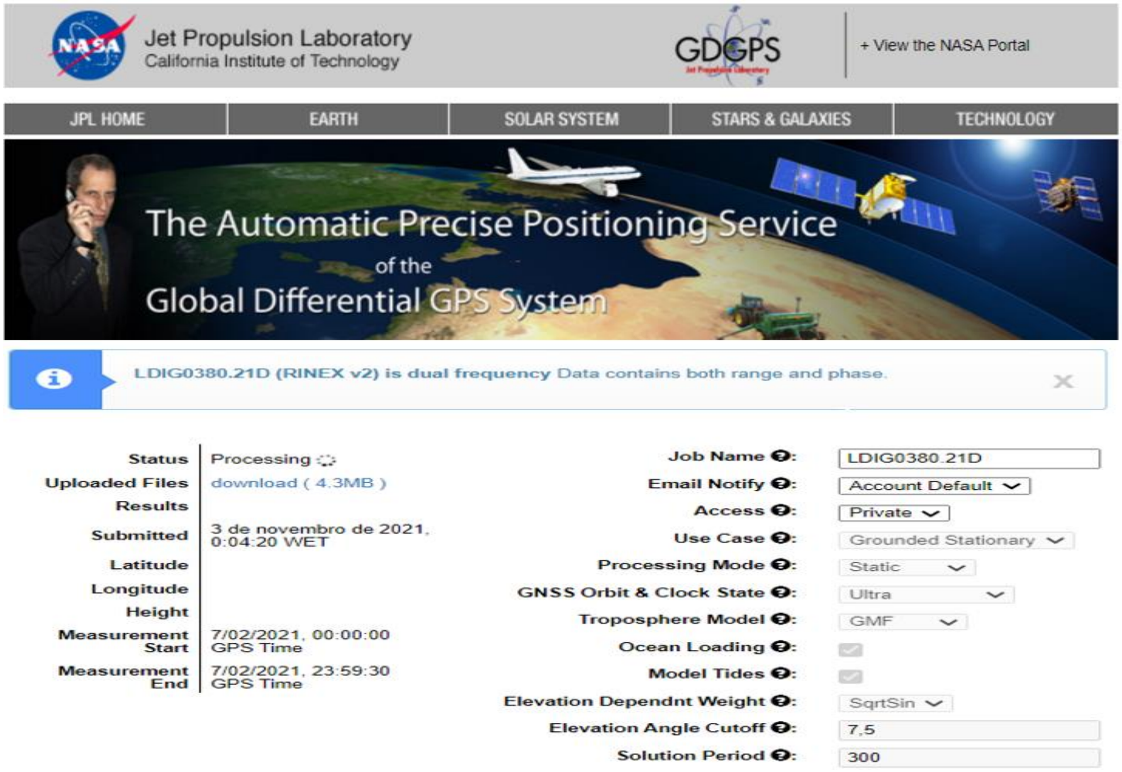

Figure 4.7 - The GNSS observations data processing from software Jet Propulsion Laboratory - Global Differential GPS.

After processing, the ZTD parameter is calculated by summing the ZHD (HZTrop in Summary file) and ZWD (WZTrop in Summary file). The result of this processing will be shown in Figure 4.8.

LUANDA_GMF_RESUL_STATION - Bloco de notas

Ficheiro Editar Formatar Ver Ajuda

#Secs_from_start	GPS_Time(yyyy:mm:dd:hh:mm:ss,ssss)	HZTrop(m)	WZTrop(m)
0,0000	2021:01:15:00:00:00,0000	2,2703	0,2425
300,0000	2021:01:15:00:05:00,0000	2,2703	0,2424
600,0000	2021:01:15:00:10:00,0000	2,2703	0,2421
900,0000	2021:01:15:00:15:00,0000	2,2703	0,2419
1200,0000	2021:01:15:00:20:00,0000	2,2703	0,2417
1500,0000	2021:01:15:00:25:00,0000	2,2703	0,2412
1800,0000	2021:01:15:00:30:00,0000	2,2703	0,2406
2100,0000	2021:01:15:00:35:00,0000	2,2703	0,2400
2400,0000	2021:01:15:00:40:00,0000	2,2703	0,2392
2700,0000	2021:01:15:00:45:00,0000	2,2703	0,2385
3000,0000	2021:01:15:00:50:00,0000	2,2703	0,2378
3300,0000	2021:01:15:00:55:00,0000	2,2703	0,2372
3600,0000	2021:01:15:01:00:00,0000	2,2703	0,2366
3900,0000	2021:01:15:01:05:00,0000	2,2703	0,2361
4200,0000	2021:01:15:01:10:00,0000	2,2703	0,2356
4500,0000	2021:01:15:01:15:00,0000	2,2703	0,2353
4800,0000	2021:01:15:01:20:00,0000	2,2703	0,2350
5100,0000	2021:01:15:01:25:00,0000	2,2703	0,2348

Figure 4.8 - Processing summary file.

4.5 Estimating Process of the PWV

4.5.1 Pressure and Temperature Parameter

The surface meteorological data were obtained from meteorological stations collocated by the SEGAL group. These stations support RINEX files. After obtaining the meteo Rinex files, the files will be used to convert the ZTD to PWV. These meteorological data is compatible with ZTD2PWV or GYPSY-X.

4.5.2 PWV Obtained from GPS and Meteorological Observations Dataset

Here, introduce the methods to derive PWV from GNSS data with meteorological parameters temperature and pressure. Elgered et al. (1991 in Bevis et al., 1992) have adopted a formula for calculating (ZHD), in millimetres, is given by:

$$ZHD = (2.2779 \_+ 0.0024)\ Ps/f\ (\phi, H) \qquad (1)$$

$$f\ (\phi, H) = (1 - 0.00266 \cos 2\ \phi - 0.00028H) \qquad (2)$$

Where Ps is the total surface pressure in millibars, ϕ is the latitude, and H is orthometric height in kilometres.

Determinating ZHD and knowing ZTD (which is the value calculated from the GDGPS – APPS software), ZWD is given by:

$$ZWD = ZTD - ZHD \qquad (3)$$

After the determination of the ZWD, it can be obtaining the amount of integrated water vapour (IWV), which can be declared by PWV and obtained by multiplying the ZWD by the variable ∏ (Bevis et al., 1994):

$$PWV \ = \prod . ZWD \qquad (4)$$

Where ∏ is given by:

$$\prod \ = \ 10\text{^}6 \ / \ ((k_3/Tm \ + \ k'_2) \ \rho Rv) \qquad (5)$$

Where Tm is the weighted mean temperature of the atmosphere, ρ is the density of water, Rv is the gas constant of water vapour, k3 and k'2 are physical constants. According to Bevis et al. (1994):

- ✓ k3 = (3.739 ± 0.012) ·10^5K^2/mbar;
- ✓ k'2 = 22.1 ± 2.2 K/mbar;
- ✓ Rv = 4.615 m3 mb/ (kg K);
- ✓ ρ = 1000 kg/m3

And lastly, Bevis et al. (1994), derived the formula to compute Tm:

$$Tm \ = \ 70.2 \ + \ 0.72Ts \qquad (6)$$

Where Ts is the surface temperature in Kelvin.

Figure 4.9 describes the scheme required to estimate the ZTD from GNSS data processing and the subsequent conversion of the wet component of the ZTD to Precipitable Water Vapour (PWV).

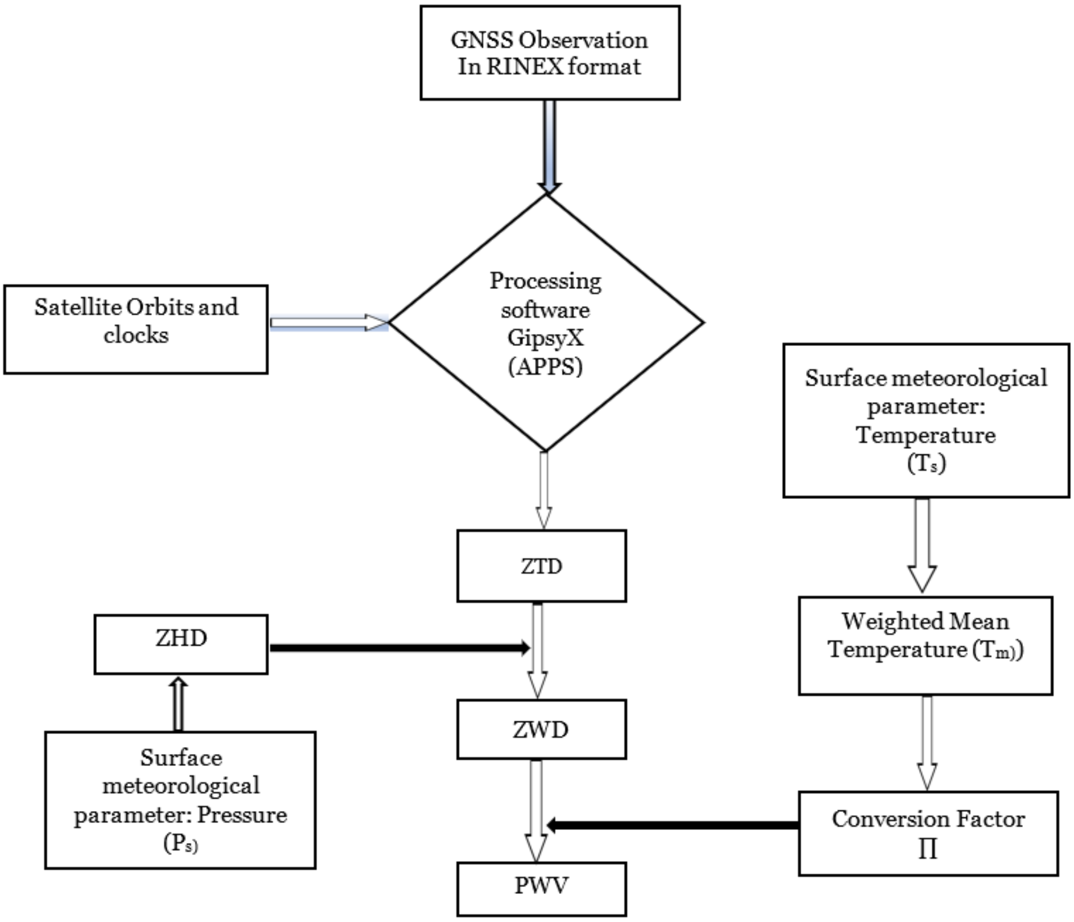

Figure 4.9 - Flowchart to obtain ZTD and Conversion to PWV (Adapted from Liu et al., 2019).

After the PWV is obtained next, it will be analysed to investigate its variations. In this dissertation, these analyses will be done, using available data over the study area.

Chapter 5

Results and Discussion

This chapter presents the ZTD time series for 16 CORS in Angola and a PWV time series for the LDIG station, then discuss them. First, starting with the analysis of the availability of data.

5.1 Network Reliability

The assessment of the reliability of the REPANGOL network is first discussed. The available observations from 11/5/2010 to 27/11/2021. These data were used to calculate some statistics.

Table 5.1 gives an overview of the total number of GNSS stations, dates of installation and when it stopped functioning. The reason for the non-acquisition of data by the GNSS stations is due to Internet connectivity or equipment failure. The table also shows the total number of files, the total number of processed and percentage value of processed files per station. Unfortunately, there are no data from Dundo and Menongue. Therefore, these two stations will not be discussed further and only results for 16 CORS will be presented.

Table 5.1 - Summary Information of GNSS Stations.

SITE	City	InitialProc	FinalProc	Years	TotalFiles	ProcFiles	Percentage (%)
BNGL	Benguela	13-05-2010	17-11-2015	5.5	920	917	45.7
CAXT	Caxito	05-09-2015	31-03-2020	4.6	208	173	10.3
CBND	Cabinda	20-10-2010	02-09-2021	10.9	410	408	10.2
CUIT	Cuito	20-07-2010	06-06-2016	5.9	850	841	39
HUAM	Huambo	13-10-2010	21-02-2020	9.4	635	634	18.5
LBNG	Lubango	02-09-2010	08-01-2016	5.4	692	686	34.8
LDIG	Luanda	23-11-2014	27-11-2021	7.0	801	792	31
LUNA	Luena	11-10-2010	29-06-2021	10.7	911	910	23.3
MBZC	M'Banza Congo	07-10-2010	12-02-2012	1.4	98	96	18.8
MLNJ	Malanje	10-09-2010	05-11-2015	5.2	329	325	17.1
NDLT	N'Dalatando	08-10-2010	17-12-2015	5.2	442	438	23.1
NMBE	Namibe	15-06-2010	30-12-2015	5.5	699	694	34.6
ODJV	Ondjiva	15-10-2010	16-01-2016	5.3	937	931	48.1
SRMO	Saurimo	19-06-2010	19-01-2016	5.6	311	305	14.9
SUMB	Sumbe	11-05-2010	13-02-2020	9.8	656	652	18.2
UIGE	Uíge	26-08-2010	18-10-2015	5.1	713	711	38.2

5.1.1 GNSS Data Availability

In Appendix A, one can find a description of GNSS data availability for each year for each station. Here we will present the results of the statistical analysis including the percentage concerning days recorded at each station of the REPANGOL network. The results were performed with data available from each station.

We found that 68.75% of the stations recorded a high percentage of measurements in 2015 and only 25% in 2010. BNGL is the one station that presented a high value of available GNSS data in 2012 while the Luanda station (LDIG) is the only one that showed the highest value (94%) among all stations. 31.25% of the station recorded a low percentage value in 2012 and 25% in 2016. Since the low value among all stations was observed in 2011 and 2020. Also, it has been observed BNGL is the only station with available data in 2013.

The lack of data recorded by each station is evident. In the period under study, datasets were lacking during the 2017-2019 period for all stations. However, it is believed the lack of maintenance of the stations has been the reason for the missing data in these years. Since 2020, maintenance was done on some stations, and the servers resumed to report data.

The other analysis performed was to compute the average percentage value per station according to the available data. Thus, Figure 5.1 illustrates the average percentage per station, with eight stations recording above average. The average percentage value of files received for this REPANGOL network is just 30.2%, with this result clearly showing that the network is not very reliable. The lack of data received by the servers by each station is the reason that can justify this result. This lack of data is caused by internet failure or malfunction of stations.

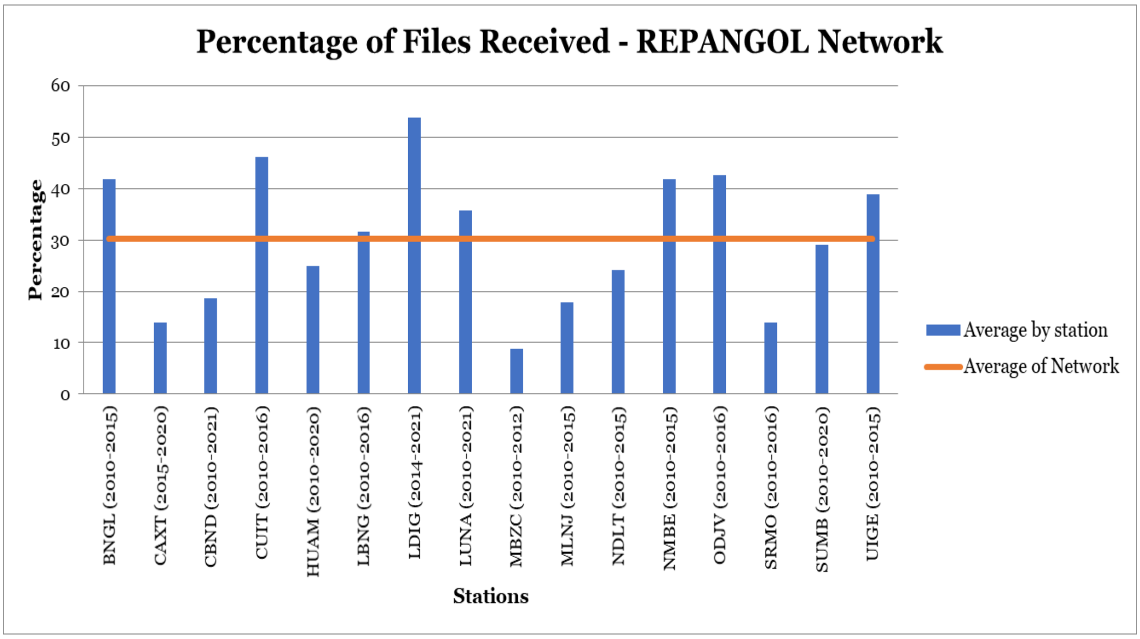

Figure 5.1 - The average percentage of data values per station.

Between 23 of January and 21 of February of 2020 was surveyed the network carried out by Gonçalo Henriques (SEGAL), Ricardo Duarte (TeroMovigo) and Edmar Rocha (IGCA). The objective of this mission was to prepare a detailed report of the current status of the GNSS stations. The report described the causes of the non-functionality of many stations and indicates internet problems as the main reason for the lack of GNSS data in the central servers.

Regarding the status of the stations, many stations were down because their batteries were drained. Only the LDIG station was online.

However, given the above it is possible to conclude the REPANGOL network is not very reliable.

5.2 Meteorological Stations Reliability

As was already discussed in the previous sections regarding the importance of meteorological data in PWV calculation, the accuracy of these data is very crucial.

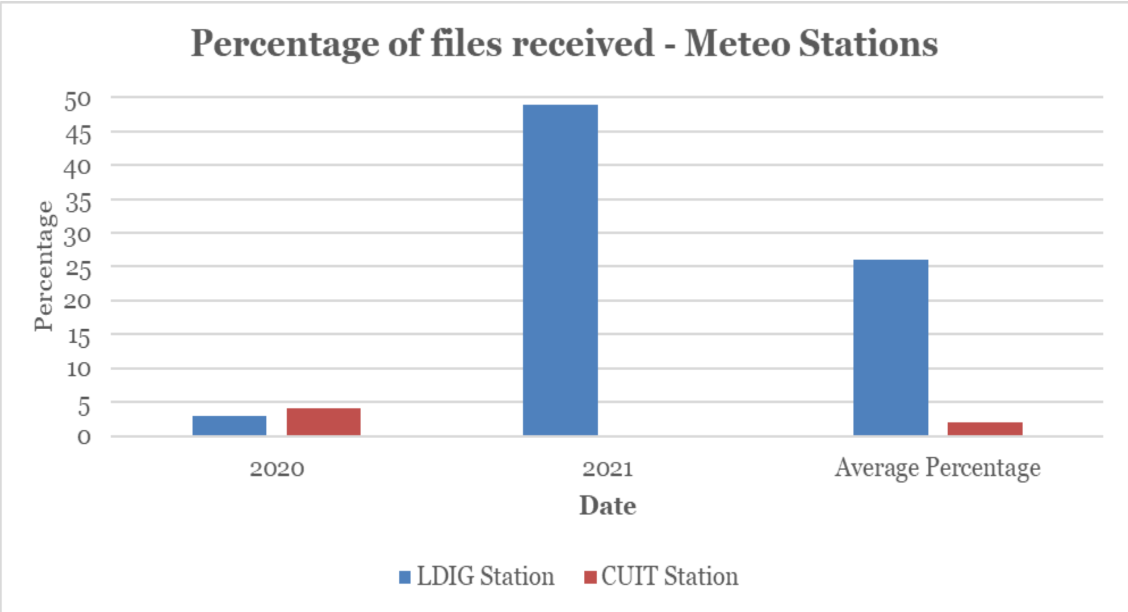

Figure 5.2 - The Total and average percentage value of the Luanda and Cuito station per year.

Luanda station presented high values of 48.8%, 178 days in 2021 while 2020 observed a low value of 2.7% (10 days). The average percentage value of files received is just 25.8%, with an average of 94 days. For Cuito station, illustrates 4.4% in the 2020 year corresponding to 16 days. 2021 does not record any data. So, the average percentage value of files received for the Cuito station is just 2.2%.

However, Luanda station showed the highest value than Cuito station. The average percentage value of files received for these stations is just 28%. During the assessment, the lack of data received by the servers by each station was evident. Therefore, this result clearly shows that these stations are not very reliable. It is believed the lack of data in meteorological stations is justified the same reason for the network REPANGOL (i.e., lack of internet).

The meteorological data used for the calculation of PWV must correspond to the location of the GNSS stations. This eliminates the uncertainties related to the spatial distance between the meteorological stations and the GNSS stations. Therefore, the analysis would be carried out on the five stations collocated near the GNSS stations. But unfortunately, only two stations recorded data.

It is important to refer that these meteorological stations were collocated in 2020.

However, what has been discussed it is possible to conclude these stations has been not reliable. This fact justifies the use of the global/regional models.

5.3 PPP ZTD Values

This section presents the ZTD time-series variations for various regions of Angola.

5.3.1 Climatological Characterization of the ZTD of Study Area

Figures 5.3 and 5.4 illustrate the ZTD time-series variations at the Cuito and Luena stations. The choices of these stations are due to presented good temporal variations among all stations.

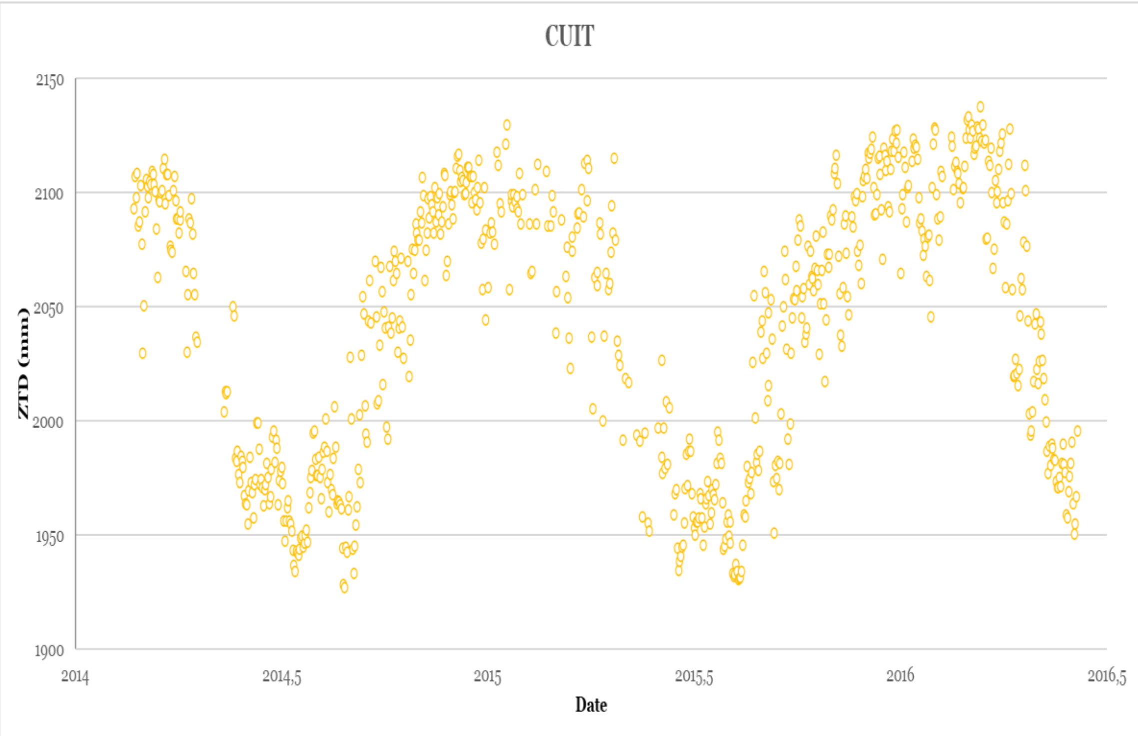

Figure 5.3 - ZTD time-series variation for the GNSS Station of Cuito.

The stations show a significant seasonal variation which is directly correlated with the wet (high peak) and dry (low peak) seasons. Note that the scale is not the same for the stations. Both stations are in the interior of Angola but, Cuito has a smaller amplitude.

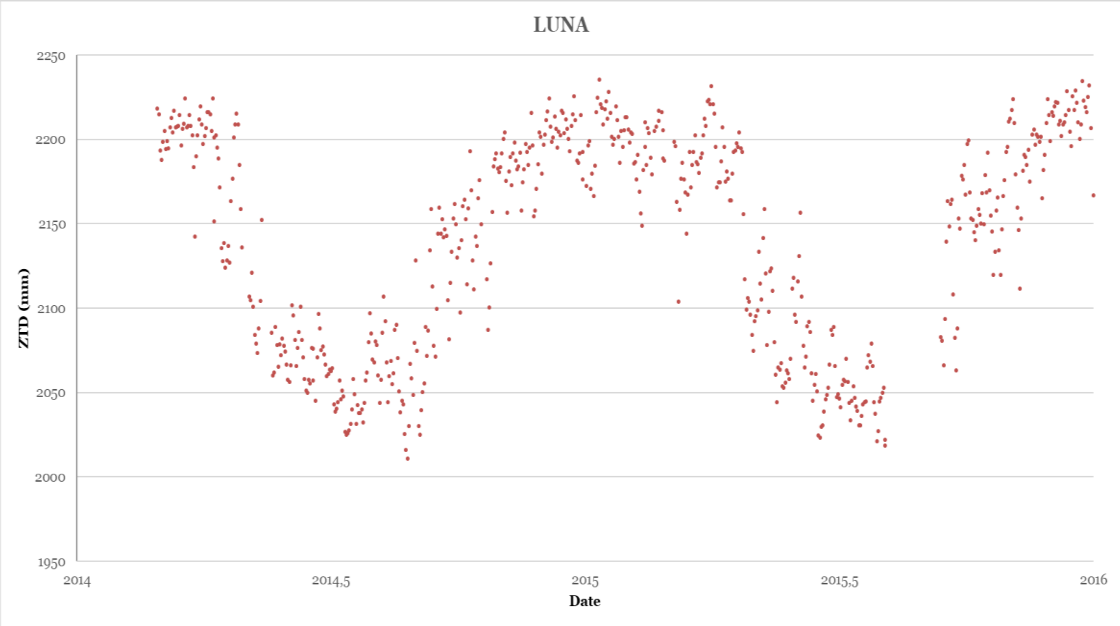

Figure 5.4 - ZTD time-series variation for the GNSS Station of Luena.

For a better understanding of the seasonality of the ZTD, Figure 5.5 illustrates monthly averages elaborated from three stations (LDIG, LUNA and CUIT) of different regions. Thus, for the elaboration of Figure 5.5, only the years that presented reliable data (2015) were chosen. These years were chosen according to the analysis performed in section 5.1.1. (See Appendix A).

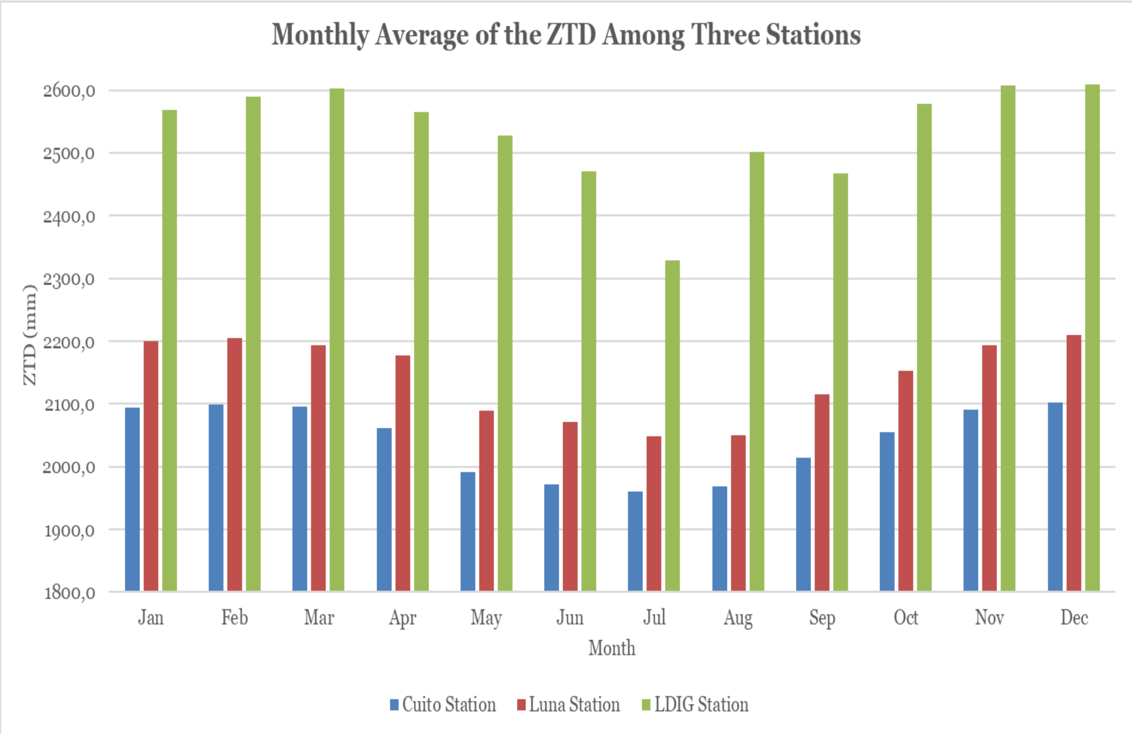

Figure 5.5 - The monthly average of the ZTD obtained from three stations.

According to Azevedo (2005); Climat (2021); Xavier (2013), the dry season starts in May and lasts until mid-September in Angola, while the rainy season begins in mid-September and lasts until April or May. Figure 5.5 illustrates a significant seasonal variation that is directly correlated with the wet and dry months. Therefore, wet months presented high values and the dry month's low values. However, it justifies the correlation of the ZTD with the seasonal variation. Figure 5.5 also shows the average values each month but, this will be discussed because this figure was elaborated only to justify the seasonal variations of ZTD.

The other analysis performed illustrates the daily average of each station per regions. In this case, Figure 5.6 shows records of the daily average of ZTD among the different stations.

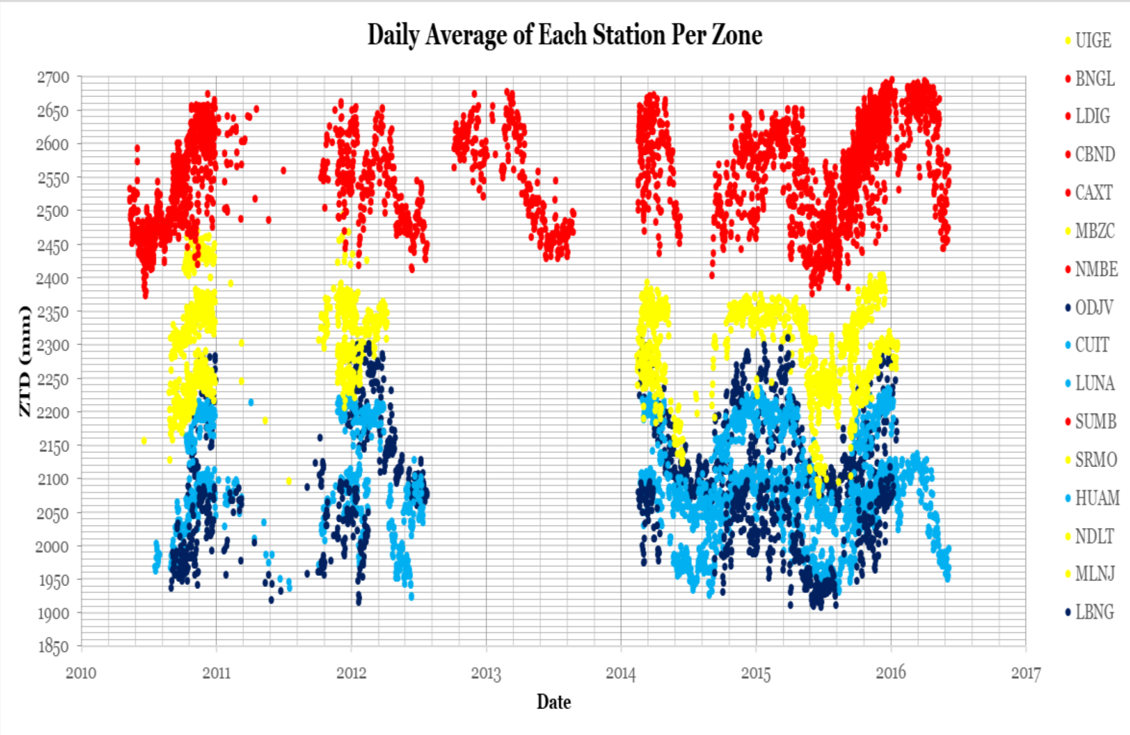

Figure 5.6 - Daily average of ZTD among sixteen stations in the different zone.

Figure 5.6 shows 16 stations that are separated by the different zones: northernmost (yellow), coastal (red), central (blue) and southern (light blue). Thus, each station is represented by a colour, where stations with the same colour are in the same zone. Therefore, Figures 5.6 clearly illustrate the correlation with the different zones. Thus, stations that are in the same region present a similarity in the time-series variation. Despite the lack of data at the stations a great similarity of ZTD values among the stations in each region was observed. This similarity permits us to study climatology for each region.

Figure 5.6 clearly illustrates that the highest values are observed by the stations that are part of the coastal zone and the low values of ZTD by the stations that are part of the central and southern zones. This is related to the climatology of each region. Coastal stations have more atmosphere above them than stations in mountainous areas. The temperature might also be a factor. Based on the discussion in section 3.2.2 on seasonal variation of temperature in the study area. It permits us to draw the conclusion that the coastal region are regions that register the highest average temperature while the northern, centrale and southern region in general present low average temperature. It is critical to note that the stations located in the central zone and some in the southern (i.e., LBNG), are in mountainous areas. These stations are strongly influenced by orographic or altitude.

One can conclude the drivers discussed in section 3.2.4 are the same that influence this similarity of the time-series variation of the ZTD values. That is, regions with higher temperatures record higher values of ZTD and vice versa.

Figure 5.7 illustrates the maximum, minimum and mean values of the ZTD, where the surfaces were generated using the kriging technique.

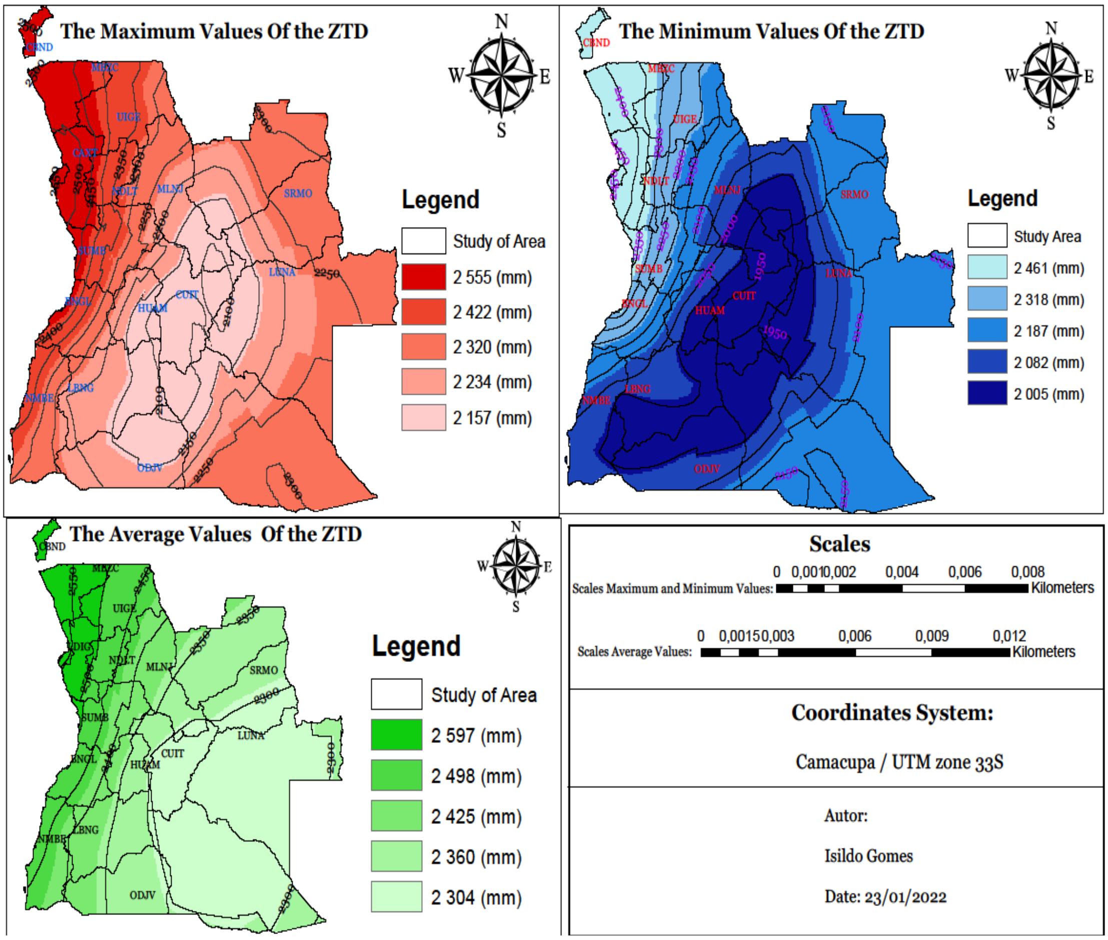

Figure 5.7 - The maximum, minimum and average values of the ZTD.

The map of the average values of the ZTD illustrates that the generated surfaces clearly show the lack of data mainly in the south-eastern area. It is important to refer that the interpolation generated in this area is not good due to lack of stations.

Figure 5.7 presents a curious correlation among stations CUIT, HUAM and LBNG. This correlation one can observe mainly in minimum values of the ZTD. Despite the LBNG being in the south zone but presents the similarity of ZTD values with the stations located in the central zone (HUAM and CUIT). The map of the minimum values of the ZTD illustrates these sites recorded low values compared with other sites. Figure 3.14 showed Huambo, Cuito and Lubango are in the plateau zone. Also, it presents high values of altitude compared with other sites. Thus, one can conclude the ZTD values decrease with increasing elevation. It is important to refer that these maps were interpolated for maximum, minimum and average annual values with all data available per station.

In Appendix B, one can find a description of the maximum, minimum and average values of ZTD per station. Here we presented the results spacially.

The climatological characterization of the ZTD in the study area is summarized in Figure 5.8.

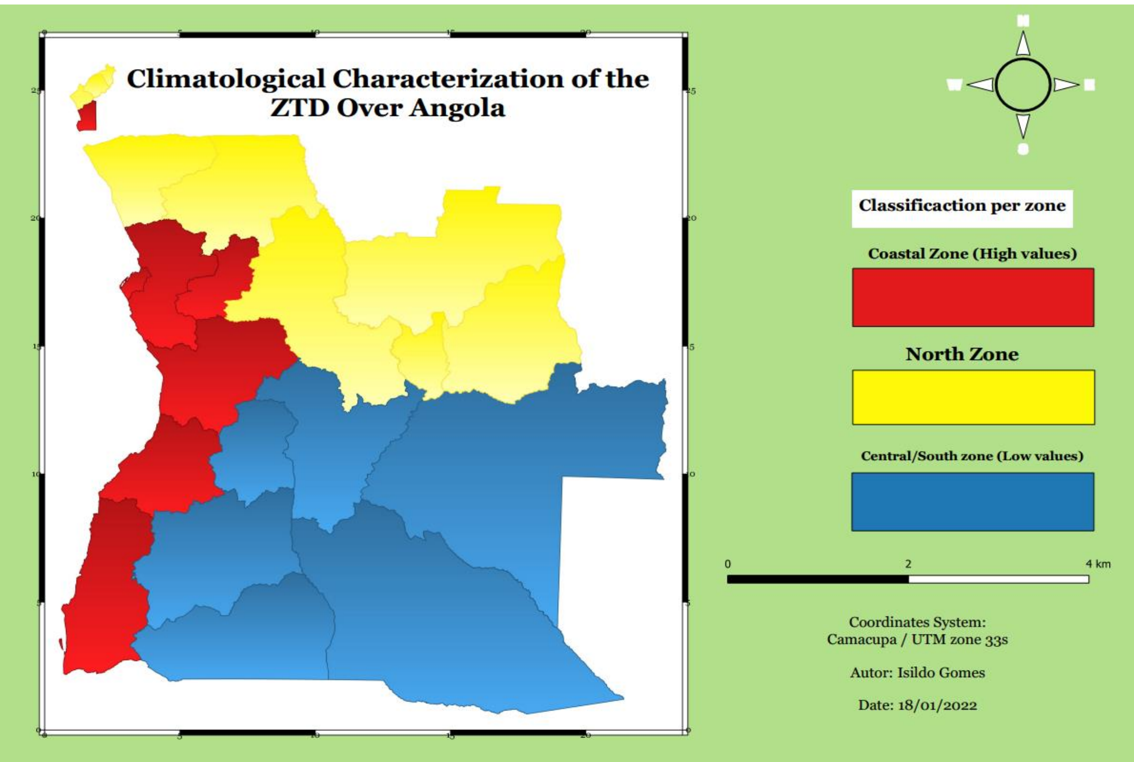

Figure 5.8 - Summary of the climatological characterization of the ZTD in the study area (Adapted from ZTD values available 11/5/2010 to 27/11/2021).

5.4 Validation of Estimated PWV

Since we already have the GNSS data processing solution (ZTD) it can be converted into the PWV. It is critical to note that this conversion will only be possible with the acquisition of temperature and pressure data. Unfortunately, the Luanda station is the only station that has this information. Thus, it will be the only station where the PWV was calculated, discussed, and analyzed.

It is essential to mention that an attempt was made to work with data from global models (ERA5). For the acquisition of temperature and pressure data.

We will analyse the data of the available PWV from 2/7/2020 to 20/7/2021 containing 258 days observation. Figure 5.9 shows the time-series variation values PWV at the LDIG station.

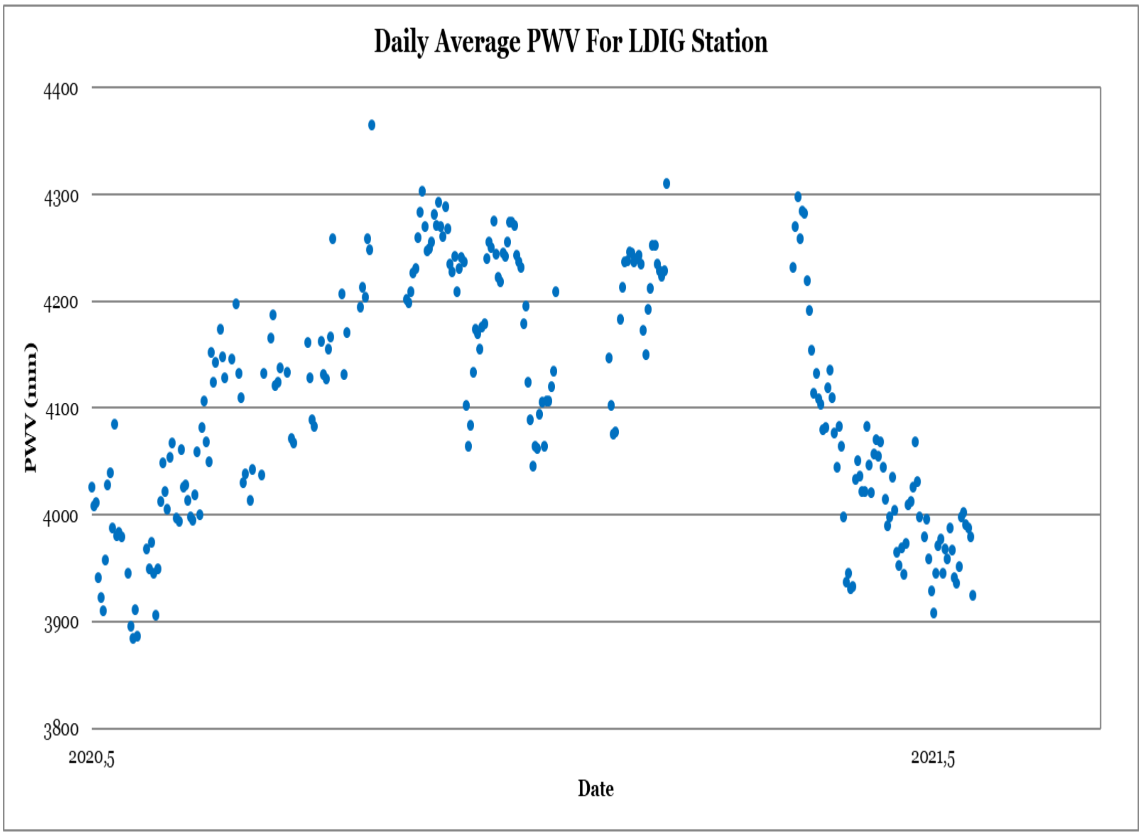

Figure 5.9 - Time-series variations average daily of the PWV at the LDIG station.

Figures 5.9 and 5.10 illustrates that the station also presents a significant seasonal variation which is directly correlated with the wet (high peak) and dry (low peak) seasons. According to the monthly average of all months available for the PWV solution the values recorded are: maximum of 4365 mm and the minimum value is 3884 mm.

Note that the maximum value recorded was in November which corresponds to the rainy season. The minimum value recorded was in which corresponds to the dry season.

In Figure 5.9 it can also be clearly observed the lack of some data for the period under analysis. Figure 5.10 illustrates this reality where one can observe the non-recording of the results for April.

Despite this failure, one can still clearly observe the consistency in the seasonal variation. Where high PWV values are in the wet months and low values are in the dry months. It is critical to note that a strong correlation is observed compared with Figure 5.5.

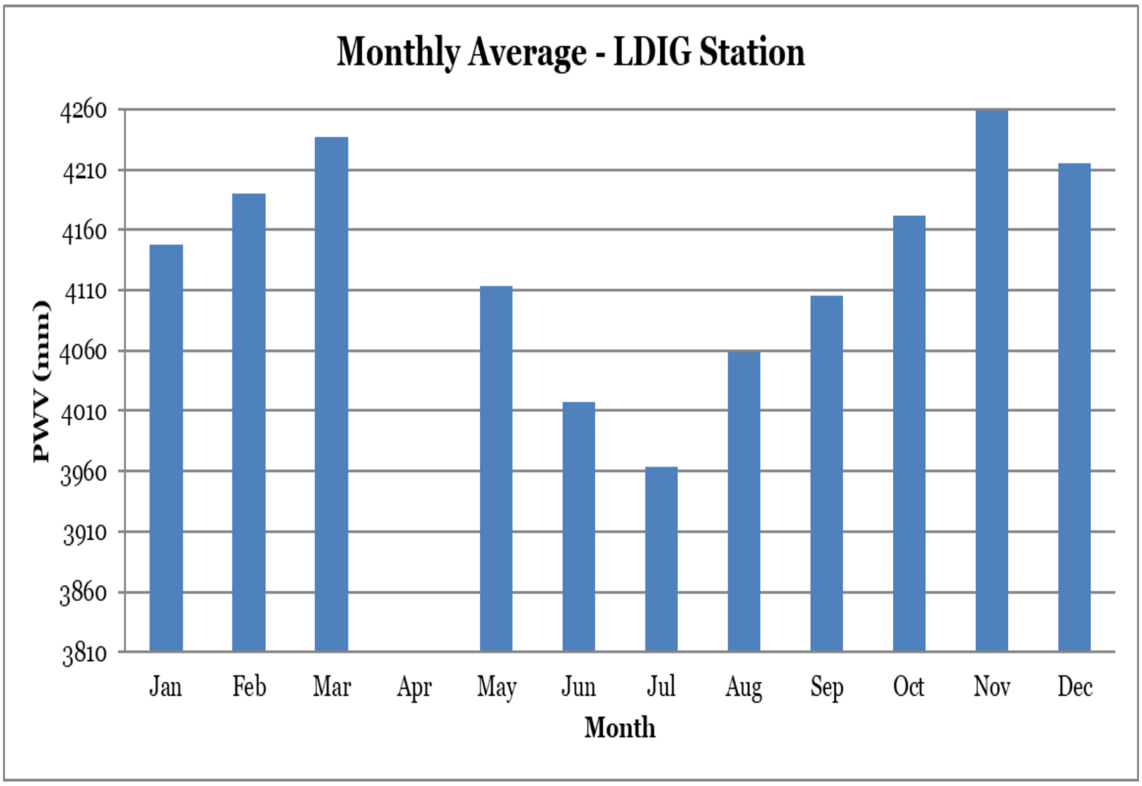

Figure 5.10 - The monthly Average of the PWV obtained from the LDIG station.

Chapter 6

Conclusion and future work

This work has analyzed ZTD for 16 GNSS stations in Angola for the period 2010-2021 and calculated PWV daily time-series variation for the station LDIG.

Analysis performed was supported by implementing the processing data flow:

- ✓ Download all data GNSS available from IGCA (through SEGAL);
- ✓ Download all meteorological observations data (Temperature and pressure) available from sensors collocated by the SEGAL group;
- ✓ Process the GNSS data to obtain the ZTD estimates;
- ✓ Convert ZTD to PWV.

In addition to the implementation of the system, it was carried out some analysis to evaluate the reliability of the implemented system, namely:

- ✓ **GNSS Data Availability:** Thus, assessments have been carried out to study how many files are missing. The conclusion is that the network has not been very reliable.
- ✓ **Meteorological Stations Reliability:** The same analysis has been carried out, for the meteorological data, but only two stations have been providing data since February 2020. This needs to be clearly improved.

Although the reliability of the GNSS network needs to be improved in order to guarantee near real-time data that can be used for weather forecasting. The historic GNSS data was sufficiently long to investigate the seasonal variations in ZTD correlate these with the dry and wet seasons in Angola and group them into coastal, northern, southern, and central regions. The results of this study are:

- ✓ The analysis of the time-series variation of the ZTD showed that is directly correlated with the wet and dry seasons.
- ✓ Their maximum values are correlated with wet months and minimum values with dry months.
- ✓ Thus, the maximum amplitude is directly correlated with maximum temperature and humidity.
- ✓ Their minimum amplitude is usually correlated with minimum temperature and altitude.
- ✓ ZTD values decrease with increasing elevation in Angola which is explained because in the Central Plateau the amount of PWV in the atmosphere is smaller than in the Coastal regions.

✓ The analysis of the time-series variation of PWV solution showed that is directly correlated with the ZTD values.

6.1 Final Notes

It is also important to note that the COVID-19 pandemic influenced the results of this work. It is not the main reason to have so much missing data on the servers (lack of maintenance and timely payment of the communications also created many data gaps). But the pandemic is the major reason why data is missing in the last years. Many stations needed to be revised in the past to get them up and running. Many stations upload the data but their upload on the servers sometimes did not happen for reasons that needed intervention. And with the borders closed, the technicians could not visit the stations to do maintenance.

Due to the lack of data, this work was to the study of daily ZTD and PWV time-series instead of the original objective to investigate short- and long-term variations of Precipitable Water Vapour (PWV) using GIS tools and GNSS data available all around the territory in Angola and the implications on its climate. It is hoped that the work will continue or become the topic of PhD research which would be the first of its kind for Angola

This dissertation has achieved its objective to provide an overview of the functionality of the GNSS stations in Angola together with the meteorological sensors placed in the framework of the project SUGGEST-AFRICA. It also explains how the data can be analysed to produce PWV time series.

As a personal note, this project was both challenging and rewarding as the goals were achieved. I was challenged to do an assignment entirely in English when my English needed improvement. It was an experience that will improve my speaking, reading and comprehension skills. I consider myself lucky to have the opportunity to analyse ZTD and PWV for the first time in Angola. And I also consider myself lucky to be part of and contribute to a project that will provide a better weather prediction in Angola.

6.2 Future Work

- ✓ There is need to Analyze the correlation between PWV and ZTD in more detail.
- ✓ Install more meteorological sensors near or at CORS in Angola.
- ✓ Establishing a method of short-term rainfall forecasting in Angola based on GNSS-derived PWV and its application.

Bibliography

Abbasy, S., Abbasi, M., Asgari, J., & Ghods, A. (2017). Precipitable water vapour estimation using the permanent single GPS station in Zanjan, Iran. *Meteorological Applications*, *24*(3), 415–422. https://doi.org/10.1002/met.1639

Alshawaf, F., Fuhrmann, T., Knöpfler, A., Luo, X., Mayer, M., Hinz, S., & Heck, B. (2015). Accurate Estimation of Atmospheric Water Vapor Using GNSS Observations and Surface Meteorological Data. *IEEE Transactions on Geoscience and Remote Sensing*, *53*(7), 3764–3771. https://doi.org/10.1109/TGRS.2014.2382713

Awk. (2021). *Linux awk command*. Available From: https://www.geeksforgeeks.org/awk-command-unixlinux-examples/

Azevedo, M. G. C. (2005). *Clima e fenomenologia da precipitação em Angola: climate and rainfall phenomenology in Angola* [UNIVERSIDADE DE ÉVORA]. http://hdl.handle.net/10174/15578

Baelen, J. Van, Aubagnac, J. P., & Dabas, A. (2005). Comparison of near-real time estimates of integrated water vapor derived with GPS, radiosondes, and microwave radiometer. *Journal of Atmospheric and Oceanic Technology*, *22*(2), 201–210. https://doi.org/10.1175/JTECH-1697.1

Benevides, P., Catalão, J., Miranda, P., & Chinita, M. J. (2013). Analysis of the relation between GPS tropospheric delay and intense precipitation. *Remote Sensing of Clouds and the Atmosphere XVIII; and Optics in Atmospheric Propagation and Adaptive Systems XVI*, *8890*(October), 88900Y. https://doi.org/10.1117/12.2028732

Benvenuto, L., Marzocchi, R., Ferrando, I., Federici, B., & Sguerso, D. (2018). A procedure to manage open access data for post-processing in GIS environment. *PeerJ Prepr.*, *6*, 7. https://doi.org/10.7287/peerj.preprints.27227

Bevis, M., Businger, S., Herring, T. A., Rocken, C., Anthes, R. A., & Ware, R. H. (1992). GPS meteorology: remote sensing of atmospheric water vapor using the global positioning system. *Journal of Geophysical Research*, *97*(D14), 787–801. https://doi.org/10.1029/92jd01517

Bevis, Michael, Businger, S., Chiswell, S., Anthes, R. A., Rocken, C., & Ware, R. H. (1994). GPS Meteorology: Mapping Zenith Wet Delays onto Precipitable Water. *Journal of Applied Meteorology an Climatology*, *33*(3), 379–386. https://doi.org/10.1175/1520-0450(1994)033<0379:GMMZWD>2.0.CO;2

Bleisch, R., Kämpfer, N., & Haefele, A. (2011). Retrieval of tropospheric water vapour by using spectra of a 22 GHz radiometer. *Atmospheric Measurement Techniques*, *4*(9), 1891–1903. https://doi.org/10.5194/amt-4-1891-2011

Blume, F. (2010). *GPS Data Collection Methods*. UNAVACO. https://kb.unavco.org/kb/article/gps-data-collection-methods-70.html

Boehm, J, Niell, A., Tregoning, P., & Schuh, H. (2006). Global Mapping Function (GMF): A new empirical mapping function based on numerical weather model data. *Geophysical*

Research Letters, *33*(January), 1–4. https://doi.org/10.1029/2005GL025546

Boehm, Johannes, Werl, B., & Schuh, H. (2006). Troposphere mapping functions for GPS and very long baseline interferometry from European Centre for Medium-Range Weather Forecasts operational analysis data. *Journal of Geophysical Research: Solid Earth*, *111*(2), 1–9. https://doi.org/10.1029/2005JB003629

Bos, M. S., Fernandes, R. M. S., Williams, S. D. P., & Bastos, L. (2012). Fast Error Analysis of Continuous GNSS Observations with Missing Data. *J.Geod*, *87*(4), 1–20. https://doi.org/10.1007/s00190-012-0605-0.

Bosilovich, M. G., Lucchesi., R., & M, S. (2016). MERRA-2: File Specification. *GMAO Office Note No. 9 (Version 1.1)*, 73. https://gmao.gsfc.nasa.gov/pubs/docs/Bosilovich785.pdf

Bosy, J., Kaplon, J., Rohm, W., Sierny, J., & Hadas, T. (2012). Near real-time estimation of water vapour in the troposphere using ground GNSS and the meteorological data. *Annales Geophysicae*, *30*(9), 1379–1391. https://doi.org/10.5194/angeo-30-1379-2012

Bosy, Jaroslaw, Rohm, W., Borkowski, A., Kroszczynski, K., & Figurski, M. (2010). Integration and verification of meteorological observations and NWP model data for the local GNSS tomography. *Atmospheric Research*, *96*(4), 522–530. https://doi.org/10.1016/j.atmosres.2009.12.012

Boutiouta, S., & Lahcene, A. (2013). Preliminary study of GNSS meteorology techniques in Algeria. *International Journal of Remote Sensing*, *34*(14), 5105–5118. https://doi.org/10.1080/01431161.2013.786850

Cai, C. (2009). Precise point positioning using dual-frequency GPS and GLONASS measurements [UNIVERSITY OF CALGARY]. In *Masters Abstracts International* (Issue August). http://www.ucalgary.ca/engo_webdocs/YG/09.20291_ChangshengCai.pdf

Climat. (2021). *Climat - Angola*. Available From: https://www.climatsetvoyages.com/climat/angola

CLOG6. (2021). *Angola*. Available From: http://www.clog6.com/Angola.html

Couto, R. G. (2016). *Automatic Local Coordinates Evaluating and automating methods to estimating 3D coordinates with respect to a specific Datum* (Issue October) [UNIVERSIDADE DA BEIRA INTERIOR]. http://hdl.handle.net/10400.6/7726

Crontab. (2021). *Linux crontab command*. Available From:

Dousa, J. (2004). Evaluation of tropospheric parameters estimated in various routine GPS analysis. *Physics and Chemistry of the Earth, Parts A/B/C*, *29*(2–3), 167–175. https://doi.org/10.1016/j.pce.2004.01.011

Dw. (2014). *ANALYSIS OF HISTORIC RAINFALL DATA FOR ANGOLA TO IMPROVE UNDERSTANDING OF RAINFALL VARIABILITY AND ITS IMPLICATIONS FOR FLOODING AND EROSION A WORKING PAPER OF THE PROJECT ON "WATER RESOURCE MANAGEMENT UNDER CHANGING CLIMATE IN ANGOLA'S COASTAL SETTLEMENTS" DEVELOPMENT WORKSHOP ANGOLA Analysis of Historic Rainfall Data for Angola*. https://www.angonet.org/dw/sites/default/files/online_lib_files/analysis_of_angolan_historic_rainfall_data.pdf

ECMWF. (2021). *European Centre for Medium-Range Weather Forecasts. 2016, updated monthly. ECMWF IFS CY41r2 High-Resolution Operational Forecasts.* Research Data Archive at the National Center for Atmospheric Research, Computational and Information Systems Laboratory. https://rda.ucar.edu/datasets/ds113.1/

Elhaty, N. M., Abdelfatah, M. A., Mousa, A. E., & El-fiky, G. S. (2019). REVIEW GNSS meteorology in Egypt : Modeling weighted mean temperature from radiosonde data. *Alexandria Engineering Journal*, *58*(2), 443–450. https://doi.org/10.1016/j.aej.2019.04.001

ERA-Interimim. (2021). *European Centre for Medium-Range Weather Forecasts. 2009, updated monthly. ERA-Interim Project.* Research Data Archive at the National Center for Atmospheric Research, Computational and Information Systems Laboratory. https://rda.ucar.edu/datasets/ds627.0/

Fernandes, R., Gomes, I., Vicente, A., Bala, I., Bos, M., & Almeida, P. (2021). Evaluating the estimation of GNSS-based PWV in Angola, Mozambique, and Nigeria. *AGU*. https://agu.confex.com/agu/fm21/meetingapp.cgi/Paper/926981

Fernandes, R., Jatau, B., Edozie, U., Armando, D., & Januário, J. (2011). Rigorous estimation of the coordinates of two new national permanent GNSS networks in Africa. *FiIG 2011*, *May*, 1–15. https://www.oicrf.org/-/rigorous-estimation-of-the-coordinates-of-two-new-national-permanent-gnss-networks-in-africa-nignet-nigeria-and-repangol-angola-

Fernandes, R. M. S., Bastos, L., Miranda, J. M., & Lourenço, N. (2006). Defining the plate boundaries in the Azores region. *Journal of Volcanology and Geothermal Research*, *156*(1–2), 1–9. https://doi.org/10.1016/j.jvolgeores.2006.03.019

Ferrando, I., Federici, B., & Sguerso, D. (2018). 2D PWV monitoring of a wide and orographically complex area with a low dense GNSS network. *Earth, Planets and Space*, *70*(1), 21. https://doi.org/10.1186/s40623-018-0824-6

Gao, Y. (2006). *Precise point positioning and its challenges, aided-gnss and signal tracking*. Inside GNSS. https://www.insidegnss.com/auto/NovDec06GNSSSolutions.pdf

Gonçalves, H. V. (2016). *Automatization of Real Time GNSS Data Acquisition , Validation , Processing for Water* (Issue June) [Universidade da Beira Interior]. http://hdl.handle.net/10400.6/6077

GPS. (2020). *GPS.gov: New Signals*. Available From: https://www.gps.gov/systems/gps/modernization/civilsignals/

He, Q., Shen, Z., Wan, M., & Li, L. (2020). Precipitable Water Vapor Converted from GNSS-ZTD and ERA5 Datasets for the Monitoring of Tropical Cyclones. *IEEE Access*, *8*(May), 87275–87290. https://doi.org/10.1109/ACCESS.2020.2991094

Hernández-Pajares, M., Juan, J. M., Sanz, J., Colombo, O. L., & Van Der Marel, H. (2001). A new strategy for real-time integrated water vapor determination in WADGPS networks. *Geophysical Research Letters*, *28*(17), 3267–3270. https://doi.org/10.1029/2001GL012930

Hersbach, H., Bell, B., Berrisford, P., Biavati, G., Horányi, A., Muñoz Sabater, J., Nicolas, J., Peubey, C., Radu, R., Rozum, I., Schepers, D., Simmons, A., Soci, C., Dee, D., & Thépaut, J.-N. (2021). *ERA5 hourly data on single levels from 1979 to present*. Copernicus Climate Change Service (C3S) Climate Data Store (CDS). https://doi.org/10.24381/cds.adbb2d47

Huang, X.-Y., & García-Moya, J. A. (2003). *Targeting optimal use of GPS humidity measurements in meteorology Special Issue "Remote Sensing Technologies for the Analysis and Modeling of Atmospheric Events" View project SINGV-A tropical Convective-Scale NWP/Nowcasting Capability for Singapore View project*. https://www.researchgate.net/publication/253678813

Huntley, B. J., Russo, V., Lages, F., & Almeida, N. F. de. (2019). *Biodiversity of Angola. Science & Conservation: A Modern Synthesis* (B. Huntley, V. Russo, F. Lages, & N. Almeida (eds.); 1.ª Edição). http://www.unescolifeonland.com/fotos/editor2/BiodiversidadeAngola_.pdf

IGS. (2021). *IGS Orbits*. Available From: https://www.igs.org/acc/gps-only/#ultra-rapid

INAMET. (n.d.). *Instituto Nacional de Meteorologia e Geofísica (INAMET)*. CIENCIA.AO. Retrieved April 30, 2021, from https://ciencia.ao/sistema-nacional-de-ciencia/instituicoes-de-investigacao-cientifica-e-desenvolvimento/92-instituto-nacional-de-geofisica-e-meteorologia

INE. (2014). Resultados Preliminares Do Recenseamento Geral da População e da Habitação de Angola 2014. *Report*, 1–137. http://censo.ine.gov.ao/xportal/xmain?xpid=censo2014

IOGP. (2021). *Camacupa 1948 / UTM zone 33S*. GeoReporsitory. https://epsg.org/crs_22033/Camacupa-UTM-zone-33S.html

IPM. (2021). *Radiossondagem*. Available From: https://www.ipma.pt/pt/educativa/observar.tempo/index.jsp?page=altitude.xml

IPMA. (2021, November 11). *Precipitable Water Vapor Derived from GNSS data in Angola*. Available From: https://www.ipma.pt/en/publicacoes/meteorologia/index.jsp?page=NWP-workshop-2021.xml

Isioye, Olalekan A., Combrinck, L., Botai, J. O., & Munghemezulu, C. (2015). The potential for observing African weather with GNSS remote sensing. *Advances in Meteorology*, *2015*(January), 16. https://doi.org/10.1155/2015/723071

Isioye, Olalekan Adekunle, Combrinck, L., & Botai, J. O. (2017). Retrieval and analysis of precipitable water vapour based on GNSS, AIRS, and reanalysis models over Nigeria. *International Journal of Remote Sensing*, *38*(20), 5710–5735. https://doi.org/10.1080/01431161.2017.1346401

Jesus, F. S. De. (2018). *Angola – Características gerais, clima, relevo e hidrografia*. GeografiaOpinativa. https://www.geografiaopinativa.com.br/2018/05/angola-caracteristicas-gerais-clima-relevo-e-hidrografia.html

Jin, S., & Luo, O. F. (2009). Variability and climatology of PWV from global 13-year GPS observations. *IEEE Transactions on Geoscience and Remote Sensing*, *47*(7), 1918–1924. https://doi.org/10.1109/TGRS.2008.2010401

Jones, J., Guerova, G., Dousa, J., Dick, G., Pottiaux, Siebren de Haan Eric Bock, O., & Malderem, R. P. R. Van. (2020). Advanced GNSS Tropospheric Products for Monitoring Severe Weather Events and Climate. In J. Jones, G. Dousa, G. Dck, S. Pottiaux, O. Bock, &

R. Malderen (Eds.), *Advanced GNSS Tropospheric Products for Monitoring Severe Weather Events and Climate*. Springer Nature Switzerland AG. https://doi.org/10.1007/978-3-030-13901-8

Joshi, S., Kumar, K., Pande, B., & Pant, M. C. (2013). GPS-derived precipitable water vapour and its comparison with MODIS data for Almora, Central Himalaya, India. *Meteorology and Atmospheric Physics*, *120*(3–4), 177–187. https://doi.org/10.1007/s00703-013-0242-z

JPL. (2021). *The Global Differential GPS System*. Available From: https://www.gdgps.net/

Kanhere, A. V., Gupta, S., Shetty, A., & Gao, G. (2022). Improving GNSS Positioning using Neural Network-based Corrections. *Available From:* http://arxiv.org/abs/2110.09581

Kaplan, E. D., & Hegarty, C. J. (2006). *Understanding GPS: Principles and Aplications* (E. Kaplan & C. Hegarty (eds.); 2nd ed.). Boston/London: Artech House. https://nguyenduyliemgis.files.wordpress.com/2014/09/understanding-gps-principles-and-applications-2006.pdf

Kitoko, D., & Painho, M. (2015). A informação geográfica em Angola : subsídios para a elaboração de uma estratégia e plano de ação de apoio à implementação do plano nacional de informação geográfica Autor (es): Publicado por : URL persistente : DOI : Accessed : Kitoko , Dilson ; Painho. In J. G. dos Santos, C. Fonte, R. F. de Figueiredo, A. Cardoso, G. Gonçalves, J. P. Almeida, & S. Baptista (Eds.), *Atas das I Jornadas Lusófonas de Ciências e Tecnologias de Informação Geográfica* (pp. 512–531). Imprensa da Universidade de Coimbra. https://doi.org/10.14195/978-989-26-0983-6_33

Kitoko, D. Z. (2014). *A Informação Geográfica em Angola: Subsídios para Elaboração de uma Estratégia e Plano de Ação de apoio à implementação do Plano Nacional de Informação Geográfica* [Instituto Superior de Estatística e Gestão de Informação da Universidade Nova de Lisboa]. https://run.unl.pt/bitstream/10362/14542/4/TSIG0103_final.pdf

Lange, A. F., & Gilbert, C. (2005). Using GPS for GIS data capture. *Geographical Information Systems*, 467–476. http://www.trimble.com/satviz.

Liu, C., Zheng, N., Zhang, K., & Liu, J. (2019). A new method for refining the GNSS-derived precipitable water vapor map. *Sensors (Switzerland)*, *19*(3). https://doi.org/10.3390/s19030698

Lo, J., & El-mowafy, A. (2011). Interpolation of the GNSS Wet Troposphere Delay. *Interpolation of the GNSS Wet Troposphere Delay*, *November*, 425–438. https://ro.ecu.edu.au/ecuworks2011/789

Munin, E., Blais, A., & Couellan, N. (2019). Convolutional Neural Network for Multipath Detection in GNSS Receivers. In *Available From:* IEEE Xplore. https://arxiv.org/abs/1911.02347

MWRa. (2021). *MICROWAVE RADIOMETER*. Available From: https://www.arm.gov/capabilities/instruments/mwr

MWRb. (2021). *MICROWAVE RADIOMETER APPLICATIONS*. Available From: http://radiometrics.com/applications/

Nas. (2021). *Nasa jet Propulsion Laboratory (JPL) - Space mission and science news, videos* *and images*. Avalaible From: https://www.jpl.nasa.gov/

NASa. (2021). *NASA/JPL. Automatic precise point service*. Available From: https://pppx.gdgps.net/

NASb. (2021). *NASA/JPL. Gipsy-oasis*. Available From: https://gipsy-oasis.jpl.nasa.gov/index.php?page=data

NOAA. (2021). *National Centers for Environmental Prediction/National Weather Service/NOAA/U.S. Department of Commerce. 1994, updated monthly.* Research Data Archive at the National Center for Atmospheric Research, Computational and Information Systems Laboratory. https://rda.ucar.edu/datasets/ds090.0/

Nykiel, G., Figurski, M., & Baldysz, Z. (2019). Analysis of GNSS sensed precipitable water vapour and tropospheric gradients during the derecho event in Poland of 11th August 2017. *Journal of Atmospheric and Solar-Terrestrial Physics*, *193*(December 2018), 105082. https://doi.org/10.1016/j.jastp.2019.105082

Okey, O. W. (2015). *Implementation of NTRIP and Management System in NIGNET Network* (Issue June) [UNIVERSIDADE DA BEIRA INTERIOR]. https://ubibliorum.ubi.pt/handle/10400.6/5840

Petovello, M. (2016). *Wath are the challenges of ray-tracing for GNSS aplications?* Available From: www.insidegnss.com

Pinto, I. (2009). *Introdução aos Sistemas de Informação Geográfica (SIG)*. 37. https://docplayer.com.br/115249-Informacao-geografica-sig-ines-pinto-instituto-de-investigacao-cientifica-tropical.html

Putri, N., Landskron, D., & Böhm, J. (2020). Assessing the performance of Vienna Mapping Functions 3 for GNSS stations in Indonesia using Precise Point Positioning. *Advances in Geosciences*, *50*, 77–86. https://doi.org/10.5194/adgeo-50-77-2020

Revuelta, A., Rodriguez, C., Mateos, J., & Garmendia, J. (1985). A model for the estimation of precipitable water. *Tellus, Series B*, *37 B*(4–5), 210–215. https://doi.org/10.3402/tellusb.v37i4-5.15025

Rizos, C, Higgins, M. B., & Hewitson, S. (2005). NEW GNSS DEVELOPMENTS AND THEIR IMPACT ON SURVEY SERVICE PROVIDERS AND SURVEYORS. In Chris Rizos, M. Higgins, & S. Hewitson (Eds.), *Proceedings of SSC2005 Spatial Intelligence, Innovation and Praxis* (Issue September, pp. 1–14). Spatial Sciences Institute. https://www.fig.net/organisation/comm/5/gnss/rizos_etal2005a.pdf

Rohm, W., Yuan, Y., Biadeglgne, B., Zhang, K., & Marshall, J. Le. (2014). Ground-based GNSS ZTD/IWV estimation system for numerical weather prediction in challenging weather conditions. *Atmospheric Research*, *138*(10), 30. https://doi.org/10.1016/j.atmosres.2013.11.026

Rsync. (2021). *Linux rsync command*. Available From: https://linuxize.com/post/how-to-use-rsync-for-local-and-remote-data-transfer-and-synchronization/

Sadoun, B., & Al-Bayari, O. (2006). On the inclusion of geographic information systems (GIS) in global navigation satellite systems (GNSS). *International Journal of Communication Systems*, *20*, 385–396. https://doi.org/10.1002/dac.868

Sadoun, B., & Al-Bayari, O. (2007). LBS and GIS technology combination and applications. *2007 IEEE/ACS International Conference on Computer Systems and Applications, AICCSA 2007*, 578–583. https://doi.org/10.1109/AICCSA.2007.370940

SEGAL. (2017). *ZTD2PWV*. SEGAL-UBI.

Sguerso, D., Labbouz, L., & Walpersdorf, A. (2013). 14 years of GPS tropospheric delays in the French-Italian border region: A data base for meteorological and climatological analyses. *International Archives of the Photogrammetry, Remote Sensing and Spatial Information Sciences - ISPRS Archives*, *40*(5W3), 7–14. https://doi.org/10.5194/isprsarchives-XL-5-W3-7-2013

Szafranek, K., Nykiel, G., Baldysz, J. B. Z., & Figurski, M. (2014). ANALYSIS OF LONG TIME SERIES OF TROPOSPHERIC PARAMETERS DERIVED FROM GPS DATA PROCESSING. In K. Szafranek, G. Nykiel, J. Baldysz, & M. Figurski (Eds.), *14th International Multidisciplinary Scientific GeoConference SGEM 2014 GPS* (p. 8). Faculty of Civil Engineering and Geodesy. https://www.academia.edu/20117886/Analysis_of_long_time_series_of_tropospheric_parameters_derived_from_GPS_data_processing

Taha, A. (2008). *Mapping The Underworld: Integrated GNSS Based Positioning and GIS Based GNSS Simulation* (Issue November) [Institute of Engineering Surveying and Space Geodesy School of Civil Engineering]. https://doi.org/10.13140/RG.2.2.32731.72489

TCSH. (2021). *Technology Tips: Csh, Tcsh*. University of Washington.

Teromovigo. (2019). *TeroNet Platform*. Available From: https://teromovigo.ubi.pt/wp-content/uploads/2019/10/TeroNet-Users-Manual-English-version-20191031.pdf

Ulukavak, M. (2019). Evaluation of GNSS Data with Internet Based Services: The Case of HRUH Station. *Open Access Books Built by Scientists, for Scientists*, 73–88. https://doi.org/10.5772/intechopen.79064

Van der Marel, H. (2004). COST-716 demonstration project for the near real-time estimation of integrated water vapour from GPS. *Physics and Chemistry of the Earth, Parts A/B/C*, *29*(2–3), 187–199. https://doi.org/10.1016/j.pce.2004.01.001

Vedel, H., & Huang, X. Y. (2004). Impact of ground based GPS data on numerical weather prediction. *Journal of the Meteorological Society of Japan*, *82*(1 B), 459–472. https://doi.org/10.2151/jmsj.2004.459

Weibel, R., & Dutton, G. (1999). Generalising spatial data and dealing with multiple representations. *Geographical Information Systems*, *1*, 125–155. https://www.geos.ed.ac.uk/~gisteac/gis_book_abridged/files/ch10.pdf

Won, J., Park, K., Ha, J., & Cho, J. (2010). Effects of Tropospheric Mapping Functions on GPS Data Processing. *Journal of Astronomy and Space Sciences*, *27*(1), 21–30. https://doi.org/10.5140/JASS.2010.27.1.021

Xavier, J. A. (2013). *Reconstrucción de la variabilidad pluviométrica en Angola en el periodo* [UNIVERSIDAD COMPLUTENSE DE MADRID]. https://eprints.ucm.es/id/eprint/23513/1/T34907.pdf

Yao, Y., Shan, L., & Zhao, Q. (2017). Establishing a method of short-term rainfall forecasting based on GNSS-derived PWV and its application. *Scientific Reports*, *7*(1), 1–11. https://doi.org/10.1038/s41598-017-12593-z

Zhang, Q., Ye, J., Zhang, S., & Han, F. (2018). Precipitable water vapor retrieval and analysis by multiple data sources: Ground-based GNSS, radio occultation, radiosonde, microwave satellite, and NWP reanalysis data. *Journal of Sensors*, *2018*(December), 13. https://doi.org/10.1155/2018/3428303

Zhao, Q., Yao, Y., Yao, W. Q., & Li, Z. (2018). Near-global GPS-derived PWV and its analysis in the El Niño event of 2014-2016. *Journal of Atmospheric and Solar-Terrestrial Physics*, *179*(April), 69–80. https://doi.org/10.1016/j.jastp.2018.06.016

Zhao, Q., Yao, Y., Yao, W., & Zhang, S. (2019). GNSS-derived PWV and comparison with radiosonde and ECMWF ERA- Interim data over mainland China. *Journal of Atmospheric and Solar-Terrestrial Physics*, *182*(November 2018), 85–92. https://doi.org/10.1016/j.jastp.2018.11.004

Zumberge, J. F., Heflin, M. B., Jefferson, D. C., Watkins, M. M., & Webb, F. H. (1997). Precise point positioning for the efficient and robust analysis of GPS data from large networks. *Journal of Geophysical Research: Solid Earth*, *102*(B3), 5005–5017. https://doi.org/10.1029/96jb03860

Appendix A

Data availability per year per station

This appendix shows for each station the percentage of available data per year.

Figure A.1 shows the percentage value that the Benguela station recorded.

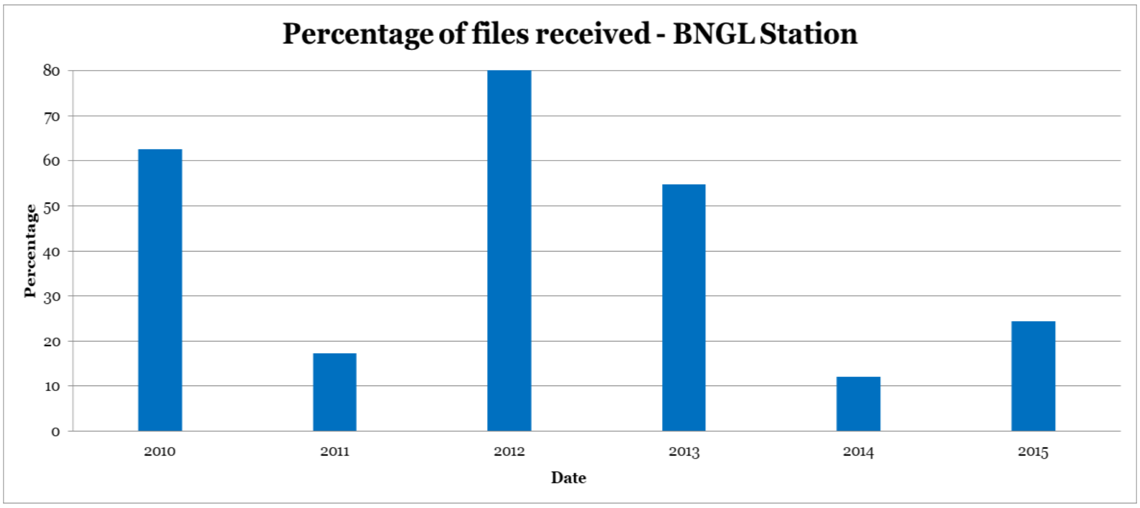

Figure A.1 - The Total possible percentage value of the Benguela station per year.

Figure A.1 shows 2012 was the year with the highest percentage value of 80.3% which corresponds to 294 days. In 2014 only 12% of data was observed which corresponds to 44 days.

Figure A.2 illustrates the percentage values that the Caxito station recorded per year.

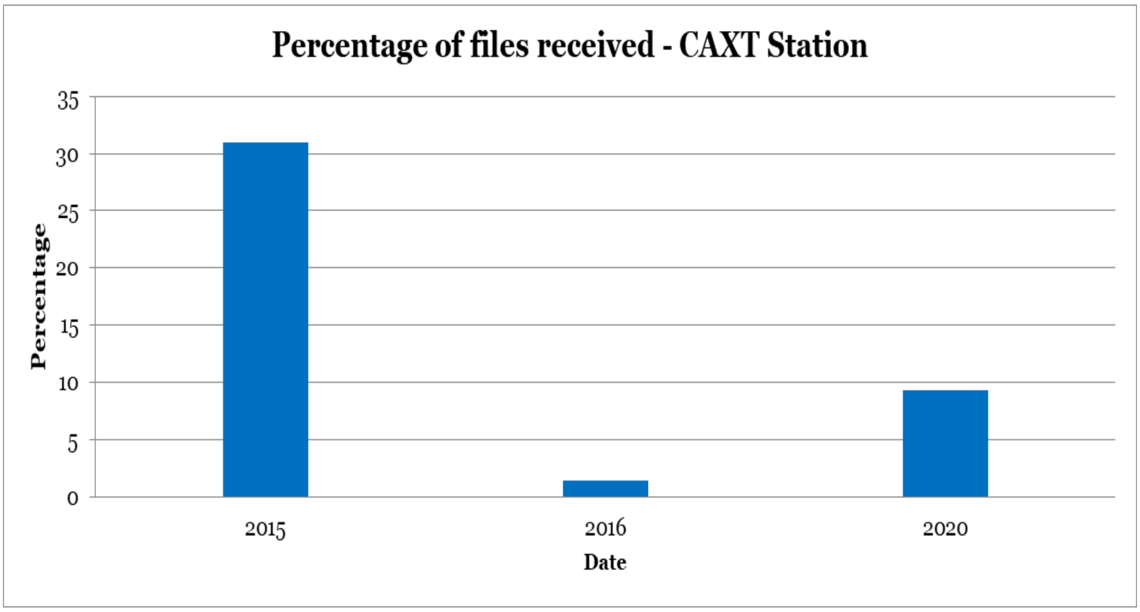

Figure A.2 - The Total possible percentage value of the Caxito station per year.

We found that, 2015 was the year with the highest percentage value of 31% which corresponds to about 113 days of data. In 2016 only 1.4% of data was collected which corresponds to five days.

Figure A.3 shows the percentage values that the Cabinda station recorded. In 2015 the most data were received with a percentage of 36% which corresponds to 131 days. In 2016 only 0.6% of data was received which corresponds to only 2 days.

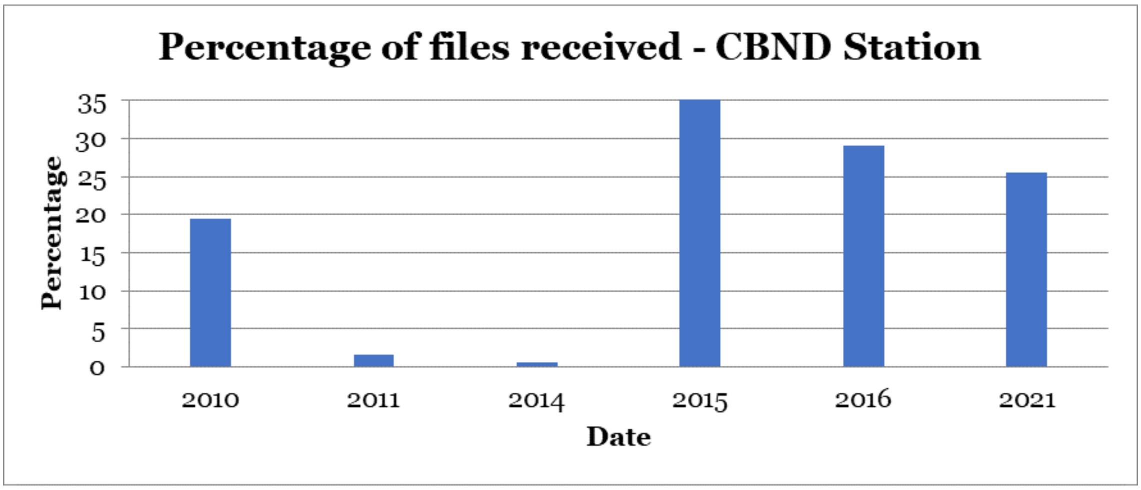

Figure A.3 - The Total possible percentage value of the Cabinda station per year.

Figure A.4 illustrates a certain balance in the high percentage values at the Cuito station. In 2014 and 2015 almost the same amount of data was stored with 2015 having just 3% more data (79.2%, 289 days).

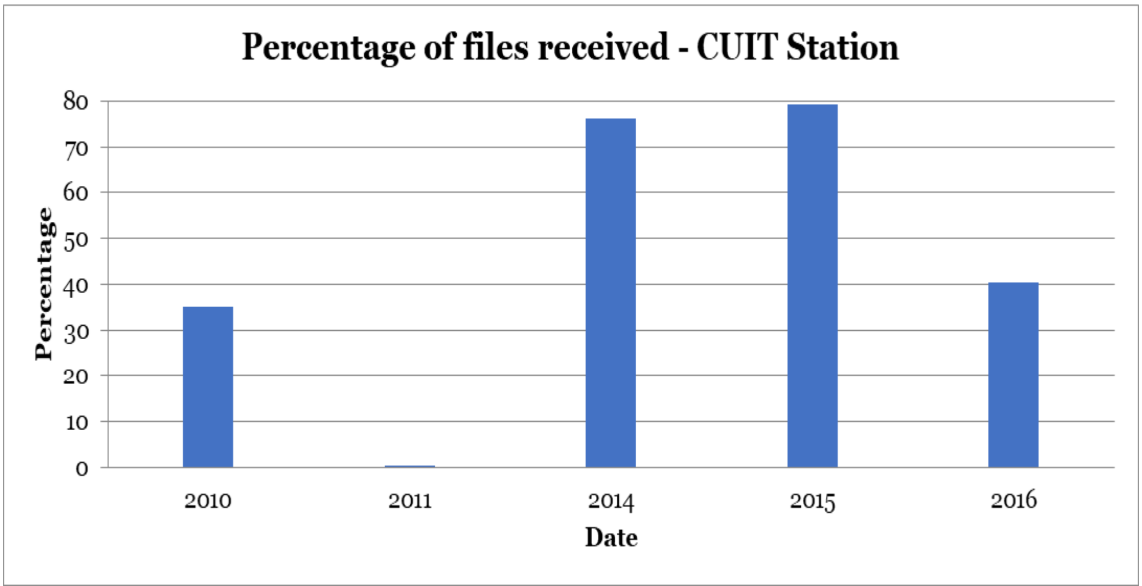

Figure A.4 - The Total possible percentage value of the Cuito station per year.

The lowest amount of data was collected in 2011 (0.3%, 1 day). Figure A.5 presents almost the same amount of data for station Huambo in the years 2010 and 2011, the difference being only one day in the transmission of information.

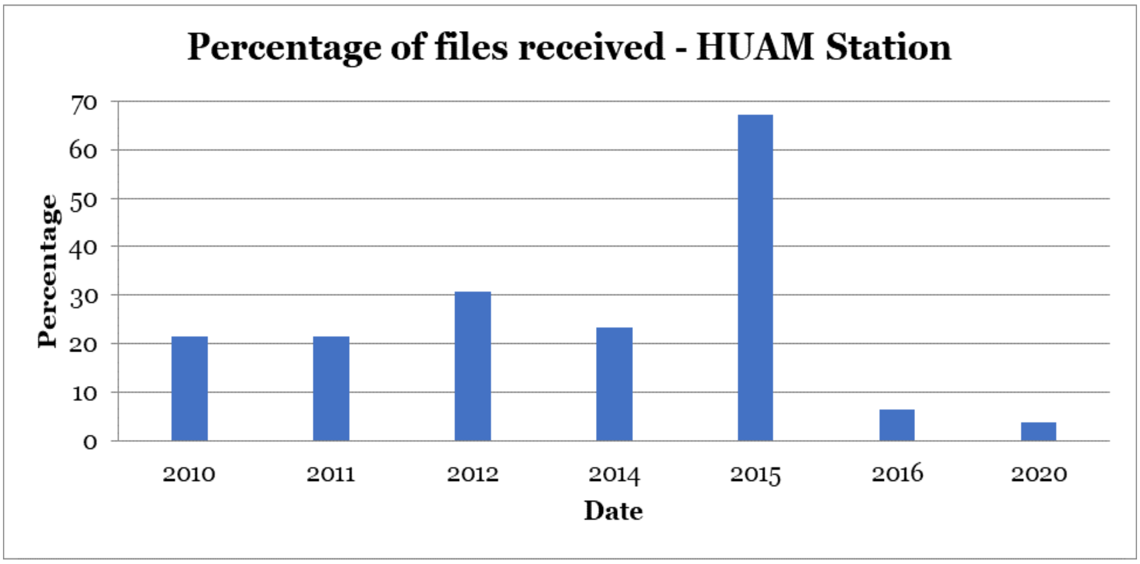

Figure A.5 - The Total possible percentage value of the Huambo station per year.

Figure A.5 shows that 2015 has a high percentage values 67.1% which corresponds to 245 days of data. In 2020, only 3.8% of data was stored which corresponds to 14 days. Figure A.6 illustrates the percentage values that the Lubango station recorded and is like Figure A.4 with the difference that in 2016 only 2.2% of data was collected which corresponds to 8 days.

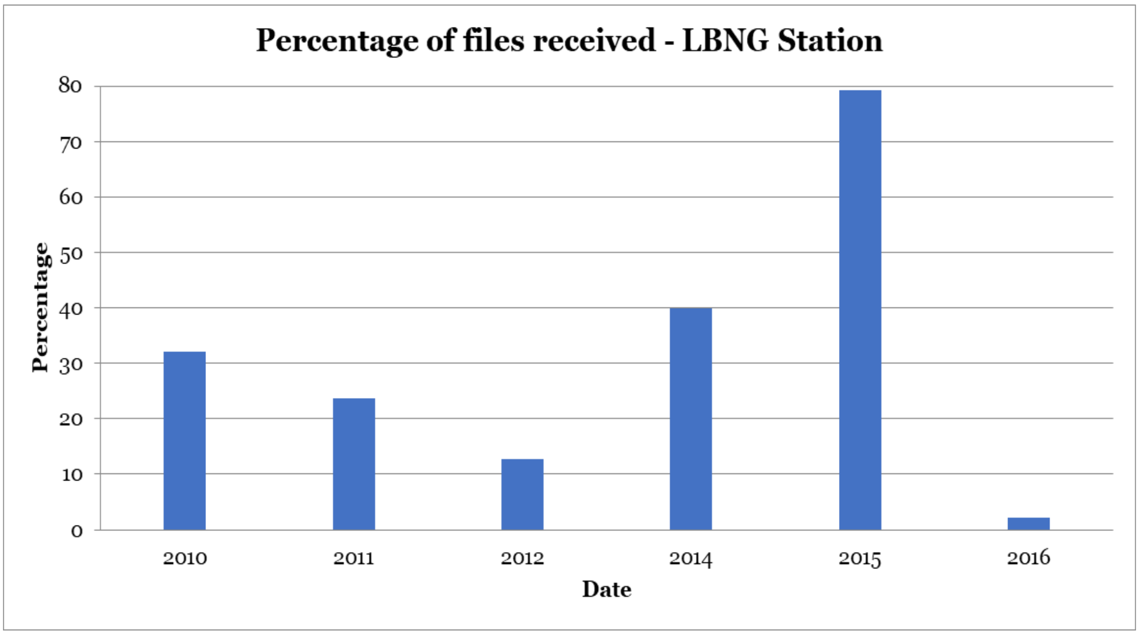

Figure A.6 - The Total possible percentage value of the Lubango station per year.

Figure A.7 illustrates the percentage values of the Luanda station where more data were recorded high value than other station, 94.2% in 2015 which corresponds to 344 days. The same station presented in 2014 with a low value of 9.9% or 39 days of data.

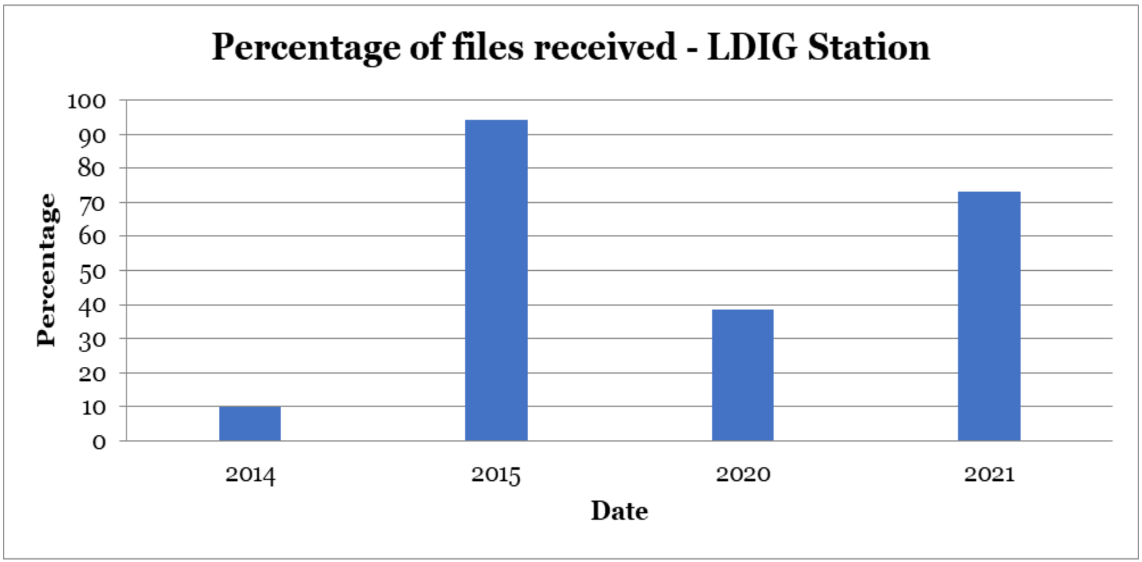

Figure A.7 - The Total possible percentage value of the Luanda station per year.

Figure A.8 presents a curious behaviour for station Luena in the years 2014 and 2015 compared with Figure A.4 when they have almost the same percentage of data, around 87% or 319 days. The lowest amount of data occurred in 2016 (2.2% or eight days).

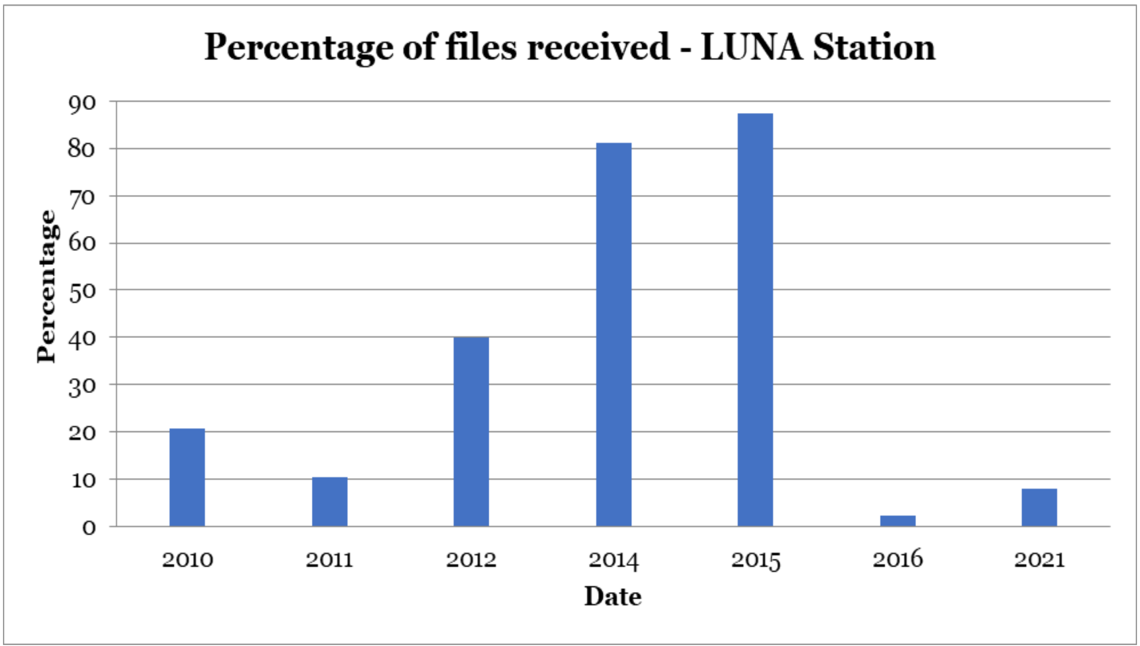

Figure A.8 - The Total possible percentage value of the Luena station per year.

Figure A.9 illustrates the records of the station Mbanza that showed much lower percentage values compared to the other stations. 2010 showed the highest value with 22.7% (88 days). 2011 and 2012 were observed the two years with low values recorded with the latter only having 0.8% or 8 days of data.

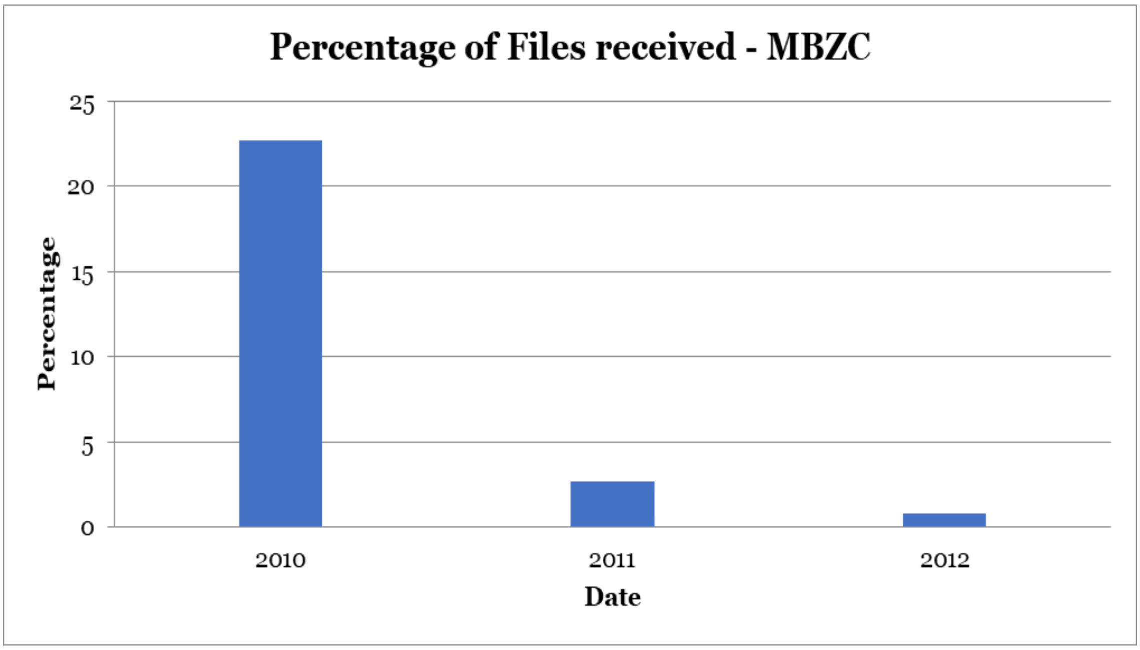

Figure A.9 - The Total possible percentage value of the Mbanza Congo station per year.

Figure A.10 also illustrates a certain stability in the high percentage values for station Malanje over the years. Figure A.10 shows the maximum percentage is obtained in 2010 with a value of 30.1% (110 days) while the lowest percentage occurred in 2012 (3% 11 days).

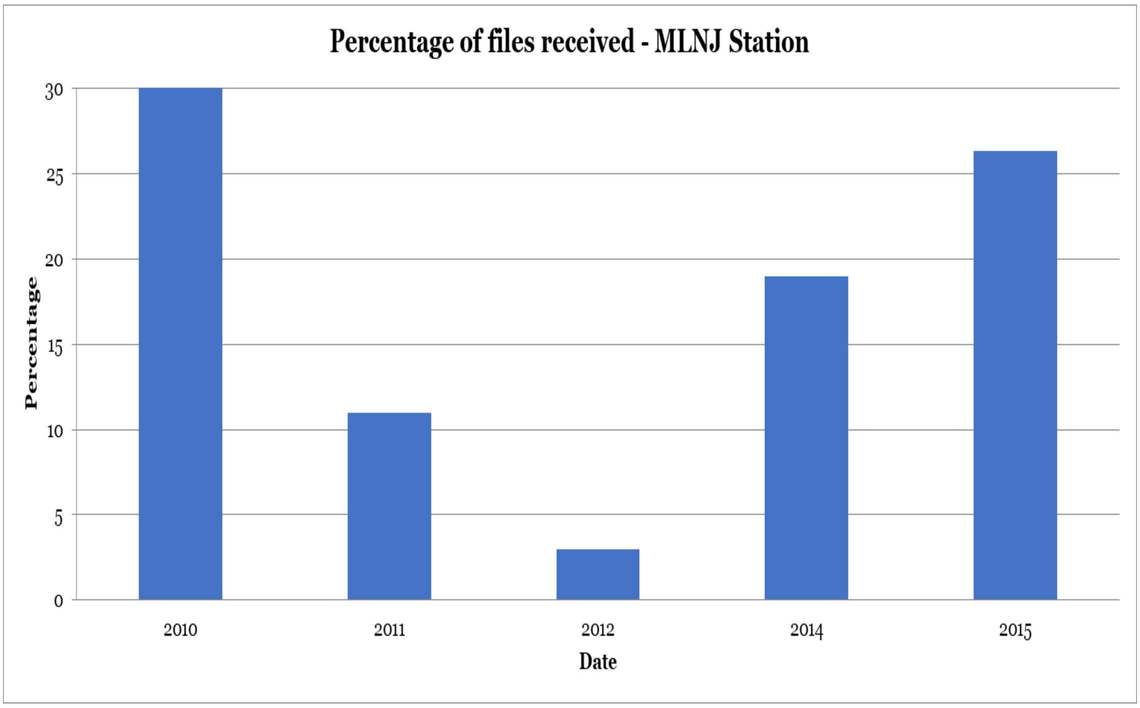

Figure A.10 - The Total possible percentage value of the Malanje station per year.

Figure A.11 also illustrates curious behaviour for station Ndalatando in 2011 and 2014 that was presented in the years 2010 and 2011 in Figure A.5. Although they are not the years with the highest or lowest value observed, they only differ by one day in the transmission of information. Figure A.11 shows 2015 with high percentage values 63% (230 days). In 2012 only 8.2% (30 days) of data was received.

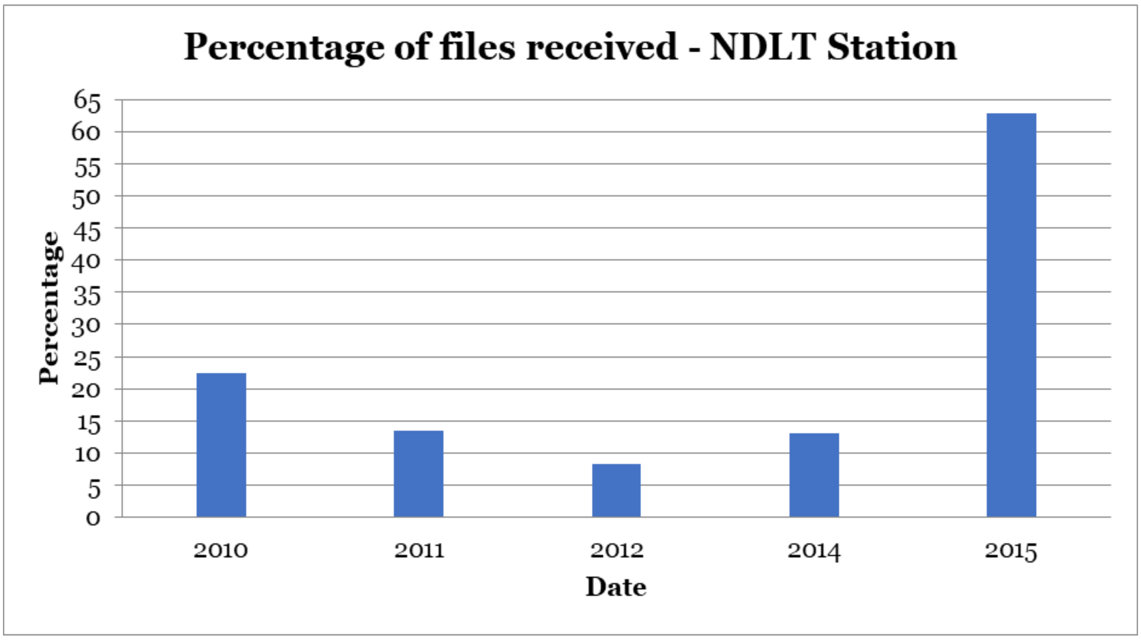

Figure A.11 - The Total possible percentage value of the Ndalatando station per year.

Figure A.12 also shows for station Namibe a high percentage in 2015 (87.4%, 319 days). In 2012 the lowest amount of data was received (3.3%, 12 days).

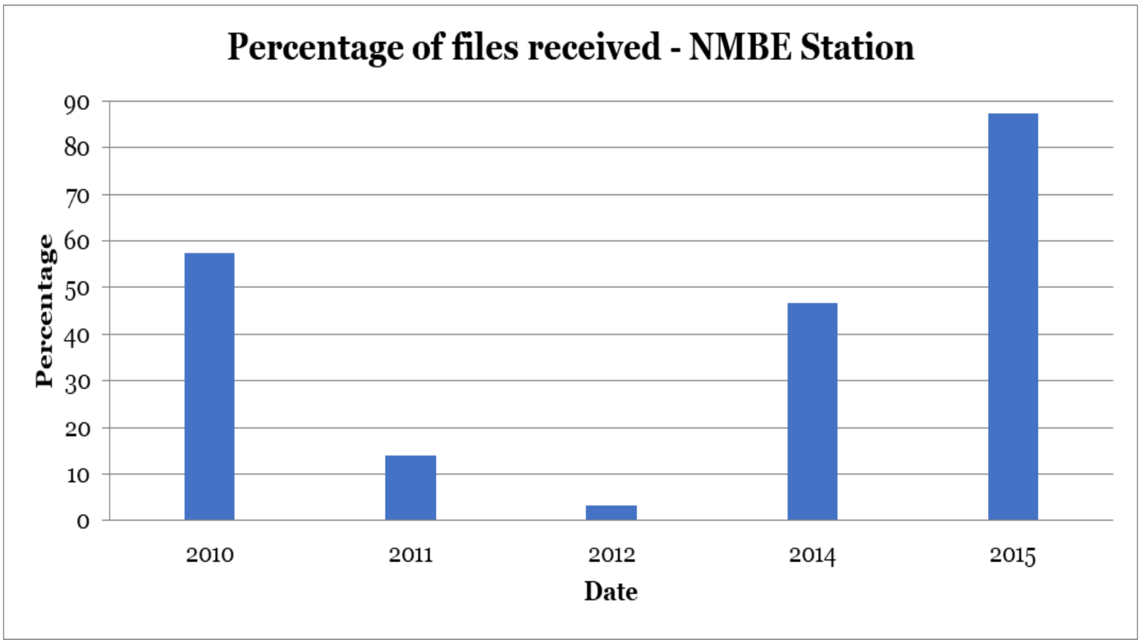

Figure A.12 - The Total possible percentage value of the Namibe station per year.

Figure A.13 also illustrates high percentage values for station Ondjiva in 2015 with 92.6% (338 days). 2016 was the year with a low value of 2.7% (ten days).

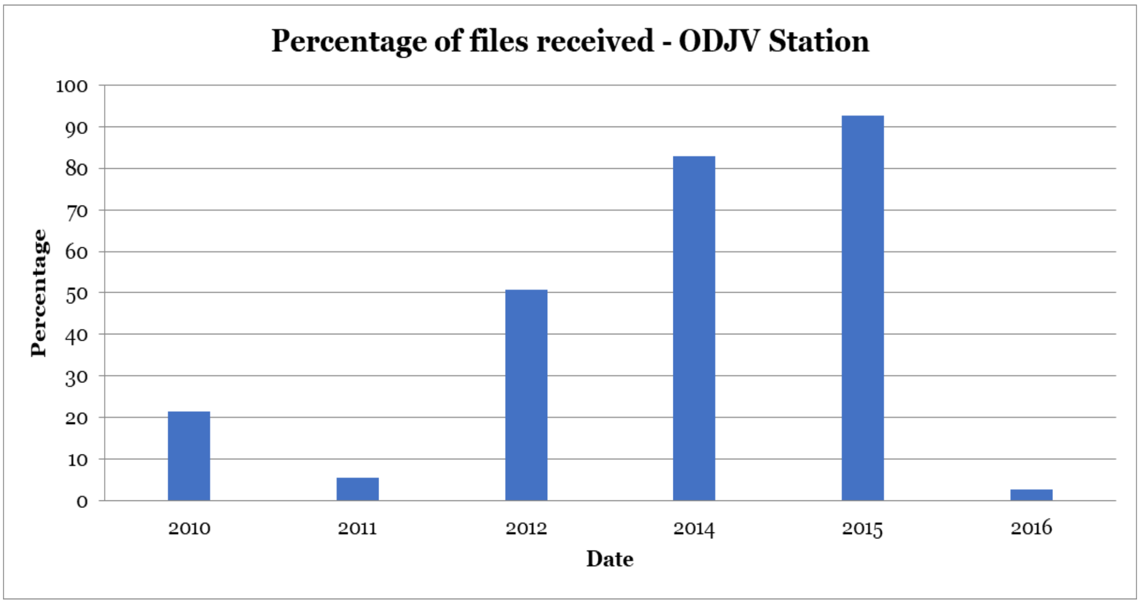

Figure A.13 - The Total possible percentage value of the Ondjiva station per year.

Figure A.14 illustrates the percentage values that the Saurimo station recorded. The most amount of data was received in 2010 (26.8%, 98 days) while the lowest amount of data occurred in 2021 (3%, 11 days).

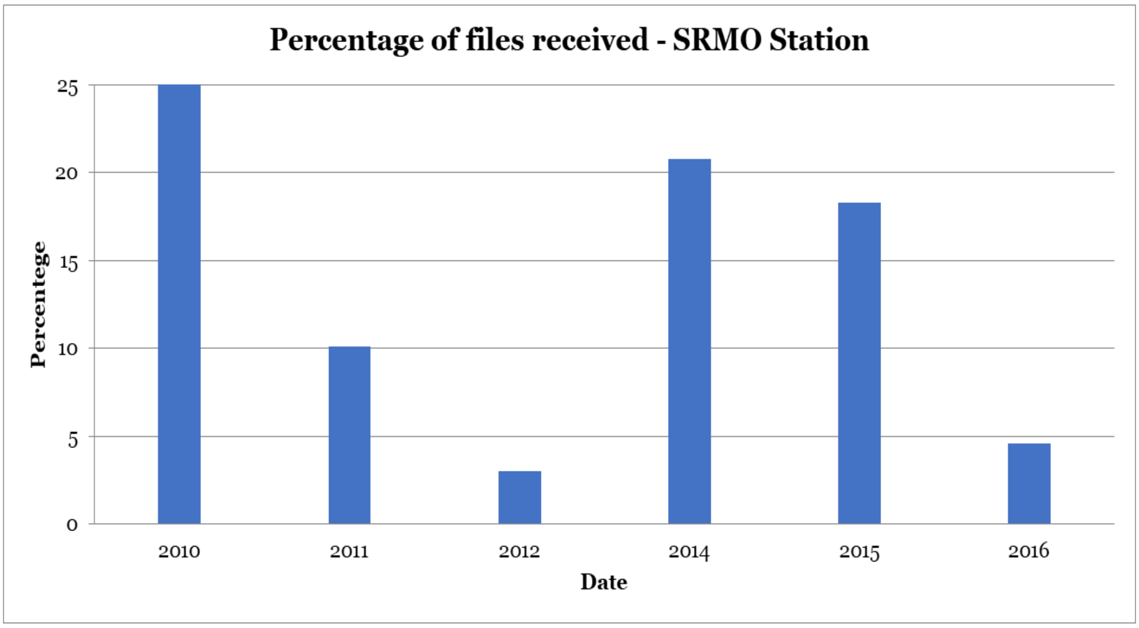

Figure A.14 - The Total possible percentage value of the Saurimo station per year.

Figure A.15 also demonstrates that for station Saurimo 2010 was a year with high percentage values (56.7%, 224 days). 2011 was the year with a low value of 2% (seven days).

Figure A.15 – The Total possible percentage value of the Sumbe station per year.

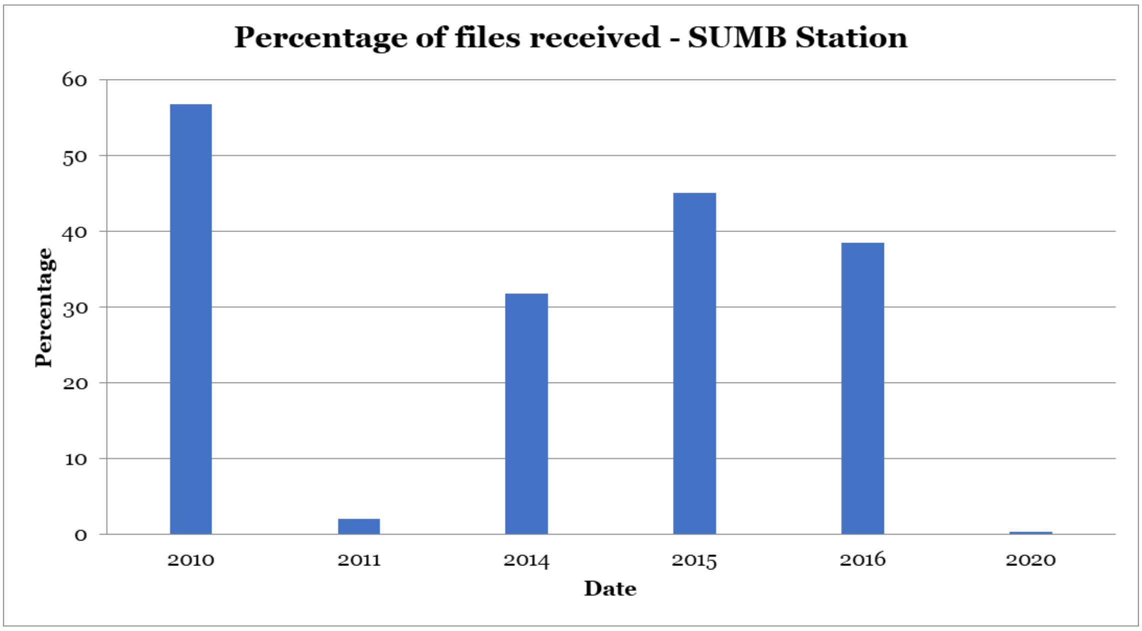

Figure A.15 - The Total possible percentage value of the Sumbe station per year.

Figure A.16 16 also illustrates low percentage values in 2011 for station Uíge (14.2%, 52 days) 2015 was the year with a high value of 69.3% (253 days).

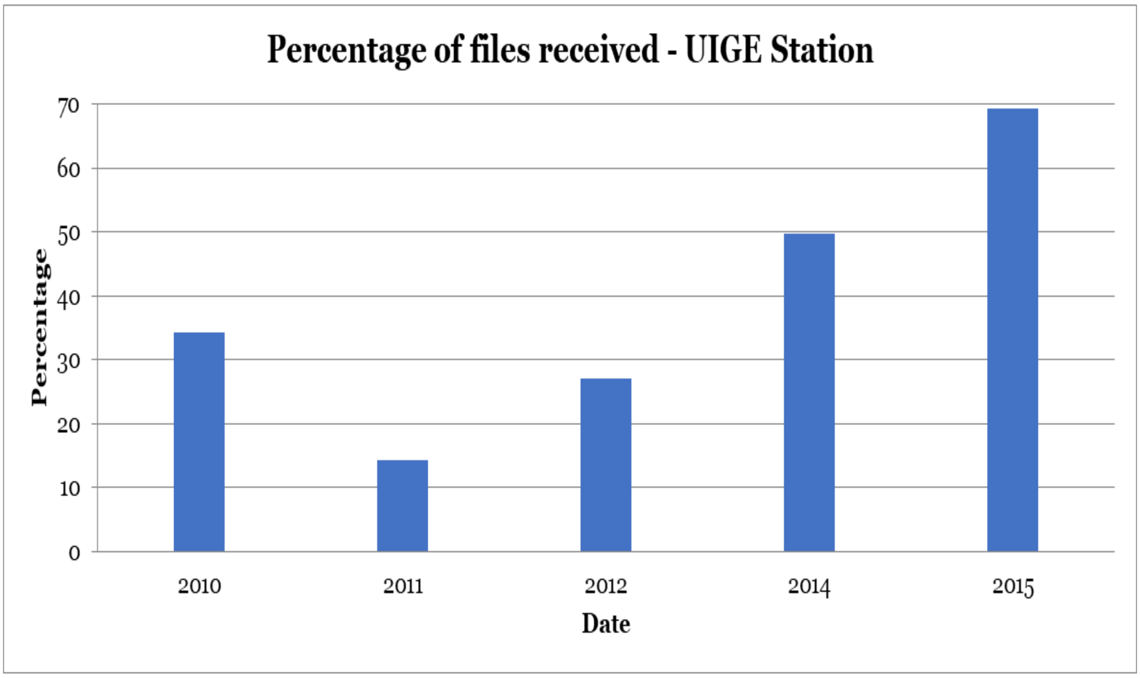

Figure A.16 - The Total possible percentage value of the Uíge station per year.

Appendix B

The maximum, minimum and average values of ZTD per station

Figure B.1 illustrates the maximum, minimum and average values of ZTD per station.

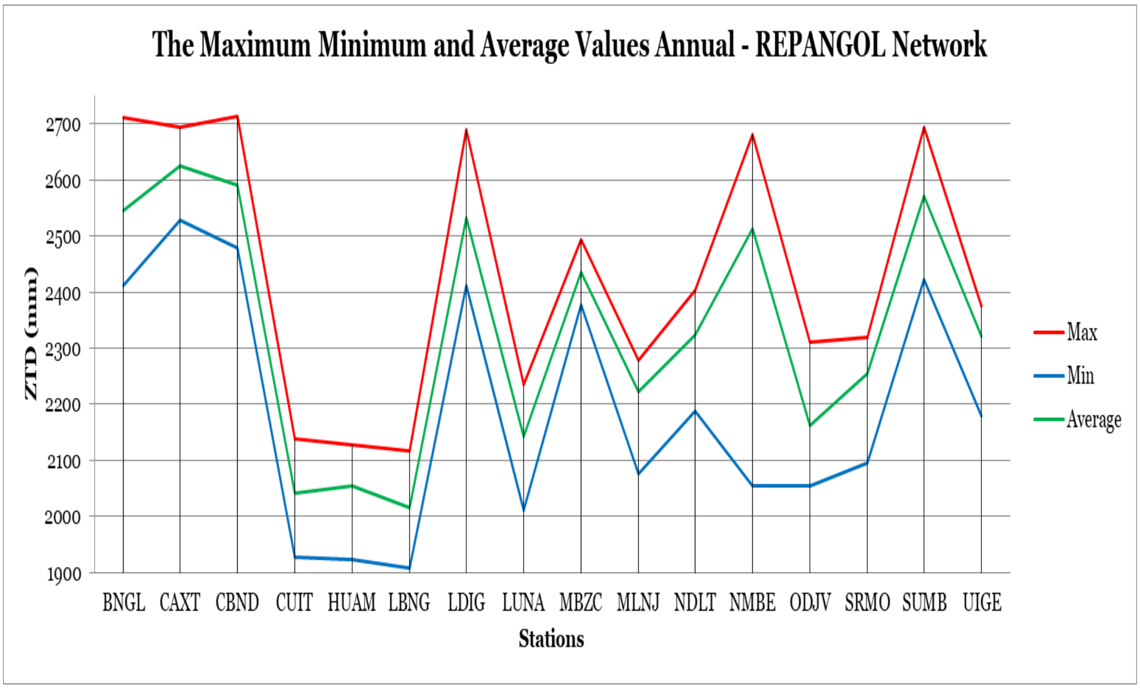

Figure B.1 - The maximum, minimum and average values of ZTD per station.

In terms of values, one can be observed clearly that the stations of the coastal region record maximum values of approximately 2713 mm. Since the minimum of the values is around 2054/2528 mm. CBND station presented higher values among the stations of coastal region. NMBE station recorded low values among the station of coastal region. The same figure 5.27 one can be observed that the stations of the northern region record maximum values is around 2375/2493 mm. Since the minimum of the values is around 2180/2375 mm. MBZC station presented higher values among the stations of northern region. MLNJ station recorded low values among the station of northern region. Finally, one can be observed that the stations of the central and southern region show maximum values is around 2117/2310 mm. Since the minimum of the values is around 1906/2055 mm. LUNA station presented higher values among the stations of central region. HUAM station recorded low values among the station of central region. ODJV station presented higher values among the stations of southern region. LBNG station recorded low values among the station of southern region. In general, the maximum and minimum values of ZTD are correlated with the average values of ZTD. Although figure 5.28 illustrates the peak values in the CAXT station since the CBND station recorded the peak values for the maximum values. The average value of received files for these stations is just 2334.5 mm.

Appendix C

Equipment Status at the Station Including the Status After Intervention (Adapted from REPANGOL – Surveying with the supervision of SEGAL).

SITES	Receiver	Router	Antenna	Energy Converter	STATUS
LDIG	OK (Septentrio)	Replaced	OK	Not working	OPERATIONAL
CBND	OK	Replaced	OK	OK	OPERATIONAL
MBZC	Faulty	Not Replaced	OK	Not working	NOT OPERATIONAL
UIGE	OK	Not Replaced	OK	Not working	OPERATIONAL
CAXT	OK	Not Replaced	OK	OK	OPERATIONAL
NDLT	Faulty	Not Replaced	OK	Not working	NOT OPERATIONAL
MLNJ	OK	Replaced	OK	OK	OPERATIONAL
DUDO	OK	Not Replaced	OK	Not working	NOT OPERATIONAL
SRMO	OK	Replaced	OK	OK	OPERATIONAL
SUMB	OK	Not Replaced	OK	OK	OPERATIONAL
BNGL	OK	Replaced	OK	Not working.	OPERATIONAL
HUAM	OK	Not Replaced	OK	OK.	OPERATIONAL
CUIT	OK	Replaced	OK	Not working.	OPERATIONAL
LUNA	OK	Replaced	OK	OK.	OPERATIONAL
NMBE	OK	Replaced	OK	Not working.	OPERATIONAL
LBNG	Faulty	Not Replaced	OK	Not working.	NOT OPERATIONAL
MNNG	Not Checked	Not Checked	OK	Not working.	NOT OPERATIONAL
ODJV	Faulty	Not Replaced	OK	OK.	NOT OPERATIONAL